NUMERICAL APPROXIMATION OF THE SCALED FRONTAL IMPACT SCENARIO OF A VEHICLE TO OPTIMIZE THE CRASH-BOXES VALIDATED VIA EXPERIMENTS TO REDUCE THE COLLISION EFFECTS

M.Sc. THESIS

Ahmad BAKHTIYAR

Department	:	**MECHANICAL ENGINEERING**
Field of Science	:	**MACHINE DESIGN & PRODUCTION**
Supervisor	:	**Assist. Prof. I. Kutay YILMAZCOBAN**

May 2019

REPUBLIC OF TURKEY
SAKARYA UNIVERSITY
INSTITUTE OF SCIENCE AND TECHNOLOGY

NUMERICAL APPROXIMATION OF THE SCALED FRONTAL IMPACT SCENARIO OF A VEHICLE TO OPTIMIZE THE CRASH-BOXES VALIDATED VIA EXPERIMENTS TO REDUCE THE COLLISION EFFECTS

M.Sc. THESIS

Ahmad BAKHTIYAR

Department	**MECHANICAL ENGINEERING**
Field of Science	**MACHINE DESIGN & PRODUCTION**
Supervisor	**Assist. Prof. I. Kutay YILMAZCOBAN**

This thesis has been accepted unanimously / ~~with majority of votes~~ by the examination committee on 03.05.2019

Dr. Öğr.Üyesi
İbrahim Kutay YILMAZCOBAN
Head of Jury

Prof. Dr. Fehim Fındık
Jury Member

Dr. Öğr. Üyesi
Gökhan COŞKUN
Jury Member

REPUBLIC OF TURKEY
SAKARYA UNIVERSITY
INSTITUTE OF SCIENCE AND TECHNOLOGY

NUMERICAL APPROXIMATION OF THE SCALED FRONTAL IMPACT SCENARIO OF A VEHICLE TO OPTIMIZE THE CRASH-BOXES VALIDATED VIA EXPERIMENTS TO REDUCE THE COLLISION EFFECTS

M.Sc. THESIS

Ahmad BAKHTIYAR

Department	:	**MECHANICAL ENGINEERING**
Field of Science	:	**MACHINE DESIGN & PRODUCTION**
Supervisor	:	**Assist. Prof. I. Kutay YILMAZCOBAN**

This thesis has been accepted unanimously / with majority of votes by the examination committee on 03.05.2019

....	....	....
Head of Jury	**Jury Member**	**Jury Member**

DECLERATION

This study is the new type of approximation for the crash box systems which has beed used for decades. The idea, design concept and orginization belong to my Advisor Dr. I. Kutay YILMAZCOBAN from Sakarya University Turkey. And all rights reserved to him. Experimental parts of the study were handled with the help of Masters Student and a Mechanical Engineer Omer ADANUR, and Mechanical Engineer Undergraduate students Mesut KOC, Okan KARAOGLU and Abdullah FEYZULLAH. Arrengements of the study, all the numerical developments for the simulations and validation checks with the experiments are belonged to me as a Master of Science Candidate for the Mechanical Engineer Department, Ahmad BAKHTIYAR.

<div align="right">

Ahmad Bakhtiyar

03.05.2019

</div>

PREFACE

TABLE OF CONTENTS

LIST OF SYMBOLS AND ABBREVIATIONS

DOF   : Degree of the freedom

E_{ab} : Absorbed energy

PDF   : Partial deferential equation

GFRP   : Glass Fiber Reinforced Polymer

GPa   : Giga Pascal

g   : Acceleration of gravity

$h_{profile}$: Length of the profile

h_{right} : Height of the right column of sample after the experiment

h_{left} : Height of the left column of sample after the experiment

$h_{average}$: Average height of the sample after the experiment

h_{stroke} : Height of the Stroke

Ke_{impact} : Kinetic energy of the drop plate at the time of collision

MPa   : Mega Pascal

$m_{vehicle}$: Sum of the mass of the vehicle, driver and sample

$m_{drop\ plate}$: The mass of the drop plate

N   : Number of the sample

Pe_{son} : Potential energy of the drop plate after collision

$V_{experimental}$: Experimental speed of the drop plate

$V_{theoretical}$: Theoretical speed of the drop plate

δ : Deformation of the crash-box

%   : Percentage

LIST OF FIGURES

vii

LIST OF TABLE

ABSTRACT

Keywords: Vehicle Crashworthiness, Crash-box and Safety, Energy Absorption, Impact Simulation.

Accidents happen in various ways in everyday use in transportation vehicles. Although extensive numbers of precaution methods are applied for prevention, the accidents are still inevitable. Especially in the field of vehicle design, many safety techniques are being developed to prohibit accidents and to reduce the loss of life and vehicle damages in the event of an accident. These security measures can be grouped under two headings as active and passive security systems. In this study, passive safety system which comprises material changes and structural improvements on the vehicle in the event of an scaled accident scenario, are examined in order to reduce as much as possible the adverse effects of the collision. Circle, hexagonal, square and the new W shaped cross-sectional steel sheet-metal crash-boxes are designed to absorb the shock waves and deformation energy between the chassis and the bumper of the vehicle as a new perspective focusing on the crash-boxes. For the frontal impact scenario, 2.88m high drop test setup was used. The designs are optimized via using thickness differences of the uniform material and shape. The deformation amounts and shock accelerations are keys to define the absorbed shock energy during the impact process. All these procedures carried out by the explicit finite element simulations also. Finally, 1mm thick St37 w shaped cross-sectional sheet metal crash-box perceived to absorb the enough amount of impact energy of the scaled version of frontal collisions with a speed around 25km/h.

ARAÇLAR IÇIN ÖNDEN ÇARPIŞMA ETKILERINI AZALTICI ÇARPIŞMA KUTUSU TASARIMININ DENEYSEL YAKLAŞIM VE SAYISAL OPTIMIZASYONLAR YARDIMIYLA BELIRLENMESI

ÖZET

Anahtar Kelimeler: Araç Kazası, Çarpma-Kutusu ve Güvenlik, Enerji Emilimi ve Çarpışma Simülasyonu.

Araçlarda günlük kullanımda kazalar çeşitli şekillerde meydana gelmektedir. Trafik kazalarından korunmak amacıyla çok sayıda önlem alınmasına rağmen, kazalar hala kaçınılmaz olmaktadır. Özellikle yeni nesil mühendislik tedbirleri ile araç tasarımı alanında, çarpışma durumunda can kaybını önlemek ve araç hasarını azaltmak için birçok güvenlik yöntemi geliştirilmektedir. Bu güvenlik tedbirleri aktif ve pasif güvenlik sistemleri olarak iki başlık altında toplanabilir. Bu çalışmada, çarpışmadaki olumsuz etkileri olabildiğince azaltmak için, bir ölçeklendirilmiş kaza durumunda malzeme değişiklikleri ve araçtaki yapısal iyileştirmelerden oluşan pasif güvenlik sistemi incelenmiştir. Daire, altıgen, kare ve yeni tasarım olarak W şeklindeki kesitlere sahip çelik sac çarpma-kutuları, bu meseleye odaklanan yeni bir bakış açısı olarak şasi ile aracın tamponu arasında bir çarpışma şok dalgalarını ve deformasyon enerjisini sönümleyici ara ekipman olarak tasarlanmıştır. Önden çarpma senaryosu için 2.88m yüksek düşme testi kurulumu kullanılmıştır. Tasarımlar, homojen malzeme ve geometrideki kalınlık farklılıkları kullanılarak optimize edilmiştir. Deformasyon miktarları ve şok ivmeleri, çarpma işlemi sırasında emilen şok enerjisini tanımlamak için bazı durumlarda kullanılmışlardır. Bütün bu işlemler dinamik olarak sonlu elemanlar simülasyonları tarafından da gerçekleştirilmiştir. Son olarak ise, 1 mm kalınlığındaki St37 ekonomik çelikten imal edilen w kesitli sac metal çarpma-kutusu, önden çarpışmaların ölçeklendirilmiş versiyonu için yeterli miktarda darbe enerjisini 25 km/s hızla gerçekleşen kazalarda sönümlediği görülmüştür.

CHAPTER 1. INTRODUCTION

Today people have immensely increased their dependency on vehicles. The number of collision and fatalities has increased with the increasing number of vehicles also. One of the most important problems of vehicles collision is frontal impact for decade. [1, 2, 3, 4]. Thus, manufacturers and establishments (Euro NCAP etc.) have been trying to facilitate rules and create different types of prevention systems. These security systems can be classified under two headings as active and passive safety measures; [5].

(a) Active safety- includes information systems to increase the control and braking capabilities of the vehicle in order to avoid the accident, and control algorithms that detect the possibility of an accident and take the vehicle out of the situation.

(b).Passive safety- describes, if an accident is encountered, design measures such as material changes and structural improvements on the vehicle in order to minimize the negative effects of the accident are examined under this heading [6].

Risk situations in accidents have started to be countered in the 1950s, and it has been noticed that measures should be taken in case of material damage accidents resulting in injury or death. In the process of accidents, the most dangerous cases come from the front collision conditions. The most important point that should not be neglected is to take measures for the frontal collision which has a high effect according to the other accident types.

Recent studies indicate about features; inside the chassis and under the hood staying in front of the Driver like protection bars to decrease the collision effects and prevent the passengers. It is called a crash box [7,8,9,10]. Crash box structures are widely used in energy absorbers in vehicles and find out their crashworthiness and numerical method. Crash box is a system converting the kinetic energy caused by the collision,

via deforming itself in plastic region of the material and absorbing the impact energy and shock waves of the accident and is expected to be collapsed with absorbing crash energy prior to the other body parts so that the damage of the main cabin frame is minimized, and passengers have saved their lives [11]. Crash box or thin walled structure, which is responsible for absorbing approximately 50% of kinetic energy of vehicles during frontal impact collision [12,13]. The cross section of energy absorber is mainly of rectangular/square shape. In Previous studies, many researchers put efforts to understand crash behavior of rectangular/shape under static or dynamic axial loading. In crash box designing; many factors are considered like energy absorption efficiency, light weight and most important design structure [14,15].

In this study, the demonstrative behavior of W shape folded crash box are selected, However, in earlier studies regular shape crash had been used for many ways. W shaped design could make many fold ways, but manufacture is capable of only this W shaped design because their machine and equipment are up-to manufacturing limits [16,17].

1.1. Literature Review

Recent studies of automobile industries are mostly focused on safety features and crashworthiness. Last few decades, manufacturing rates of automobile has been continuously increasing. Worldwide automobile production 2000-2017 in millions, in 2017, some 73.5 million cars were produced worldwide [18]. This figure translates into an increase of around 2.4 percent, compared with the previous year. The number of accidents and cars collision is increased with the increasing manufacturing rate of automobiles. That's why crash-box and frontal impact analysis is very important. This analysis mainly aims to protect the occupants of a car, so there are many new safety features such as airbags, crash box, seat belts, and ABS brakes are added day by day. Unlimited data is available in research domain based on crash-box analysis but in this studies, geometrical design of crash box differentiate from previous studies.

This study is to find out the crashworthiness of multi-cell hexagonal crash-box below and axial and oblique load. Crashworthiness of sectional configuration, such as one single walled, two double walled, and four multiple cell hexagonal crash box tube have been analyzed. These results are validated by both experimental and analytical results. In these comparative studies, multi cell tubes were performing better than other crash-box tube configurations [19].

In this work, the analysis of crash-box with different cross-sectional area and of the joining system is found out. At the time collision crashing is affected by the loading rate and depend upon the materials behavior, which has been examined in many non-common continuous welding or joining system with different cross-sectional area of the crash - box. In this study, three different types of joining system have been used such as adhesive acrylic, one component epoxy and two non-epoxy and laser welding method. Due to continuous joining spot welding used wieldy to improve the performance of structures; an adhesive and laser welding can be used as an alternative. The more energy absorption properties in these methods have adhesive due to continuous connection of the sheet, the other is finding an interesting solution by laser welding. If compared with a spot welding it gives better results and even similar to adhesive joining [20].

Nowadays composite materials used in making of the crash - box, have good energy absorbing characteristics at the time of frontal impact collision. GFRP (Glass Fiber Reinforced Plastics) one of those composite materials are used in crash-box. In this study, investigation of GFRP material is to find out energy absorption characteristics with different model of crash-box. Crash box is compared use of triggered and non-triggered mechanism. To get a significant result of crash behavior and energy absorption properties if choosing a proper combination of the trigger mechanism and cross-sectional area of the cross - box [21].

(a) Traffic Collision -In this topic, a literature review of traffic collision and accidents injuries in developing/developed countries has been given.

In our daily life numbers of people die and face causalities on the road accidents worldwide. But accidents and traffic collision are preventable to upgrade traffics system, road and more importantly to increase safety features system in vehicles. In developed countries, a formatted set of intervention contributes to significant reduction in the accidents and road traffic injuries. In opposite way, road traffic injuries and accidents are increased in developing countries. The rate of road side accidents and getting effected by it is higher in developing countries. To get rid of this scenario millions of advancement and developments are required to achieve these goals.

(b) Definition of Road Accidents- The definition of road accident is defined as; "the number of person causalities and death due to a traffic collision on the roads". In this road accident measurements are not included suicide by using the motor vehicles. The meaning of automobiles is vehicles connected with an engine as a mean of propulsion those normally have been used to carry goods or people on the road. The road vehicles having many types of transportation such as buses, trolleys, coaches, tramways, cars to transport goods and passengers. The countries, where motor vehicles are registered, Road motor vehicles are attributed to the countries where they are registered, while deaths are attributed to the countries in which they occur. This indicator is measured in number of accidents, number of persons, per million inhabitants and million vehicles [22].

The following data is measured in number of accidents, number of persons, per million inhabitants and million vehicles of Republic of Turkey from 1994 to 2016.
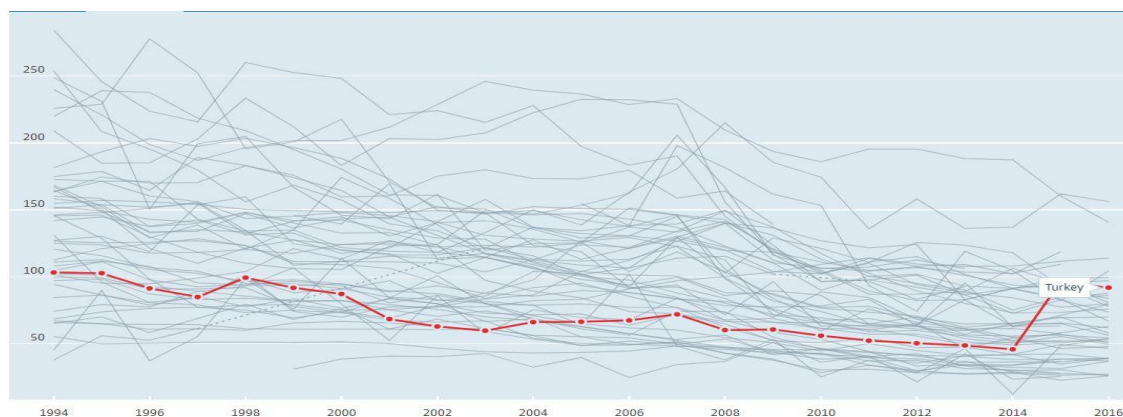
Figure 1.1. Death in Turkey due to Road Accidents in 1994-2016
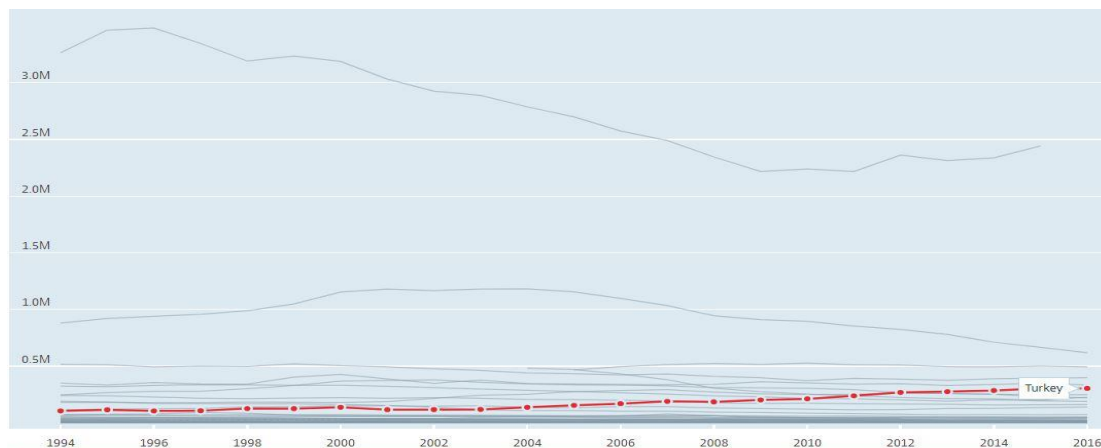
Figure 1.2. Injuries in Turkey due to Road Accidents in 1994 to 2016

The crash-box is an energy absorbing device installed vehicles bumper structure and side rail in order to prevent the kinetic energy transfer to occupant's chamber in the time of the frontal collision (Figure 1.3.). Crash-box tried to absorb the maximum amount of the energy from the raise of the collision and shocking. A large part of the energy is absorbed by the plastic deformation of the crash-box.
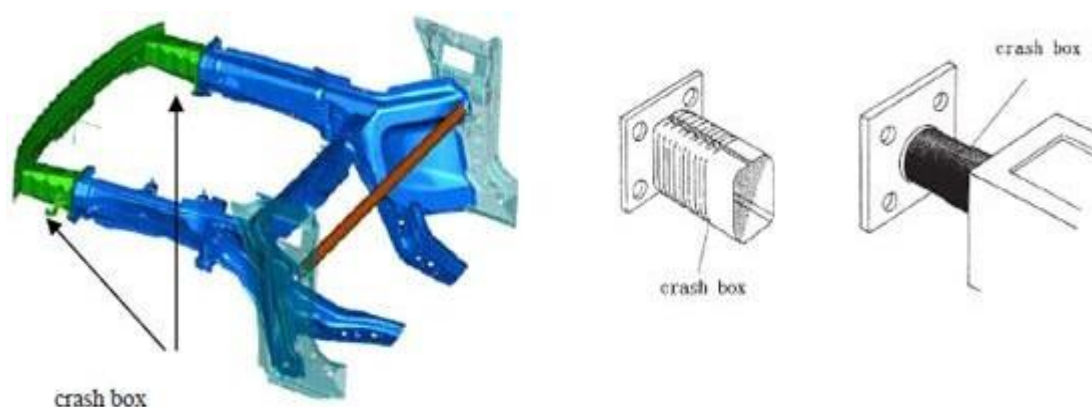
Figure 1.3. Location of the crash-box in the vehicle

The number of studies has been completed regarding to structure absorb the maximum amount of energy. However, the researcher are trying to make light vehicles to help of using different design and materials of the crash-box and parts of the vehicles to could achieve these goals.

In the case of collision at low speed, crash- boxes absorb the energy of the collision and reduce the impact load due to arise collision [23]. In order to ensure that these crash-box absorb all kinetic energy at low speed collision, it is necessary to assure the

impact forces is equally distributed in the boxes and less than maximum force value that allows the box to protect the other parts of the vehicles [24]. There are following principle should be considered in the designing of the crash-boxes to achieve these objectives;

a) The crash-boxes are changeable and low cost. Therefore after collision of the vehicles easy to manufacture and replaceable.

b) The kinetic energy must be converted into irreversible deformation energy as much as possible. For metal crash-boxes, this energy must be converted into plastic deformation energy (Figure 1.4.).
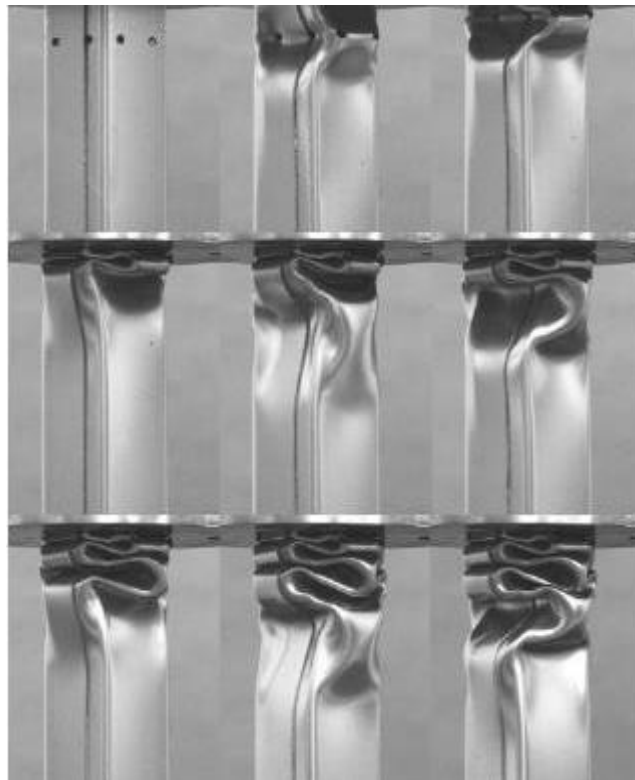
Figure 1.4. Absorbing energy in a crash boxes

The bumper structure in modern cars consists of glass fiber, composite or plastic materials on the steel or aluminum support rod. The bumpers of luxury cars are produced from PC / ABS materials called polycarbonate (PC) and Acrylonitrile butadiene styrene (ABS). However, despite all these developments, the results of the

crash tests performed speed until 50 km / h. According to this idea, the folding of thin walled dampers are investigated. There are some basic examples of the dampers design are presented [25] (Figure 1.5.-1.6.).

Figure 1.5. Folding of properly triggered elements, often subjected to axial impact loading

Figure 1.6. Square columns resulting from the development of symmetric and 'inverted' folding modes indicated by white arrows

In order to increase the maximum amount of energy absorbed, different section geometries (Square, Hexagonal, and Circle) have been proposed and lighter vehicle weights have been targeted with the use of high strength materials. The high reaction force during the plastic deformation of the shock absorbers means that the amount of energy absorbed is high. However, it is undesirable to have a high initial reaction force at the beginning of the collision of the vehicle. Therefore, local sprains on shock absorbers should be start at minimum response forces.

The geometric projections and indentations are formed on the profile. In a study conducted at Dalian University of Technology, models with different dimensions of buckling initiator were solved and the results were compared. In this study, which was

conducted by two people, it was seen that the indentations provided more regular plastic deformations after the collision (Figure 1.7.).

According to a researched in 2014, the behavior of the sample obtained by filling the inside of a hollow square section with the honeycomb structure made of glass-fiber reinforced polyamide (GFRP) was tested during the collision [26] (Figure 1.8.).
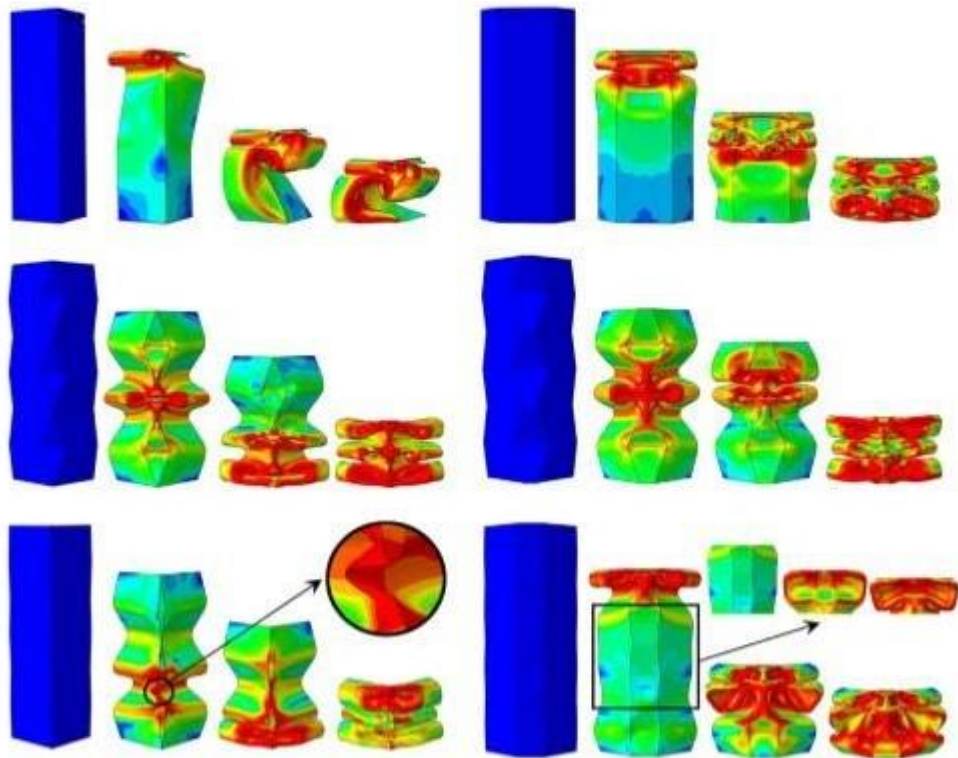
Figure 1.7. The effect of recesses and protrusions on agglomeration in the crash-box origami
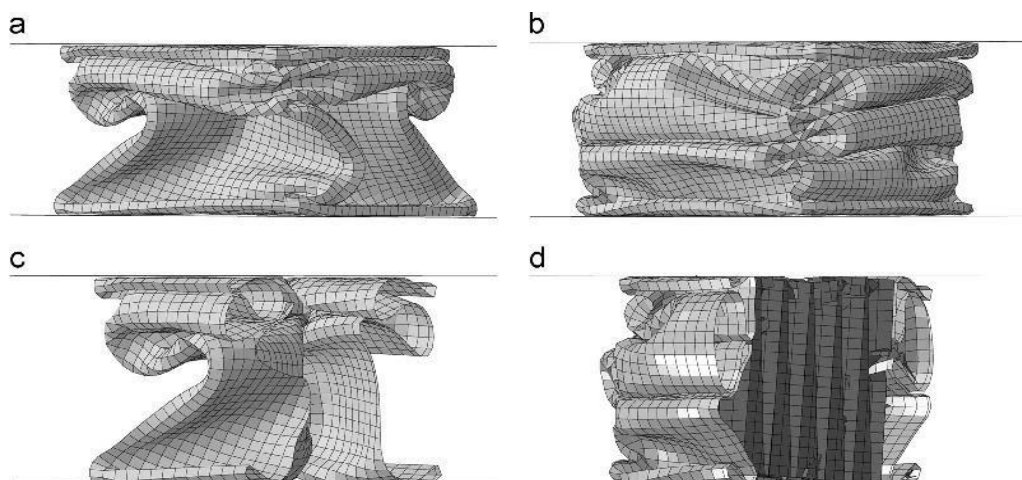
Figure 1.8. Reinforced Hollow Square cut samples of the crash-box

In order to increase the energy damping capability of hollow steel tubes, steel tubes with different geometries were analyzed by LS-DYNA and the highest geometry with collision conformity was tried to be found [27]. The samples used in this studied were determined as square, hexagonal, octagonal and 12-sided hollow tubes.

Then a vehicle model was created and the samples were placed in this model and collision analysis was performed at a speed of 56 km / h (Figure 1.9.).
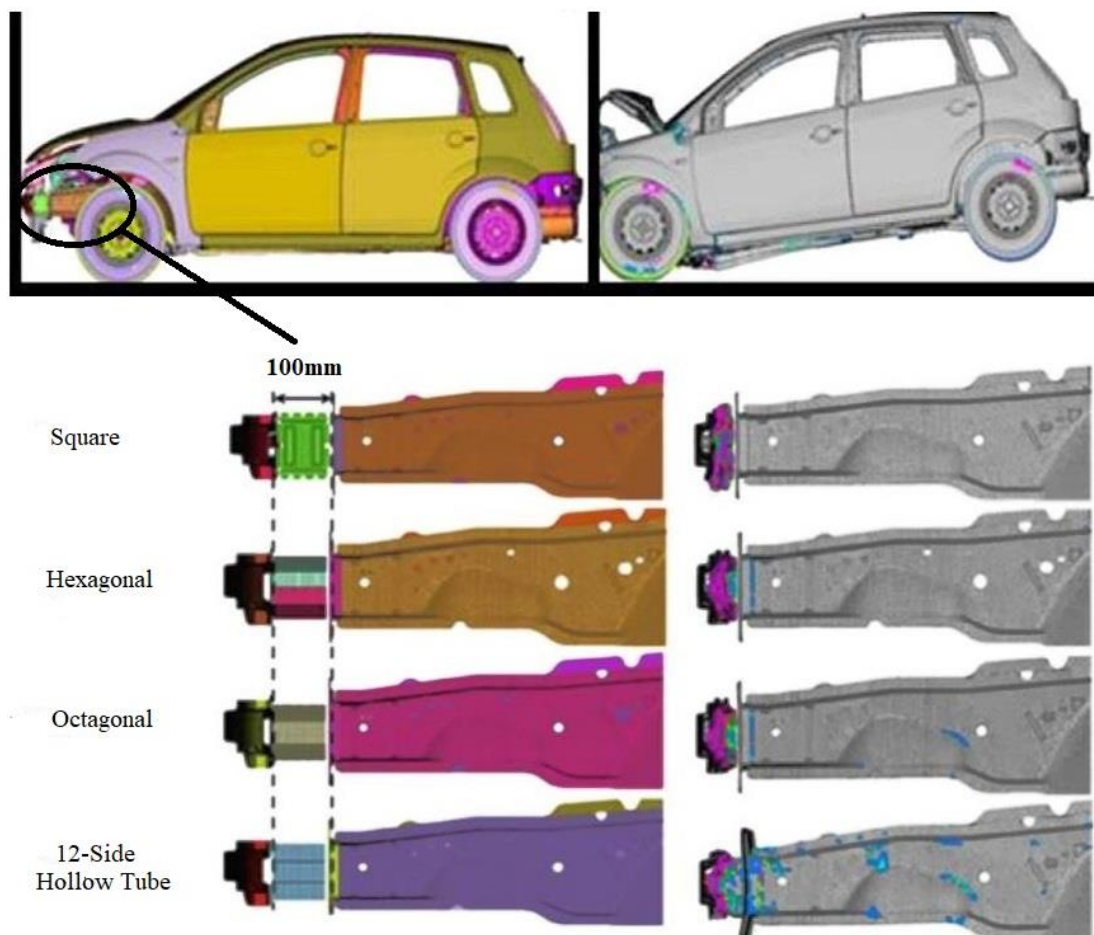
Figure 1.9. Crash test of the vehicle at 56 km / h & deformation according to sample geometries

When the results of the analysis are examined, it is seen that square and hexagonal specimens can be folded by excessive deformation immediately and12 edge section samples absorbed a part of the energy at 90ms and still have the capacity of damping.

1.2. The Evolution of Vehicles Safety System

In the early 1900s, increasing using of the automobiles vehicles also the increase in accidents and fatalities. Due to accidents every year there is a huge loss of lives a general statement has been formed that this is because of unsafety of automobiles. Manufacture firms and independent organizations try to improve safety system of the vehicles, traffics rules and pedestrian safety studies are taken into consideration. However, today the automobile's industry is touching the sky it is not merely the efforts of years but it has taken centuries to make the vehicles more safety system are listed below in a chronological order. In the previous section described active and passive safety system. These are following categories of active and passive safety system.

1.2.1. Active safety system

Active safety includes information systems to increase the control and braking capabilities of the vehicle. These following are some systems.

(a) 1966: Anti-lock brakes (ABS)- ABS system is a system that provides full control of the steering wheel by preventing the wheels from locking in sudden braking situations in all road conditions and various speeds in case of any load in the vehicles.

Figure 1.10. Johnson Car with ABS system

The application of this ABS system have been developed long time ago than might be you think, in 1929's first time used in the aircraft. ABS system is unveiled for four wheel-drive car in 1966 [28] The system, implemented by the English manufacturer Jensen, makes The Jensen FF & the Ferguson Formula (Figure 1.10.) the first mass production car to be equipped with mechanical anti-lock braking based on aircraft technology.

(b) 1995: Electronic stability control- Electronic stability system prevents the loss of steering and out of control in curves by controlling your car when it begins to start it doesn't follow your intended path. Electronic Stability Control (ESC) is a technology that improves vehicle stability by sensing and reducing traction loss. The ESC is a highly effective system to enable the driver to control the vehicle and thus reduce the collisions. With the help of Bosch; Mercedes- Benz became the first manufacturer to use the ESC and the S-Class again led the way [29]. The ESC simulation is shown in Figure 1.11.
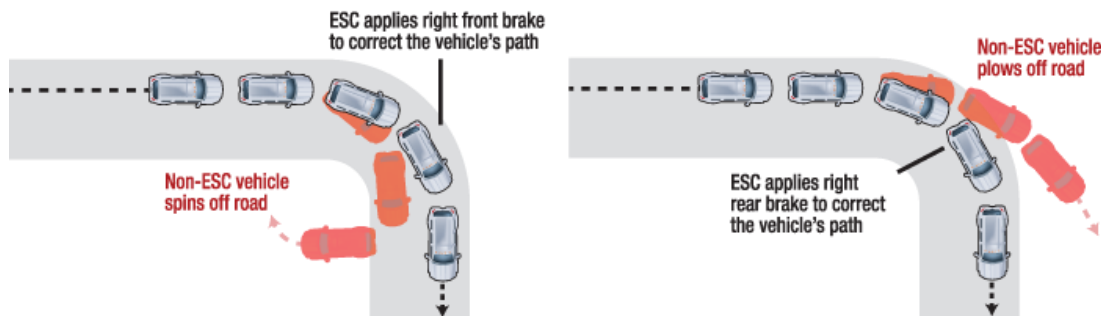
Figure 1.11. ESC simulation system

(c) 2003: Child safety system- There are three aspects of the protection of child occupant: 1) the child restraint system in the side and frontal impact test 2) different sizes and designs of child occupant's protection system have vehicles 3) accommodation of child in the vehicles for safe transport. For the manufacturers providing these points is much more difficult. These aspects of child occupant protection are giving more difficulty to the manufacture to full fill requirement of this security measure system test [30].

(d) 2008: Autonomous braking- The vehicle is a system that allows the vehicle to slow down by detecting this sudden braking by means of sensors and slowing the vehicle due to the sudden braking in the front vehicle due to heavy traffic during driving or due to a different reason [31]. This system is available in 2008 with the Volvo XC60.Added more tests.

1.2.2. Passive safety system

Passive safety system; if an accident is encountered, design measures such as material changes and structural improvements on the vehicle. These are following system with their discovering year.

(a) 1934: Crash test- The history of safety vehicles started when first automobile accident and fatalities had been found on the 31 August 1869 in the recorded. In this accident, one Ireland women lost her life. This accident & fatalities probably triggered the awareness and need of safety system in the vehicles and traffic rule of the road which protect the occupant of the vehicles as well as pedestrian of the road [32].

Figure 1.12. In 1934, the crash test has been done by General Motors

Therefore, after many years of this event, In 1934 the General Motors performed first collision test with a vehicle see in the Figure 1.12. This movement, which is a revolution, has attracted the attention of all car manufacturers and security institutions, after it has been performed by The General Motors and many companies and institutes started crash test of the vehicles such as Ford, Volvo etc. and since then, these tests

have become standard among all automotive manufacturers and state security agencies
[33]. It has come. Thanks to this test, the safety insufficiency of the cars in the period
has been seen and paved the way for improvements. The Figure 1.13. also shown
current scenario of vehicles which has been tested on the vehicle Chevrolet Bolt EV
2017.

Figure 1.13. Crash Test of Chevrolet Bolt EV 2017

(b) 1959: Safety belt- In 1955's the first time modern three belt concept is patented by
Roger Griswold and Hugh De Haven.

Figure 1.14. Safety engineer Nils Bohlin shows the 3-point seat belt used in 1959 Volvo cars

The Swedish car manufacture company Volvo has recognized this danger Volvo and employed Nils Bohlin for further design studies see in the figure 1.14. After research upon thousands of car accidents and patented more advancement invention of three seat belt system, which have been used till to date and is one of the most effective security systems. Although it has many variants, as double-point, three-point, and four-point. Before 1959 only two-point seat belt is used. This belt system is only used to hold the body and can cause serious trauma to the body of the driver and passengers during the accident because it had not been impose any restrictions on the body. By 1959, congress began regulating automobile safety standards, and by 1968 required all new American automobiles to be built with seatbelts. In 1970, Victoria, Australia became the first place in the world to require the wearing of the seatbelts in a moving vehicle [34].

(c) 1960: Filled Front Console- In the occurrence of a frontal clash, serious injuries may be caused by the front console for frontal seat passenger. In order to prevent these injuries, the front console is covered with soft padding and composite rubber material [35]. This coating reduced face and chest injuries. It was introduced by Volvo in 1960.

(d) 1973: Airbag- The air bag is a protection system made of flexible material, which prevents the passenger from getting injured by flexible air or gas balloon, which can be opened very quickly in the time of a collision.

Figure 1.15. Air bag system in the car

A typical airflow opens in less than 1 / 10th of a second and makes it easier for the passenger to move and leave the vehicle within a few seconds. The first airbag was developed in 1953 by John W. Hetrick. In 1973, the first airbag for sale was presented in the Oldsmobile Toronado series [36]. At the end of the 1990s, almost all new cars had become standard air bags. Airbag system see in this Figure 1.15.

(e) 1991: Side impact protection- Although injuries from airbags and belts recently have been reported to decreased, the serious injuries encountered due to side impact of collision of the vehicles. The space between both sides of the vehicles is not sufficient to prevent of the serious side impact collision than head on traffic collision. A high-quality wheelchair should be equipped in the appropriate direction with the stability properties against shock and vibration raise at the time of collision. The side collision protection should also prevent injury to the child on back side seat of the vehicles. Therefore, a side impact protection system is designed to meet this requirement to protect by side impact collision. The manufacturers have been given different ideas regarding side impact protection. For example, the Volvo side impact protection system (SIPS) combined with side-acting arms on the horizontal rails see in the Figure 1.16. [37].

Figure 1.16. Side view of Volvo S80

(f) 1996: Knee airbag- The knee airbag inflates under the steering column to reduce the risk of injury to the knees and lower legs of the driver (Figure 1.17.). The knee

airbag is always triggered with the driver's front airbag. Kia Sport-age SUV had been used the first knee airbag [38].

Figure 1.17. Knee airbag system in car

(j) 1998: Active head restraints or headrests *(AHR)*- Now days every vehicles are equipped of the active head rest restraints system. This restraints system is prevent from the rear collision to reduce the chance of serious injuries of head and neck. Active head restraints are move forward and backward in a rear-end collision to support the head and reduce the risk of a whiplash injuries.
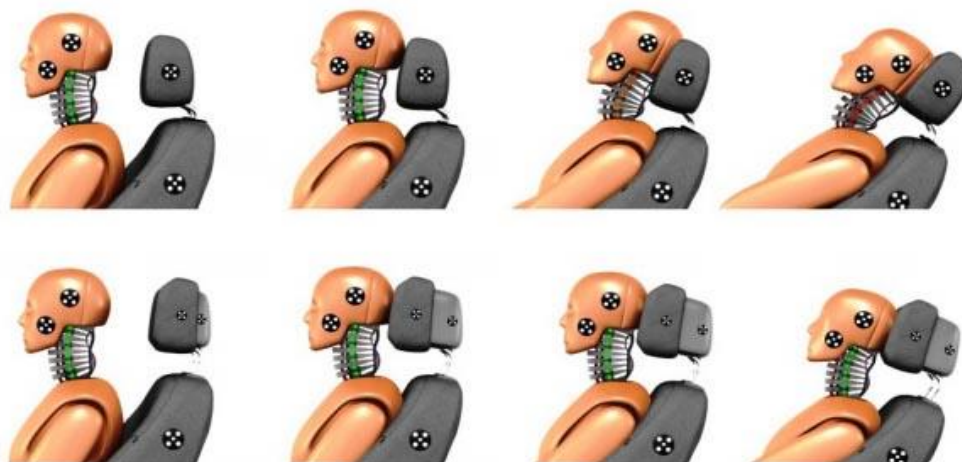
Figure 1.18. Headrest restraint system

Active head restraints with two flexible swings that are optional and individually detachable provide a good side grip and offer more comfort (Figure 1.18.). This will

reduce the physical injuries that will occur in the neck portion when the heads of the occupants are thrown with the force during the rear collision. The first example of head support is seen in 1968 in Volvo's mass production vehicles. North America started headrest in the cars on optional basis since 1960's, but later in 1969 it was made mandatory by the U.S. National Highway Traffic Safety Administration (NHTSA) for all new manufactured cars [39].

(k) 2005: Lane tracking system- The Lane Follow Assist warns the driver with the steering wheel vibrations when the vehicle is unintentionally leaving the lane, thus helping to prevent accidents [40]. First time this system applied in the Europe in this model, Citroen C4, C5 and C6.

(l) 2005: Pop-up bonnet- It was developed to reduce the risk of injury to pedestrians when cars hit pedestrians. In order to minimize the risk of pedestrian injury in such collision examples, the first examples of this study were applied to the Jaguar XK and Citroen C6 blades [41] see in the Figure 1.19.

Figure 1.19. Pop-up bonnet design

(m) 2007: Blind spot alert system- The blind spot warning system is the system that provides visual information to the driver with the LED lamps inside the mirror if the vehicles within two hundred feet of the rear bumpers of the vehicle are detected from behind and the vehicles within 50 meters distance.

(n) 2015: Obstacle detection in the dark, barrier detection- This technology is available from the Volvo XC90. Enhanced pedestrian detection shows people in the dark.

Barrier detection and lane tracking system intervenes in autonomous driving with cruise control and brake control.

1.2.3. Highway administration and rule

From last few centuries, increasing number of automobiles, vehicles uses common in the human being also increased the roads accidents and fatalities. Decade to decade, American Congress, the European Union and some government's organization passed acts and established new departments regarding this vehicle manufacturing and traffic rules.

(a) 1959: Road safety insurance institute (IIHS)- The Institute of Road Safety Insurance is an independent and non-profit scientific and educational organization dedicated to reducing deaths, injuries and physical damage from motor vehicle accidents. This organization has been operating in the USA since 1959 and aims to raise the awareness of consumers by rating the cars crash tests. In this test, the deformations of the cars will be formed by a 25% overlap at a speed of 64km / h. With this test, which is normally much more challenging than the tests with 40% overlap, IIHS demonstrates the importance placed on safety by trying to show the behavior of vehicles in the most extreme case [42]. The crash test of the Hyundai cars see in the Figure 1.20.

Figure 1.20. IHS-2010 Hyundai Tucson GLS & 2009 Hyundai Sonata Crash Test.

(b) 1966: National highway traffic safety authority (NHTSA)- In the time of 1950s & '60s increasing number of the accidents and vehicles fatalities due to lack of traffic

rules and regulations and increased public outcry about traffic injuries, and when American researcher and lawyer Ralph Nadar introduced publication Unsafe at Any Speed(1965), which criticized the American automobile industries for its unsafe products. After this situation in 1966 American congress organized a series of hearing regarding traffic rule and unsafe at any speed and should be created regulatory agency for traffic safety. Later the year Highway Safety Act was passed, which established the national Highway Safety Bureau (NHSB) became NHTSA in 1970 under the newly established Department of transportation [43].

(c) 1996: Euro NCAP founded- The government of number of European countries have been working under the European Experimental Vehicles Committee (EEVC), dealing with various type of aspect of the car and secondary security in 1970's. Before 1990s, this committee research given a concept in the full scale crash test, for protection of vehicles drivers in the side and frontal impact collision and also in the development of component test procedure for precaution of pedestrians, collision by a front of the vehicles. The EEVC test proposals for adoption was strongly opposed by the automobile industries in the European legislation in 1970s. In November of 1996, the Swedish National Road Administration (SNRA), the Federation Internationale de l'Automobile (FIA) and International Testing was the first organization to join the car safety test programme. This resulted in Euro NCAP being formed. Its inaugural meeting was held in December 1996. Twenty years later, 9 out of 10 cars were produced under the Euro NCAP certification [44].

(d) 2009: New euro NCAP score- In 2009, a strict rating was made in Euro NCAP. The scores of adult passengers, children's passengers, pedestrians and security assistants were started. In 2014, these ratings were further amended with more recent ratings [45].

1.3. Crashworthiness and Occupant Safety

In the early 1950's the term crashworthiness is used in aircraft industries. Crashworthiness means the ability of aircraft or vehicles to withstand collision or crash

to minimize injuries of the occupants. Crashworthiness has two main aspects are structure and restraint. First, its need to be energy absorber occupant shell that will provide a protection occupant from being crashing. Other, more important structures need to be more crashing zone where the force of impact can be absorbed by crashing part of structure more than occupants shell and also need to be stronger side structure to manage exerted force from the side collision. The restraints also provide to important role in strength crashworthiness. Seatbelt and Air bags have been reduce injuries due to vehicles accidents and even prevent death.

1.3.1. Safety of motor vehicles

In 1889, the first occurrence of death by accidents of vehicles in the New York City; genuinely these accidents are being a birth of safety features of vehicles as the field of research work. After this, manufactured realized to demonstrate research work of safety features in the automobile industries. There are three different eras of automobile safety in the development history. First is starting period of safety from century to 1935, second is 1935-1965, this was an intermediate period of safety and last period is started from 1966.

Early period of safety only focused on to understand the extremely complex process of vehicle frontal collision. During this period, manufactured to tried basic improvement of the vehicles such as reduction of tire blowouts, introduction of self-starter, improvements of headlamps, installing laminated glass, steel body structure for better occupant protection. In the row in this development series of safety features of vehicles, the first crash test of the full model of cars was done early 1935's. According to statistical data the fatality rate is approximately 17 per 100 million vehicle mile travelled.

The second period from 1935-1965 was intermediate safety period. In this period most common and valuable crash avoidance device are developed by the manufactured including as turn single lighting, dual windshields wiper, improved headlamps, how to test head impact into instrumental panel, high penetration resistant glass, frontal crash

test conducted by General Motor and one most significant safety device development of this era that concept of the seat belt in the 1956 [45].

Third period starts in 1966, when the President Lyndon Johnson signed into law of highway security act, and authorized the creation of National Highway Traffic Safety Administration (NHTSA) [46] and many mandatory safety standards, known as a Federal Motor Vehicles Safety Standards (FMVSS), were introduced. In this era, safety of the occupant and kinetic energy transfer to absorbing energy from frontal collision and side collision had been integral part of the vehicles development process. The summation of these automobile safety technologies, collaboration improvement of the traffic highway rules and driver skill education has played role of drastically changes in the rate of traffic fatalities. Statistical data that the fatality rate is approximately 1.6 per 100 million vehicle mile travelled in 1996. This is about only 10% fatalities of 1935 [47].

Nowadays automobile safety system depends on crashworthiness, driver skill performance, crash avoidance features, highway construction and traffic rules, last some decade automobile manufactured and researcher introduced many advanced safety features system to help out accidents and fatalities of vehicles like an anti-locking braking system (ABS), Automatic emergency braking (AEB), Forward-collision warning (FCW), Blind-spot warning (BSW), Rear cross-traffic warning, Rear automatic emergency braking (Rear AEB), Lane-departure warning (LDW), Lane-keeping assist (LKA), Lane-centering assist, Adaptive cruise control and day time running lamps [48]. In addition features to related crashworthiness are added in the vehicles such as variable types of crash-box to absorb maximum energy transfer by frontal collision into form of kinetic energy, using of sheet metal type materials to decrease a weight of vehicles and absorb crashing energy as possible as an addition of this row of including features as an absorbing energy steering columns, three points belt, two side air bags and demonstrated design of bumper to minimize a fatalities of vehicles. The content is only with structural crashworthiness and related to injuries.

1.3.2. Design of vehicles

The statics and dynamics analysis is a primary aspect of automobile design to encounter with life cyclic vehicles. The main prospective of design is integrity which provides adequate protection at the time of crashing and accidents. The evolution of the automobile structure from decade to decade to depend upon the research work of manufactured to satisfy customer requirements and demands. Sometimes may be arising conflict each other regarding these constraints are material and energy availability, safety features, economics, ergonomics, competition in market, technology engineering and manufacturing capabilities.

Current scenario; there are two type of body frame structures that have been used. One is a body frame structure and other is one body structure. The body frame structural is an automobile constructed method. In this method separated body mounted on relatively rigid the chassis or body frame. The chassis frame is consisting of an engine, transmission, power train, suspension and other accessories. This is an original method of manufactured vehicles but now days this method has only been used in light duty trucks and SUVs model vehicles. In addition in this method, the frontal sheet metal and body frame most of them absorb crash energy by plastic deformation in frontal impact collision. One body structure, chassis and frontal sheet body make a single unit construction from stamped sheet and jointed by spot welding. This vehicles construction method also known as a unit frame or frames less body, is also reducing the weight of vehicles and supported whole vehicles rigidity [49]. Under the unit frame body construction it's have been used for passenger car manufacturing.

1.3.3. Need of crashworthiness

The vehicles structure should need energy absorber properties and provide protection an occupant. The bending and torsion properties of vehicles structure must be sufficiently to provide a proper handling and driving of the vehicles. The yield criteria and yield strength that satisfied to range of occupant size, ages and crash speed for both occupants.

The frontal structure as a bumper, crash-box to absorb a kinetic energy from the frontal collision by plastic deformation and prevent the occupant shell from serious crashing intrusion. The occupant shell especially has provided protection from offset collision with the small object such as trees, short vehicles fronts end collision, its present considerable challenge for crashworthiness engineer to get rid of this situation with economic and acceptable solution. Crumple rear structure to prevent rear compartment of the occupants and also fuel tank. Side structure zone and door design should be proper designed to prevent intrusion of side impacts and roof structure also would be in proper designed.

The restraint system plays very important role to vehicle structure design to provide an occupant stability riding and protection in different scenario. The demonstrated chassis designed and location of power train is also provided stability in vehicles structure [50].

1.3.4. Requirements of crashworthiness model and crash test

The following requirements of crashworthiness model are accuracy, speed, robustness, development time, should be fulfill at a minimum condition. The yield criteria and strength of model should be able to accurate prediction of essential features and also model should be allow iteration a reasonable time regardless its size and complication analysis, not exceed many hours to executing it. Robustness is allow to small variation in parameter of the model but should not be exceed yield response and the model of crashworthiness should be completed in reasonably time period, not exceed one or two months.

Last few decades tremendous achievement of crashworthiness analysis in aircraft as well as vehicles. Apart this, the crashworthiness simulation of the vehicles structure components or full scale simulation vehicles, using latest computational mechanics techniques and super computers analysis to find out final crashworthiness still depends upon a laboratory test. This is an essential for vehicles certification. There are many types of test is conducted for crashworthiness of vehicles [51]. There are three main

categorize: components test, sled test, and full impact barrier test. The crash analysis and energy absorption capacity on isolated components is identified by components test. Sled test is conducted for vehicles interior system such as occupant compartment, seat, belt, steering system air bags etc. sled test is generally evolution of restraints system. Full vehicles analysis is done by full impact barrier test.

1.4. Crash-Box Principle

The crash-box, an absorbing device installed between main frame and front bumper of the car is called Crash box. The occupant of vehicles is not only protected by crash-box but also reducing the damage of vehicles, effects of damages and external pedestrian safety. The basic principle of Crash-Box is a system converting the kinetic energy caused by the collision and absorbing the impact energy and shock waves of the accident and is tried to be collapsed with absorbing crash energy prior to the occupant of vehicle and reducing damage of cabin frame and saved life [51]. In this study, the thin- walled square, circle, hexagonal or w-shape structural is a defined as Crash-box fixed between the bumper of vehicle and chassis structural.

1.5. Drop Test (Free Fall Assembly Test)

The test set consists of a falling table with a weight of 150 kg, which is mounted on 4 cylindrical pistons, a magnet holding the table with magnetic force, and an electric motor that provide the up and down movement of the magnet. At the same time there are two speed sensors for measuring the speed of the table and a digital display for reading the data on the sensor.

Last few decades, the number of collisions and fatalities has increased with the increasing number of the vehicles also. Therefore, there is a dire need of security system in the vehicles. These security systems are defined as an active and passive security system. The crash-test is the most important system lies under this heading. After introducing crash-test in the vehicles, crashworthiness and occupant safety system have increased the use of the automobile sector because before 1950's, the term

crashworthiness was used only in aircraft industries. Crashworthiness means the ability of aircraft or vehicles to withstand collision or crash to minimize injuries of the occupants. The frontal structure as a bumper, crash-box to absorb a kinetic energy from the frontal collision by plastic deformation and prevent the occupant shell from serious crashing intrusion. The basic principle of Crash-Box is a system converting the kinetic energy caused by the collision and absorbing the impact energy and shock waves of the accident. These properties of the crash-box depends upon material which would be used in the manufacture of the crash-box and geometric design of the crash-box. Material properties and design of the crash-box will be discussed in the next chapter and will be explained in the detail of the experimental analysis of these crash-box studies.

CHAPTER 2. MATERIALS & EXPERIMENATL SETUP

In previous chapter it has been discussed that the evolution of the safety features in the vehicles, crashworthiness, occupant safety, the crash-box principle and important of the crash-test in the vehicle safety system. Although, the above explanation was about highway administration-rule for vehicles and for decreasing accidents and fatalities due to collision of the vehicles. Further it is elaborated that material's properties which will be used in the crash-box manufacturing. The design and geometry also will be discussed in a detailed way and explanation of the experimental set-up of Crash-box test where it is conducted.

2.1. Materials Properties

To intend to improve safety features in the vehicles and reducing the damage effects due to frontal impact collision and accidents. The design of samples should to be capable of absorbing the maximum energy to plastic limits deformation and the same time that is resistant to collision. In this type of working selection of materials is very important. The many types of materials are used in the manufacturing of the crash-box such as steel, aluminum, GFRP (Glass Fiber Reinforced Plastics),syntactic foam material & composite materials [52]. In the materials of the aluminum crash-boxes, in the hollow section of the boxes are modeled by filling empty section with some types of syntactic materials such as micro glass bubbles, epoxy etc. it is considered that using the syntactic foam materials which show high performance under sudden impacts and dynamic weight [53]. Composite materials have good kinetic energy absorbing properties and resistance against impact and arising shock wave at the time of the collision. Nevertheless, it's not used commonly and economical vehicles because it's so expensive and analysis of composite materials is so complex and difficult. So most commonly used steel and Aluminum in the crash-box Also, the number of designed with different geometries are considerable in this research analysis. The designer need

to be consider of these material properties such as strength, toughness, formability, durability, weld ability etc. for good structures.

In the present work, steel alloy used in the manufacturing of Crash-Box. The main advantages of using steel in the vehicle components are decreasing the weight of vehicles and make an economical vehicle. St37 steel is a low carbon steel with the 0.20 % of carbon other chemicals composition are Silicon, 0.15-0.25%, manganese 0.35 - 0.75%, phosphorus, max, 0.050%, Sulfur, max, 0.050%, Nitrogen, max, 0.011%. St37 steel having more important properties to suitable for this work [54] (good durability, formability, good tensile and yield strength and also great corrosion resistance properties). The stress and strain diagram as shown on Figure 2.1. of the steel and also mechanical properties as shown in the table 2.1.
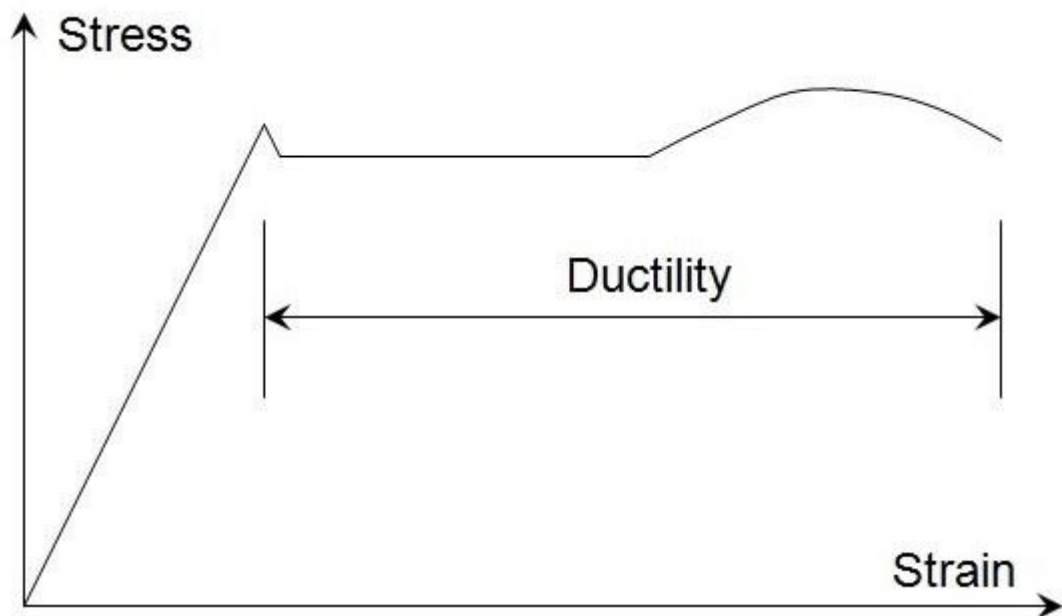
Figure 2.1. Stress and strain graph

Table 2.1. Mechanical Properties of Steel St37

Steel Grade	Yield Stress min, [MPa]	Tensile Strength [MPa]	Elongation , min, δ, %	Density kg/m^3
St37	235	360-460	25	7860

2.2. Geometry Section and Origami Pattern

Geometry selection of crash boxes was discussed in this section, we tried some kind of open loop profile crash boxes and would be compared and validated with previous closed loop crash boxes used in studies. Besides the thickness of the crash box sheet was also decided.

2.2.1. Selection details of origami

According to browsing the internet, we got plenty of closed loop crash-boxes with various pattern. But we tried that some kind of open loop crash-box which could be studied. Lots of design and pattern came into mind, but it is important that what so ever comes into mind, need to be assured that, whether ability to manufacture it is possible for us or not. In various academic literatures and different school of thoughts, some geometrical shapes have been drawn into Auto cad and it is confirmed by manufacturer that the one, who possess such abilities and skills to either manufacture it or not. Two geometrical profile (1st & 2nd mentioned in the Figure 2.2.) of the crash-box have been confirmed by the manufacturer. So, it has been decided that 1st W-shaped profile is economically feasible and titled as W01.
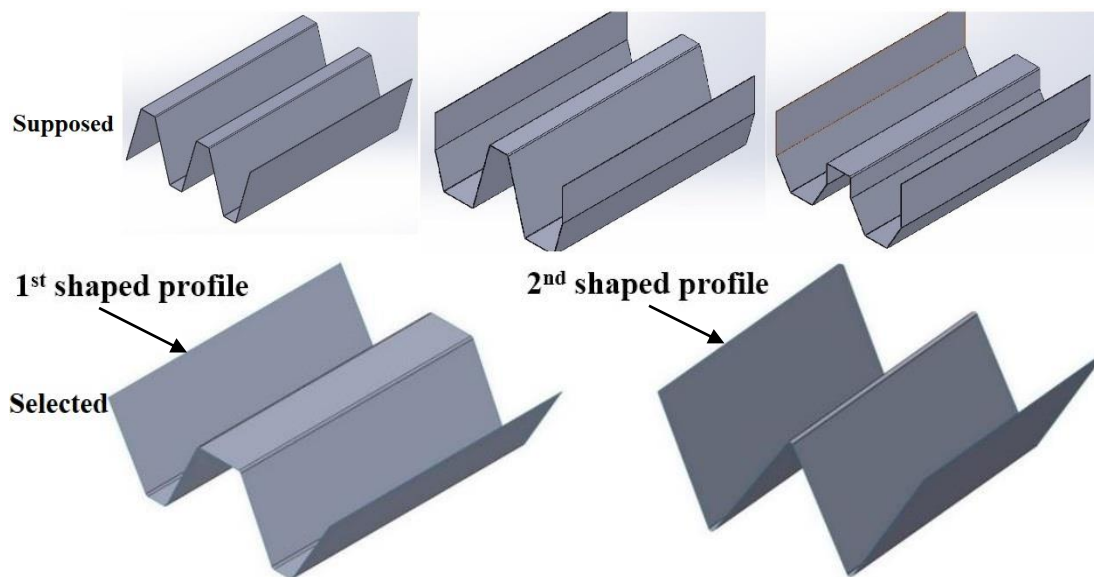
Figure 2.2. Supposed and selected pattern of the crash-boxes

1st shaped profile has number bends like zigzag profile because it gives good buckling strength and energy absorbing properties to this type of profile. Thus the studied selected 1st shaped profile with more bends than 2nd profiles.

2.2.2. Selection of the thickness of the origami

Selection of the geometry of origami has been completed. Further, there has been tried that which thickness would be appropriated for crash-box whose absorbing maximum energy which arise from frontal impact collision of the vehicles. Firstly, different sheet thicknesses might have been investigated and it has been started from the steel W01-shaped profile made of 2 mm thick St37 material which can be easily obtained economically. It is seen that 2mm thick sample is too rigid and the test speed does not affect the desired damping effect. Otherwise, the sample will transmit the energy to the vehicle carrier elements and cause damage to these points and also see the result in the section (4.1.1). Next, 1.5mm of the crash-box thickness will be investigated. After investigating 1.5mm thickness sheet, it has been found almost same result in 2mm thickness sheet and the test speed does not affect the desired damping effect. Although could see results in the section (4.1.2.). Now, it has been understood after these two analyzed sheet thickness that sheet of thickness would be less than 1.5mm which might be a good energy absorbing properties. So, many different thicknesses have been further analyzed in this study such as 1.2mm, 1.0mm & 0.8mm sheet thickness.

W01 shaped profile has been selected for study and also would be compared with another that have different number of bends shaped profile (2nd shaped profile). However, in this profile have less bends than W01 shaped profile and also given to name this profile is W02 shaped profile.

After selection of the geometries and thickness of the sheet of crash-boxes, the next step would be validation of these shaped profiles with previous studied and researched work [55] Therefore, according to work based on the different geometry profile of the crash-boxes, it has been considered three more shaped profile of the crash-boxes such

as the Circle (C01), Hexagonal (H01), & Square (S01). So, the cad model of different type of the crash-boxes has been shown in the Figure 2.3. & 2.4. which would be used in this study.
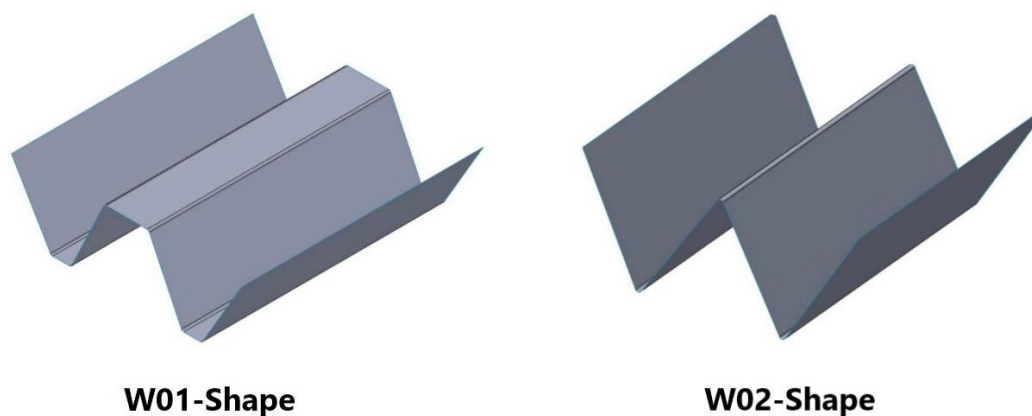
W01-Shape   **W02-Shape**

Figure 2.3. Figure 2.2. Cad modelling of W01 & W02 shape profile crash-boxes

Hexagonal (H01)   **Circle (C01)**   **Square (S01)**
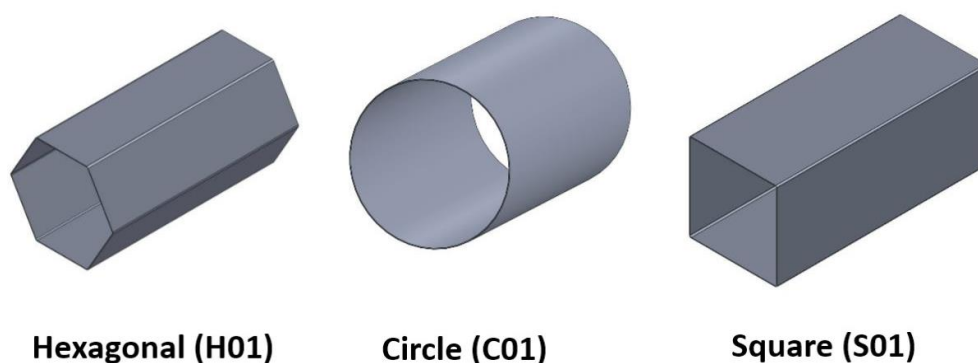
Figure 2.4. Cad modelling of H01, S01 & C01 shaped profile crash-boxes.

2.3. Numerical Analysis

In this section, theoretical speed and method of calculation of absorbed energy are explained in a details. In the drop test setup is able hold 150 kg and drop it from 2.88m height with maximum speed of 25 km/h because of sample height is 300mm, it can reach a crash box max. Speed of 24.604 km/h. Conservation of energy- energy can change from the kinetic energy to potential energy and vice versa. The total energy of the system at the initial time will be same the sum of the kinetic energy($0.5mv^2$) and

potential energy (mgh) at the any other time. Therefore, it has been calculated drop plate velocity with the help of conversation of energy formula.

By conservation of energy:

Before energy = After energy

$$\frac{1}{2}mv^2 + mgh = \frac{1}{2}mv^2 + mgh$$

$$0 + mgh = \frac{1}{2}mv^2 + 0$$

$$mgh = \frac{1}{2}mv^2 \tag{2.1}$$

(a) Theoretical speed of the drop plate

From equation 2.1

Potential energy of the plate = kinetic energy of the plate

$$mgh = \frac{1}{2}mv^2$$

$$m_{sample} \times g \times (h_{stroke} - h_{profil}) = \frac{1}{2} \times m_{sample} \times V^2_{theoretical} \tag{2.2}$$

$$m_{sample} \times g \times (h_{stroke} - h_{profil}) = \frac{1}{2} \times m_{sample} \times V^2_{theoretical}$$

$$g \times (h_{stroke} - h_{profil}) = \frac{1}{2} \times V^2_{theoretical}$$

$$V^2_{theoretical} = g \times (h_{stroke} - h_{profil}) \times 2$$

$$V_{theoretical} = \sqrt{g \times (h_{stroke} - h_{profil}) \times 2} \tag{2.3}$$

$$V_{theoretical} = \sqrt{9.81 \times (2.88 - 0.3) \times 2}$$

$$V_{theoretical} = 7.11 \, ^m/_s \tag{2.4}$$

From the speedometer of the drop test setup

$$V_{experimental} = 6.815 \; ^m/_s \tag{2.5}$$

After calculation of the theoretical velocity of the drop plate set setup is 7.11 m/s (From Eq. 2.4) and has been compared with the actual velocity of the drop plate that find out speedometer which connected in the drop test set-up. is almost same 6.815 m/s (From Eq. 2.5).

(b) Method of calculation of absorbed energy- Energy is defined as the ability to do work. During an impact, an object's energy is converted into work. The energy of a moving object is called kinetic energy and the energy of the object at its point of impact if know the height from which it was dropped. This type of energy is known as gravitational potential energy. So, absorbed energy after impact collision defines the kinetic energy is subtracted from potential energy.

Absorbed Energy (E_{ab}) = Kinetic Energy (KE_{mapcat}) − Potential Energy(PE_{last})   (2.6)

From the Equation 2.6

$$E_{ab} \quad = KE_{impact} - PE_{last} \tag{2.7}$$

From the equation 2.5

$$V_{experimental} \quad = 6.815 m/s$$

According to the formula of the kinetic and potential energy

$$KE_{impact} \quad = \frac{1}{2} \times m_p \times V_{experimental}{}^2 \tag{2.8}$$

$$PE_{last} = m_p \times g \times h_{average} \qquad (2.9)$$

$$h_{average} = \frac{h_{right} + h_{left}}{2} \qquad (2.10)$$

To obtain the necessary parameters to calculate the amount of energy that the samples have absorbed and transmitted without damping, a rough calculation to be made in this way has been applied. The values found by this method will not coincide with the actual values, but it was found to be reasonable to use them in terms of making ideas.

The numerical analysis of the velocity and energies have been discussing in the above section. These theoretical values would be compared with experimental analysis, which would have been done in the subsequent headings. The experimental analysis of the crash-boxes have been performed by the drop plate test (Free fall assembly set-up).

2.4. Experimental Analysis

The crash tests of the produced samples could not be performed as real vehicle crash tests due to laboratory conditions and financial means. Instead, tests were carried out by the drop tester, which was available at the university laboratory facilities. The data obtained from the existing test setup were analyzed by experimental approach method.

In this experimental analysis, the number of samples of crash-box with many variants such as shape, length size, thickness. So for experimental purpose in a proper manner and in a systematically way, a code has been made for a crash-box "unique code" number so that the samples can be identified in an easy way. The unique code numbering system is explained below for the collision and compression tests. First code box is mentioned in which the type of profile (W01, W02, C01, H01 & S01), where second box is defined as crash box thickness (2mm, 1.5mm, 1.2mm, 1.0mm & 0.8mm) and third is a crash-box length (S01-300mm, S02-250mm, & S03- 200mm). Last code is mentioned that number of sample will be tested in this analysis (T01, T02 etc.). The crash-box are many variants in this analysis on the behalf of shape, length

and thickness. For these details see Table 3.1 with sample code of the crash-box and number of samples which has been used for the drop test.
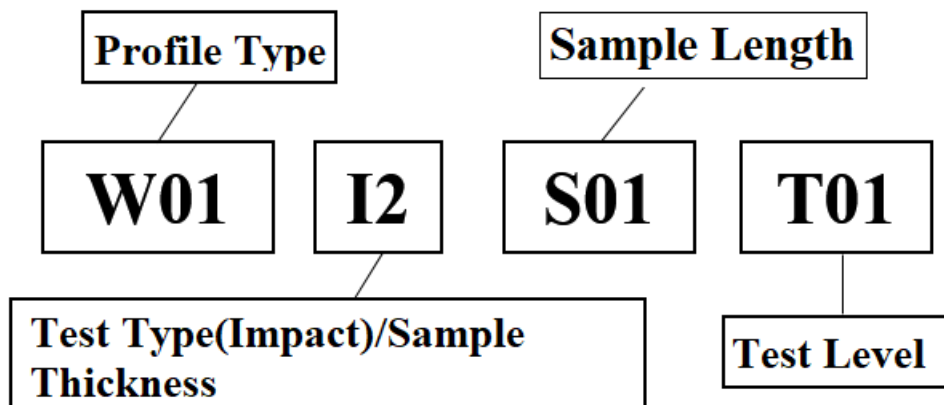
Figure 2.5. Nomenclature of the crash-box coding system

Table 2.2. Details of the crash-boxes shape & size

Length (mm)	Profile Shape	Thickness (mm)	Sample code	No of samples for Experiment
300	W01	2	W01-I2.0-S01-T01	2
		1.5	W01-I1.5-S01-T01	2
		1.2	W01-I1.2-S01-T01	9
		1.0	W01-I1.0-S01-T01	18
		0.8	W01-I0.8-S01-T01	7
	W02	1.5	W01-I1.5-S01-T01	5
		1.2	W01-I1.2-S01-T01	5
		1.0	W01-I1.0-S01-T01	9
		0.8	W01-I0.8-S01-T01	5
	C01	1.0	C01-I1.0-S01-T01	8
	H01	1.0	H01-I1.0-S01-T01	8
	S01	1.0	S01-I1.0-S01-T01	7
250	W01	1.0	W01-I1.0-S02-T01	10
	W02		W02-I1.0-S02-T01	8
	C01		C01-I1.0-S02-T01	4
	H01		H01-I1.0-S02-T01	4
	S01		S01-I1.0-S02-T01	4
200	W01	1.0	W01-I1.0-S03-T01	10
	W02		W02-I1.0-S03-T01	9
	C01		C01-I1.0-S03-T01	4
	H01		H01-I1.0-S03-T01	3
	S01		S01-I1.0-S03-T01	4

2.4.1. Crash-box test

The manufactured specimens could not be carried out in the form of actual vehicle crash tests due to collision tests, laboratory conditions and material availability. Instead, tests were carried out using the drop test method, which is available in university laboratory facilities. The data obtained from the current test setup were analyzed and evaluated by the experimental approach method. In this drop test setup is able hold 150 kg and drop it from 2.88m height with maximum speed of 25 km/h because of sample height is 300mm, it can reach a crash box max. speed of 24.604 km/h.

The magnetic holder is placed in the center of the upper plate, the switched of the electrical panel is on and the magnetic holder is expected to hold the upper plate. The table is then lifted up with the help of the electric winch so that the sample can be placed on the bottom plate. Here, the top of the table due to a power failure of the magnetic holder to lose function and fall down against the table is not upward too high.

Crash-Box samples are prepared before testing. The acceleration sensor is mounted on the sample using the sensor wax. The prepared sample is placed on the 80 x 80 cm test plate. One of the two speed sensors, which will measure the speed of the top table during the profile collision, is aligned to the top of the profile, and the other is positioned at a distance of 45 cm with the first sensor. By moving the table with the help of a crane, it is checked whether the sensors determine the speed or not. Three cameras are placed at designated points to record the experiment at different angles. The upper table is then raised to a maximum stroke distance of 2.88 m. Video recordings are started and the sample number and test number are specified. The switched is switch off and the free holder makes a drop on the table profile by releasing the magnetic holder from the tray. The switch is then opened and the magnetic holder is lowered to contact the table. The table is lifted up and the profile is taken from the test setup. Finally, the speed is read from the speedometer by reading the speed of the plate during contact with the profile. One sample experiment have been completed, the other sample test will proceed in same manner.
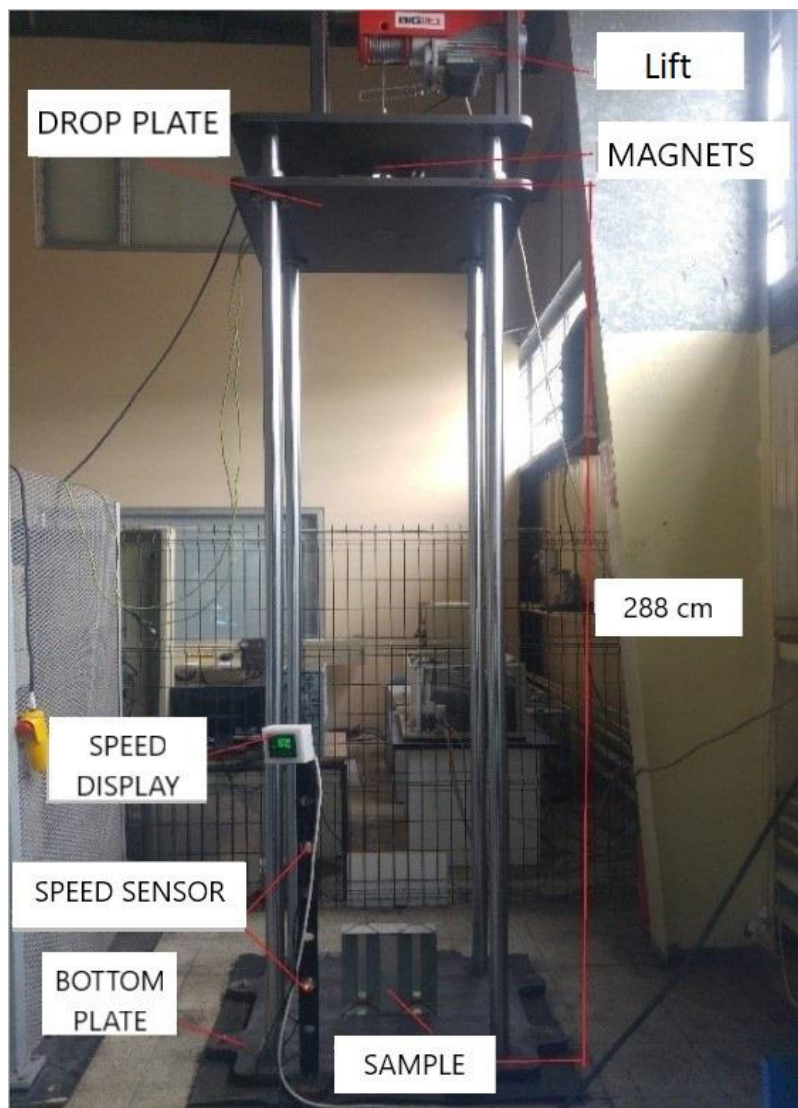
Figure 2.6. The set-up of the Drop test in our laboratory

Material properties have been decided as steel St37 because steel also economical as well as good mechanical properties. The differential geometry of the crash-boxes which have been mentioned in the above section. After all, the different shaped profiles and distinct sheet thickness of the crash-boxes have been analyzed experimentally in the laboratory. These experimental analysis results also compared and validated with the finite element analysis of the samples. Therefore, next chapter would be giving the details about the finite element analysis of the crash-boxes. FEA method, cad modeling of the crash-boxes in Ansys & LS-Dyna, and also analysis procedure are included in chapter three.

CHAPTER 3. FINITE ELEMENT ANALYSIS (FEA)

In this work, the analysis of the crash-boxes will have been done experimentally as well as finite element analysis. The experimental analysis has been elaborated in the last chapter. Subsequent chapter, there would be a discussion between the FEA and the experimental approximation procedures.

Finite element analysis procedure is the most common used one in engineering analysis and in this current scenario also. This is a numerical method of solving engineering and mathematical problems. Engineers use this method to analyze and optimize the components for developing better products. To identify any physical properties or phenomena such as statics or dynamics; structures, fluid mechanics, heat transfer as well as comprehensively understand of mathematics used in finite element analysis (FEA). Partial differential equations described most of these processes (PDFs). From last few decades, engineers and researchers have been trying to develop a technique for a computer to solve these PDEs numerical analysis. One of the best among PDFs is "Finite Element Analysis". In which no need of very complicated structures (like stresses (ϵ), strains (ϵ), etc.) to estimate a certain behavior of the analyze component under a given condition load. Therefore, partial differential equations are complicated equations to need a relevant quantities structures to the investigated component under a given load. To get an approximate solution of the problem by FEA and is a numerical approach to find a real result of these PDEs.

Basically, FEA is a numerical method used for the prediction of material part, stress-strain behavior or assembly behaves under given load condition. Some modern software and research works help to find out a stress behavior of the material, areas of tension, weak spots, load condition etc. in their designs. The simulation results are based on the FEM are usually explained by a color scale that shows the pressure or force distribution on the part. The numerical method is being used to predict the material part stress strain behavior or assemble the behaviors under given load

condition. To find out the material areas of tension and weak spots, some soft wares have been developed to help the researcher to find out the stress behavior in the designs [56] and the line diagram of the manufacturing of the advance engineering system also shown in the Figure 3.1.
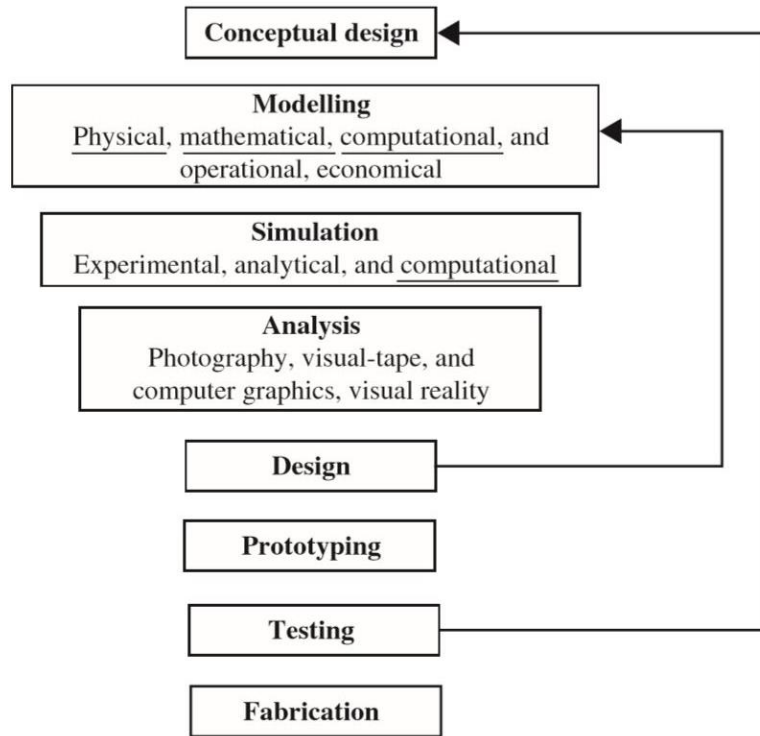
Figure 3.1. Processes leading to manufacturing of advance engineering system

The major step in using FEA methods are given below:

a) Discretization of real structure,

b) Identify unknown primary quantity,

c) Defined the interpolation function,

d) Derivation of element equation,

e) Combination of the element matrix to make a global matrix for the entire domain,

f) Drive the stiffness equation,

g) Solve for primary and secondary unknown,

h) Solution of equation, display and result interpretation.

These are different approaches to use in finite element analysis which one can formulate the properties of the elements in the domains such as direct approach, variational approach, energy approach and weighted residual approach [57].

Introduction of matrix notation

The number of method and tools are used solving the finite element analysis, matrix method tool one of them. The purpose of this tool is simplifying and solving the formulation of the stiffness matrix equations, long hand solution of complex problems. The main important purpose is using in programming method for high speed digital computers. Matrix notation method represents as a simple way to use the notation for solving and writing the number set of an algebraic equation. As an example of matrices, number of forces components acting on the various point of the elements (nodes) of any linear or nonlinear material structure and the corresponding set of displacements elements. Force components $\{F_{1x}, F_{1y}, F_{1z}, F_{2x}, F_{2y}, F_{2z}\ldots\ldots\ldots\ldots F_{nx}, F_{ny}, F_{nz}\}$, Displacements components $\{u_1, v_1, w_1, u_2, v_2, w_2, \ldots\ldots\ldots u_n, v_n, w_n\}$ these are components can expressed in the matrices.

$$\{F\} = \begin{Bmatrix} F_{1x} \\ F_{1y} \\ F_{1z} \\ F_{2x} \\ F_{2y} \\ F_{2z} \\ \vdots \\ \vdots \\ \vdots \\ F_{ny} \\ F_{ny} \\ F_{nz} \end{Bmatrix} \qquad \{d\} = \begin{Bmatrix} u_1 \\ v_1 \\ w_1 \\ u_2 \\ v_2 \\ w_2 \\ \vdots \\ \vdots \\ \vdots \\ \vdots \\ u_n \\ v_n \\ w_n \end{Bmatrix} \tag{3.1}$$

The subscripts of the F represented as node and direction of the forces such as F_{1x} identify the force applied at the node 1 and direction of the force is x. At a node 1, u, v, & w represent the displacement components in the x, y & z direction respectively. The matrices mentioned above equation is called n x 1 size column matrix. {F} or {d} is simplest form of the set of force or displacement valves in the column matrices.

The rectangular matrices will represent braces notation [ ] in the more general case. For instance, element stiffness matrices [k] and global structure stiffness matrices.

$$[k] = \begin{bmatrix} k_{11} & k_{12} & \cdots & k_{1n} \\ k_{21} & k_{22} & \cdots & k_{2n} \\ \vdots & \vdots & \vdots & \vdots \\ \vdots & \vdots & \vdots & \vdots \\ k_{n1} & k_{n2} & \cdots & k_{nn} \end{bmatrix} \tag{3.2}$$

$$[K] = \begin{bmatrix} K_{11} & K_{12} & \cdots & K_{1n} \\ K_{21} & K_{22} & \cdots & K_{2n} \\ \vdots & \vdots & \vdots & \vdots \\ \vdots & \vdots & \vdots & \vdots \\ K_{n1} & K_{n2} & \cdots & K_{nn} \end{bmatrix} \tag{3.3}$$

Where, in the structure theory, k_{ij} & K_{ij} are always referred to as a stiffness influence coefficient. According to (Eq. 3.1 & 3.2), find out global nodal force {F} and global nodal displacement {d} are related use of the global stiffness matrix [K]. To clear understating of this elements matrix k_{ij} (Eq.3.3), with use of Eq. 3.1 and to write out expand form of Eq. 3.3 as

$$\begin{Bmatrix} F_{1x} \\ F_{1y} \\ \vdots \\ \vdots \\ \vdots \\ F_{nz} \end{Bmatrix} = \begin{bmatrix} K_{11} & K_{12} & \cdots & K_{1n} \\ K_{21} & K_{22} & \cdots & K_{2n} \\ \vdots & \vdots & \vdots & \vdots \\ \vdots & \vdots & \vdots & \vdots \\ K_{n1} & K_{n2} & \cdots & K_{nn} \end{bmatrix} \begin{Bmatrix} u_1 \\ v_1 \\ \vdots \\ \vdots \\ \vdots \\ w_n \end{Bmatrix} \tag{3.4}$$

From Eq.3.4, to suppose an element structure to be forced into displaced configuration defined by $u_1 = 1, v_1 = w_1 = \cdots w_n = 0$

$$F_{1x} = K_{11} \quad K_{1y} = K_{21}, \ldots \ldots, F_{nz} = K_{n1} \tag{3.5}$$

Equation (3.5) contain all elements in the first column of [K]. These equation are better understating of the meaning of stiffness influence coefficient [58]. The matrix represents the resistance of the element to change when subjected to external

influences. Matrix notation method represents for solving and writing the number set of an algebraic equation. In the finite element method which method must be used is called matrix method. The matrix methods and related finite element method were not acceptable only for solving complex problems. Although the finite element method was being used to describe complex structures, the resulting large number of algebraic equations related with the finite element method of structural analysis made the method extremely difficult and impractical to use. However, with the advancement of the computer, the number of equation solve within in minute become possible these method. The description of the finite element analysis equation see in the Figure 3.2.

$$\{F\} = [K]\,\{u\}$$

Array of applied forces   Matrix of stiffness   Array of displacement

(one for each DoF)   (DoF x DoF)   (one for each DoF)
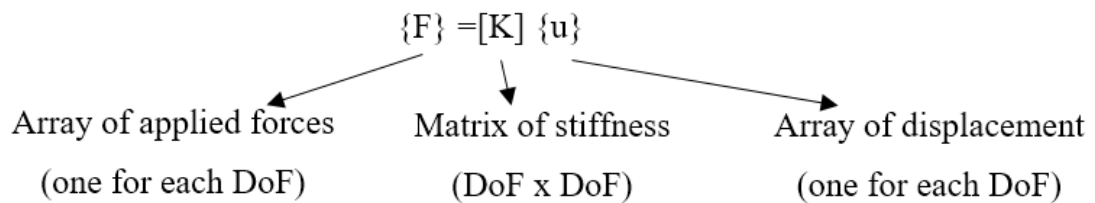
Figure 3.2. Description of the finite element analysis equation.

[K]= (geometries, material properties.......element)

{u}= Displacement

{F}= Load

This is can be solved by using matrix method

$$\{F\} = [K]\,\{u\} \tag{3.6}$$

Also, can be solved by using matrix inversion method

$$\{u\} = [K]^{-1}\,\{F\} \tag{3.7}$$

These equations show that how to do "finite element analysis" for many elements.

-Nonlinear Finite Element Analysis- Nonlinear analysis does not follow the linear relation of displacements and force curve (polynomial). These nonlinearity categorized in a two major parts, Geometric nonlinearity, wherein significant changes in geometry are observed due to large deformations, large strain, stress stiffening,

softening, material nonlinearity means changes in the relation of the stress-strain graph elasticity to plasticity section (some material can be highly non-linear like rubber, but elastic) even though for plastic material, stress-strain graph started with a linear then become non- linear post the proportional limit. Nonlinear material behavior are categorized in Ansys Software, Plasticity is defined as a permanent and time-independent deformation, creep is also permanent but time-dependent deformation, nonlinear elastic, viscoelastic and hyper elasticity like a rubber materials.

Some engineering problem could be solved by only non-linear finite element analysis such as collapsing or buckling of structures due to sudden over load applied on the structures. High-temperature loads in nuclear reactor components, cables transmission tower. These type of structure need to be nonlinear analysis phenomenon for service and load calculation.

In recent year, the need of nonlinear analysis has been increased day by day. Many branches of engineering has depended upon the nonlinear finite element analysis (see in the Figure 3.3.) such as automobile industries, earthquake engineering, nuclear engineering, defense industries, aeronautical engineering, offshore engineering etc. [59].
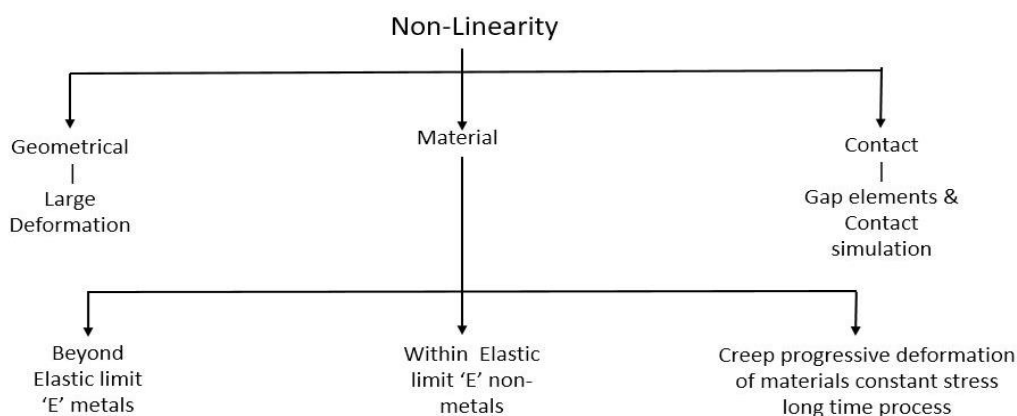
Figure 3.3. Description of the non-linear finite element analysis

The second and main approach was to use analytical models and simulation. For this section studied different types software have been used. Ansys Software have been used for created models and simulation have been done with LS-Dyna Software.

The finite element analysis is a method to solve the problem of engineering structure and physical phenomenon. There are number of software to use for finite element analysis, such as ANSYS, ABAQUS, NASTRAN, LS-DYNA, CALCULIX etc. In this study, simulation has been done by LS-DYNA software and CAD modeling have completed by PTC-Creo Software.

3.1. CAD Modeling

The designers and engineers use a computer aided design software or CAD software to create a two dimensional (2-D) and three dimensional (3-D) designs of the physical components. With the specific dimension, Crash-box 3-D geometries is created in the PTC-CREO computer aided design software, number of geometries such as Square, Circle, Hexagonal, and W-Profiles. In this geometry, the crash-box is base element with shell model geometry (surface model) and drop plate modeling is a solid model. There are all shape profile technical drawing with 3-D geometry pictures see in the Appendix A.2.

3.2. Finite Element Modeling

The finite element method (FEM) is a numerical technique used to perform finite element analysis (FEA) of any given physical phenomenon. Finite element modeling means which model have been created in the CAD software, in this model to give a physical phenomenon condition of this work. After creating a CAD model, CAD model file has been imported in the ANSYS, LS-DYNA software for finite element analysis. This file have a crash-box geometry model with drop plate model. In this software has been given a physical condition in the model such as types of model (shell & solid), meshing, boundary condition, load applied, etc. In this model, drop plate and crash-box are created as solid and shell model respectively shown in the Figure 3.2. and material definition is defined/specified as a Steel St37 and including set of material properties. Steel St37 as linearly elastic material behavior and also elastic-ideal plastic behavior defined in following Table 3.2. & 3.3. Finite element analysis has been

completed step by step such as selection of the boundaries, velocity control and the contacts of the crash-box with drop in the LS-Dyna software.

Table 3.1. Linearly Elastic Material Behavior of St37

Density	7850 kg/m³
Young Modules	E=205000 MPa
Poison Ratio	0.29

Table 3.2. Elastic-Ideal Plastic Behavior St37

Yield stress	235 MPa
Tangent Modules	763 MPa
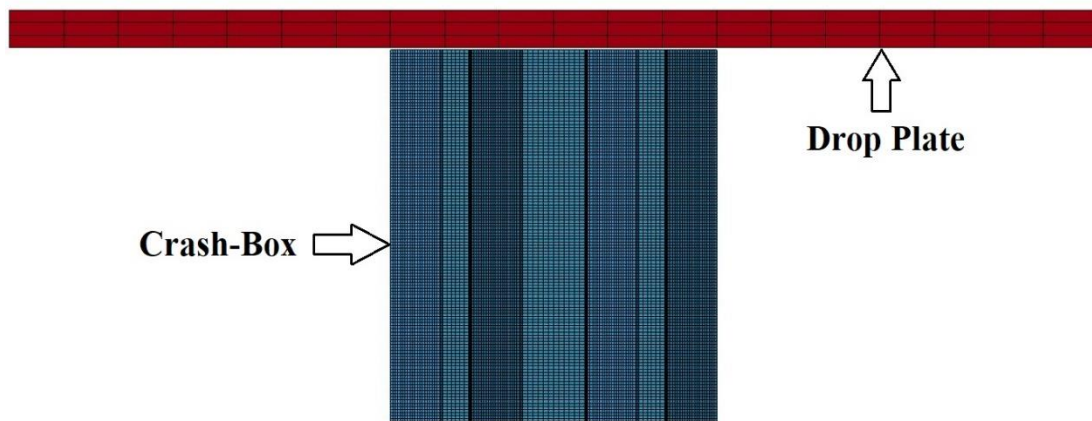
Figure 3.4. FEA model of the Drop plate & Crash-Box

In this work two types of approaches can be used in the FEA model such as solid model and shell model. So first model of crash-box including drop plate is a solid model as well as crash-box FE model. This is a model called solid model. In LS-Dyna software, this solid approach did not work properly means analysis until did not run and get any result of this solid analysis. Therefore, in this work shell model of crash-boxes has been used.

Finite element analysis has two types of approaches which are being used in the analysis such as implicit analysis and explicit analysis.

(a) Implicit Finite Method- This method is used for time independent finite element analysis. The solution result does not depend upon the time factor in the implicit finite

method (such as model analysis, structural analysis, harmonic analysis etc.). Quasi-static problem is also solved on the implicit finite method, in which studies problem is unconditionally stable for large time intervals.

The function of time is not defined the displacement (x=constant) the time derivatives of displacement as a velocities and acceleration. This is considered out at zero and mass and vibration factors can be neglected. The implicit analysis can be based on Newton Raphson Method and Newark's method, etc. The advantage of this technique is that usually solution is obtained in less number of time-steps than the explicit analysis techniques. The advantage of this method is that problem solution is obtained in minimum number of time-steps than explicit finite method.

(b) Explicit Finite method: Explicit method is a useful for crashing simulation and dynamics analysis where the time dependency of the solution is an important factor as well as for highly nonlinear problems with contact definition. The velocity and acceleration as well as the mass and vibration effect need to be considered as a function of time in this technique. Impact and blast problems are usually solved in these techniques and does not need inverting stiffness matrix because inverting matrix use of implicit techniques, it does not require more memory space with computer and solution is only conditionally stable [58].

(c) Element types and definition: The thin walled steel material crash-box has been analyzed in the LS-Dyna/Ansys with nonlinear explicit finite analysis code. The quadrilateral four node thin shell elements known as Belystchko-Lin-Tsay formulation, it's based on Reissner-Mindlen kinematic assumption (5. DOF in local coordinate system yield globally 6. DOF). These Belystchko-Lin-Tsay shell elements selected from the LS-Dyna elementary library. [60]

In this study, crash-box is manufactured by steel alloy as have a Young's module of 205 GPA, Elastic yield stress of 235 MPa, Tangent Modulus of 763MPa and poison ration 0.29. The Figure 2.1. shows a strain stress graph of Steel St37. The main advantages of steel alloy crash-box using in vehicles is economically than aluminum

alloy and reducing the weight of the structure and also cost. Steel material models in LS-DYNA are many type but in this analysis two types of material was selected one is MAT_RIGID_ (020) this is a rigid body material properties such as density, poison ration, young modules are specified. Other is a MAT_PIECEWISE_LINEAR_PLASTICITY_ (TITLE) _ (024) for shell modeling, this material suited to inelastic model with effect of rate changes.

(d) Contact definition -The contact definition between drop plate and the crash-box model in LS-Dyna is AUTOMATIC_NODE_ TO_ SURFACE & AUTOMATIC_SINGLE_ SURFACE. The automatic option detects hitting timing coming from the master part (Drop plate) automatically. In the drop test, the drop plate is specified to be a target material and master part is a crash-box [61].

(e) Meshing Information- The crash box modeling was created in the PTC Creo 3.0. The finite element analysis of the each size and shapes of the crash-box modelling was prepared in the ANSYS- LSDYNA software. For every shapes meshing information see the Appendix A.1.

CHAPTER 4. RESULTS & DISCUSSION

In this chapter, both experimental and finite element analysis results are explained in detail. The experimental result of the drop tests is carried out, and at the time of frontal collision it was investigated that how much of the crash boxes was deformed and energy was absorbed by a 1000 kg vehicle. The Finite element analysis results are prepared by using LS-Dyna software and all crash-boxes FE analysis results.

4.1. W01 Shaped Profile Results

In the experimental analysis, several sheet thicknesses have been analyzed and it has been started from the W-shaped profile those made of 2mm thick steel St37 material, it is easily available in the market and most importantly it is economical.

4.1.1. 2.0mm thickness of the sample

Two samples of 2.0mm thickness of W01 Shape Profile have been used for experiment in the laboratory.

-W01-I2-S01-T01- The pre-collision status of the sample having a thickness of 2mm is given in Figure 4.1. After drop test of this sample, slight buckling was observed on the left surface. In the right column of the profile, it was observed that the folds were observed 69mm above the ground, 79mm on the left column and 75mm above the middle column. It was determined that the length of the specimen which was 304mm decreased to 279mm on average. The distance between the right and left columns at the base and peak points remained the same see in the Figure 4.1.
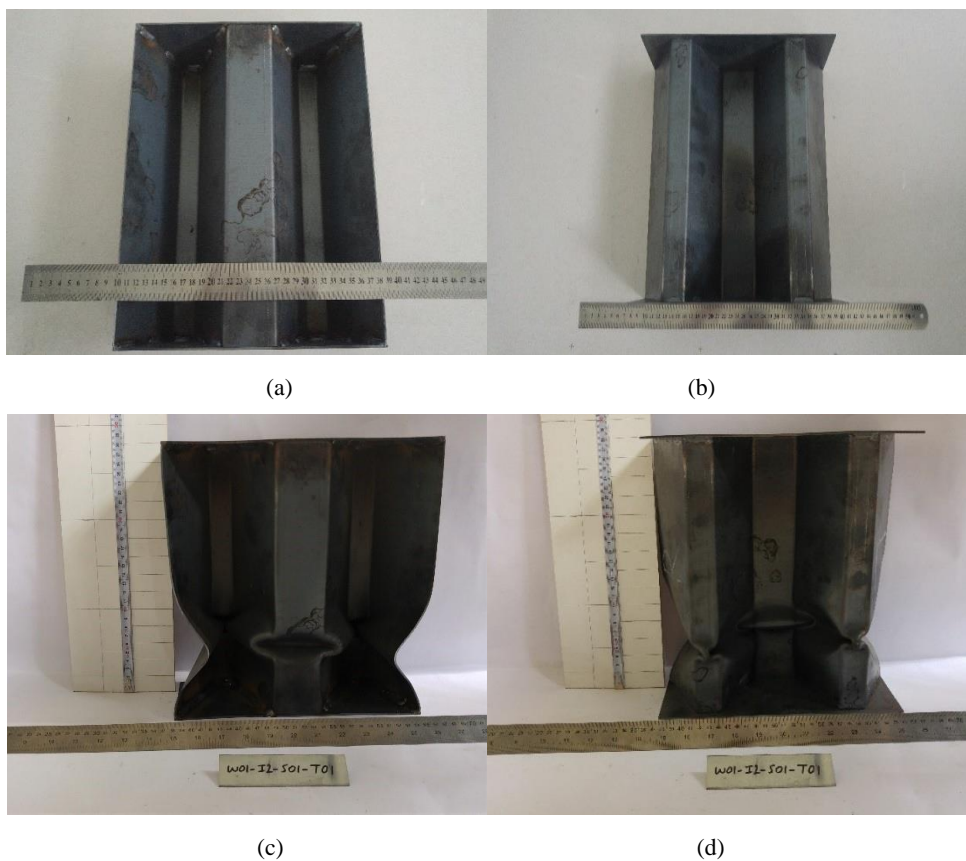
Figure 4.1. W01-I2-S01-T01 sample before deformation (a) front side (b) back side and after deformation (c) Front side (d) back side

When the slow motion videos were examined as shown in Figure 4.2., it was observed that the lowering plate contacted the inclined profile. The first contact was seen on the left side of the upper surface (Figure 4.3.).
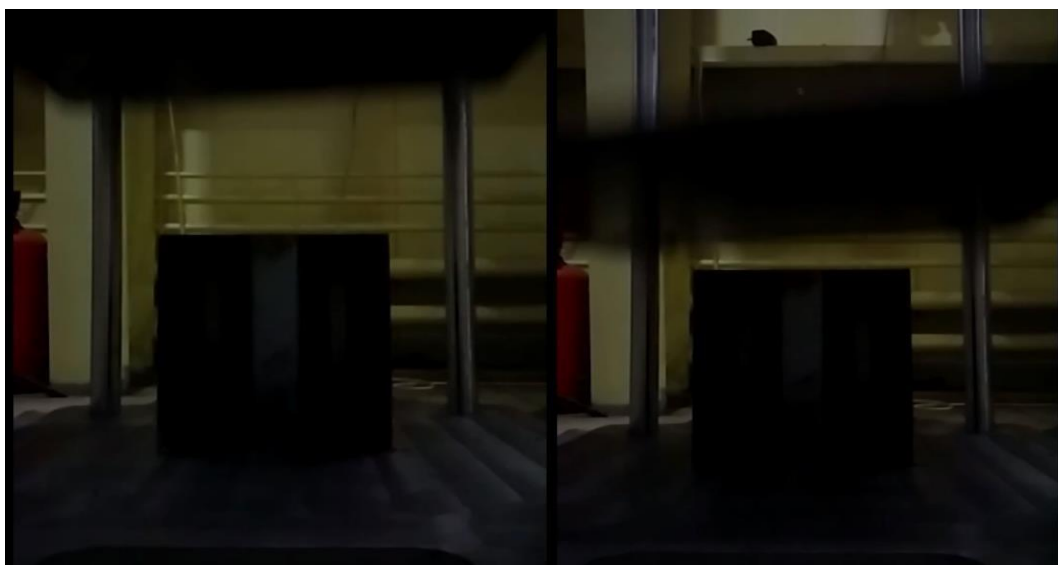
Figure 4.2. W01-I2-S01-T01 sample slow motion recording photographs when the drop plate hit the crash-box

It was determined that the deformation occurring in the 2mm thickness sample and the ability to dampen the sufficient energy by spreading over time was low and accordingly it was determined at this point that it is appropriate to gradually thin the sheet thickness. The amount of energy absorbed by the sample is calculated below:

$$KE_{Impcat} = \frac{1}{2} \times 150 \times (6.815)^2 = 3.48 \text{ KJ}$$

$$PE_{Last} = 150 \times 9.81 \times \frac{279}{1000} = 0.410 \text{ KJ}$$

$$E_{absorb} = 3.48 - 410 = 3.069 \text{ KJ}$$

The experimental speed data measured due to improper connection of the sensors used for the measurement of the experimental speed was greater than the theoretical velocity value. As a result of the calculation, the resulting energy value is not accurate. For the second sample result see Appendix A3.

It is seen that 2mm thick sample is too rigid and the test speed does not affect the desired damping effect. Otherwise, the sample will transmit the energy to the vehicle carrier elements and cause damage to these points.

4.1.2. 1.5mm thickness of the sample

Considering the thickness of the sheet, which is easily available under 2 mm, is 1.5mm sample which is prepared with the same size for the next test. There are two sample of this thickness for drop test.

-W01-I1.5-S01-T01- The pre- and post-collision of 1.5 mm thick specimen is shown in Figure 3.4. After the drop test, the left and right surfaces were wrenched. It was observed that the sprain on the left surface was more than the right surface. After the initial folding reached the base, the second folding was observed to be 33mm high from the base in the right column and it was observed that the left column had a deformation of 29mm in height. The sprain in the left column was more than the right column. Plastic deformation was observed from the peak of the sample at 14 mm in

the right column, 16 mm in the left column and 15 mm in the middle column. The height of the right column decreased from 300mm to 247mm and the height of left column decreased from 300mm to 243mm. It should be noted that this difference is due to the fact that the lowering plate has a slight inclined as it move downwards (Figure 4.3.). Finally, the distance between the columns was measured at the lower and upper points and the difference was 19mm (see Figure 4.3.).

(a)   (b)

(c)   (d)
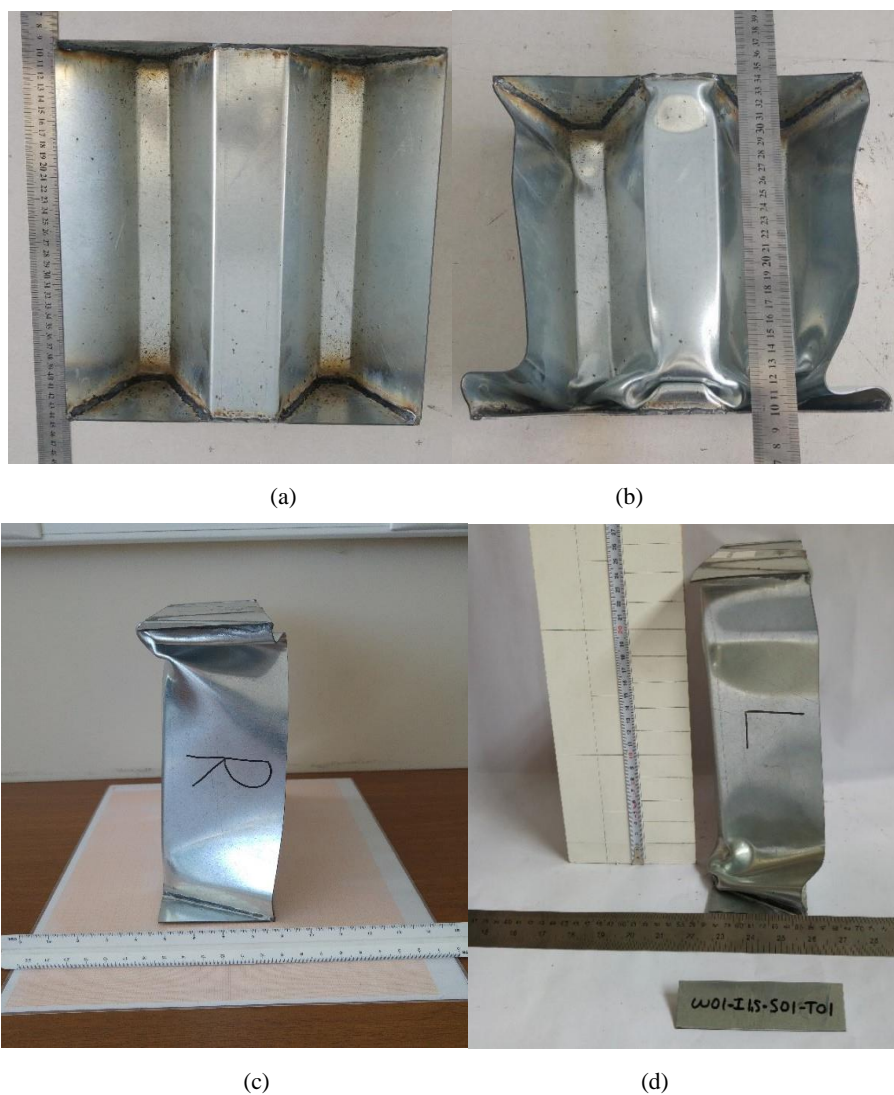
Figure 4.3. W01-I1.5-S01-T01 sample (a) Before Deformation (b) After Deformation (c) Left Side View (d) Right Side View.

When the slow motion videos were examined, it was observed that the lowering plate contacted the inclined profile. The first contact on the left side of the upper surface (Figure 4.4.).

Figure 4.4. W01-I1.5-S01-T01 sample slow motion recording photographs when the drop plate hit the crash-box

After the drop test, it was understood that the amount of deformation with sample having a thickness of 1.5 mm is not sufficient for absorbing energies as per the requirement and deformation is approximately same as that of a 2mm thickness sample. Here are the calculations taking into consideration the change in the height of the sample as a result of deformation.

$$KE_{Impcat} = \frac{1}{2} \times 150 \times (6.815)^2 = 3.48 \text{ KJ}$$

$$PE_{Last} = 150 \times 9.81 \times \frac{247}{1000} = 0.363 \text{ KJ}$$

$$E_{absorb} = 3.48 - 0.363 = 3.12 \text{ KJ}$$

As a result of the calculation, the amount of energy absorbed by the sample was found to be 3.12 KJ. As the connection of the sensors to the test setup is not proper, the measured value is above the theoretical velocity value and it is understood that the energy value found as a result of the calculation is inaccurate due to this speed value if used in the calculation. The more efficient this amount will be, the more efficient it will be. Otherwise, in this case deformed part of sheet will not absorb the sufficient amount of energy, then this excess amount of energy will be undesirably deformed to the vehicle chassis and this extra amount of energy will be transmitted to the occupants. This will be an undesirable situation.

4.1.3. 1.2mm thickness of the sample

There are nine sample of 1.2mm thickness which have been tested in the laboratory. The following description is about first sample and for remaining samples' experimental results see Appendix A3.

-W01-I1.2-S01-T01- After the experiment of sample having a thickness of 1.2mm, it is seen that the upper surface of the sample is very stable where the table was hit. There are signs of folding near the lower side. Almost symmetrical sprain is observed on the left and right surfaces of the sample. Peak force of the plate, signs of buckling on the front of the specimen were determined. When measured from the front side, the sample height was measured as 224mm from the rear. To obtain more accurate information about the 1.2 mm sample, it was appropriate to repeat the experiments. With the speed sensors in the measuring device, the approximate speed of the plate at the time of impact was measured as 6.819 m/s (Figure 4.5.).

<table>
<tr><td>(a)</td><td>(b)</td></tr>
<tr><td>(c)</td><td>(d)</td></tr>
</table>
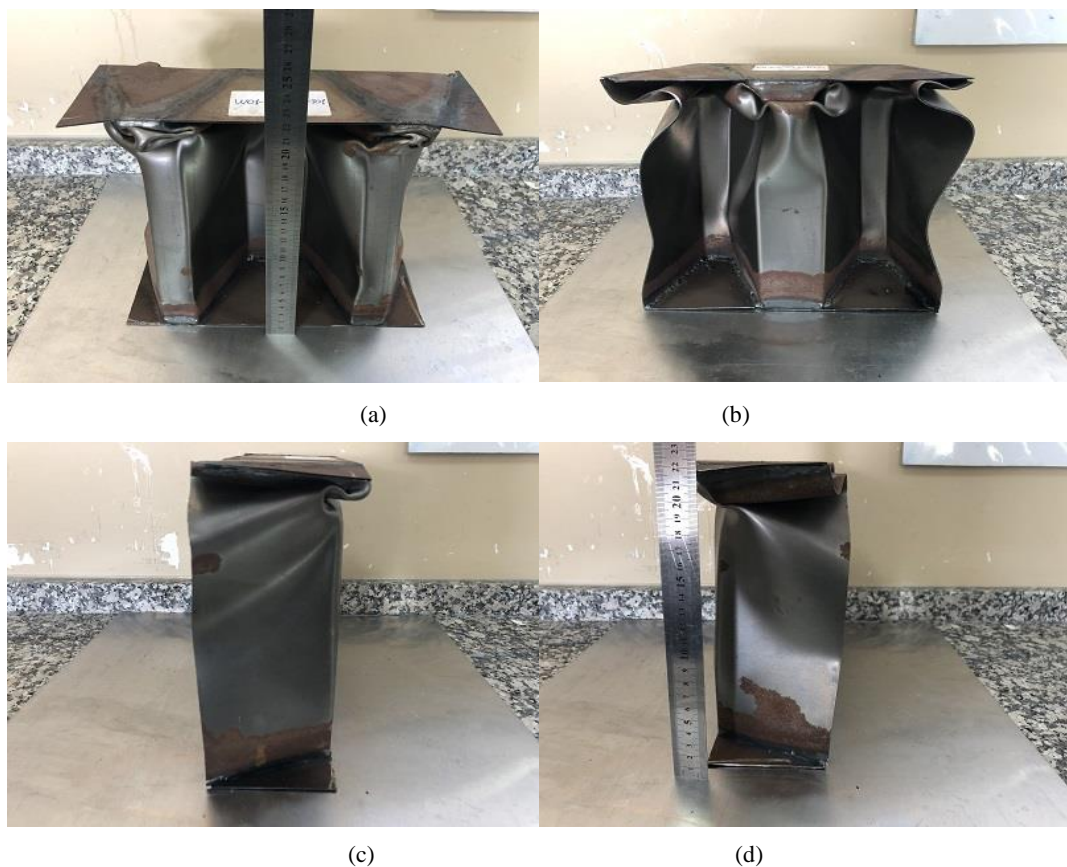
Figure 4.5. W01-I1.2-S01-T01 sample after deformation (a) Back side (b) Front side (c) Left Side (d) Right Side

The amount of energy absorbed by the sample is given below:

$$KE_{impcat} = \frac{1}{2} \times 150 \times (6.819)^2 = 3.48 \text{ KJ}$$

$$PE_{last} = 150 \times 9.81 \times \frac{223}{1000} = 0.328 \text{ KJ}$$

$$E_{absorb} = 3.48 - 0.363 = 3.152 \text{ KJ}$$

As a result of the calculation, the amount of energy absorbed by the sample was found to be 3.152 KJ.

4.1.4. 1.0mm thickness of the sample

Considering those situations, it was decided to use 1mm sheet thickness, which is easily reachable as a sufficient condition, though absorb the maximum amount of energy after 1.5mm thickness. Thus, 1mm thickness sheet have different shape of geometries such as W01, W02. There are a number of samples of W01 profile shape. According to situation and time of experiments have completed on many samples in laboratory. W01 Profile having 18 samples with length 300mm. Remaining 20 samples are of lengths 250mm and 200mm. W01-I1-S01-T01, W01-I1-S02-T01, and W01-I1-S03-T01 are explained here while remaining samples' experimental results can be seen in Appendix A3.

-W01-I1-S01-T01- For the first sample with a thickness of 1mm, the geometric dimensions and the material are the same and only the thickness is reduced from 1.5mm to 1mm.

After the drop test, the left and right surfaces were sprained. It was observed that after the initial folding reached the base, the second folding was observed at the height of 33 mm in the right column and 29 mm in the left column. It is observed that the sprain in the left column is more than the right column. Plastic deformation was seen from the peak of the sample at 14mm in the right column, 16mm in the left column and

15mm in the middle column. The height of the right column decreased from 300mm to 247mm and the height of left column decreased from 300mm to 243mm. The distance between the columns was measured at the lower and upper points and the difference was found as 19 mm. Post-collision photographs of the sample are shown in Figure 4.6.

(a)	(b)
(c)	(d)
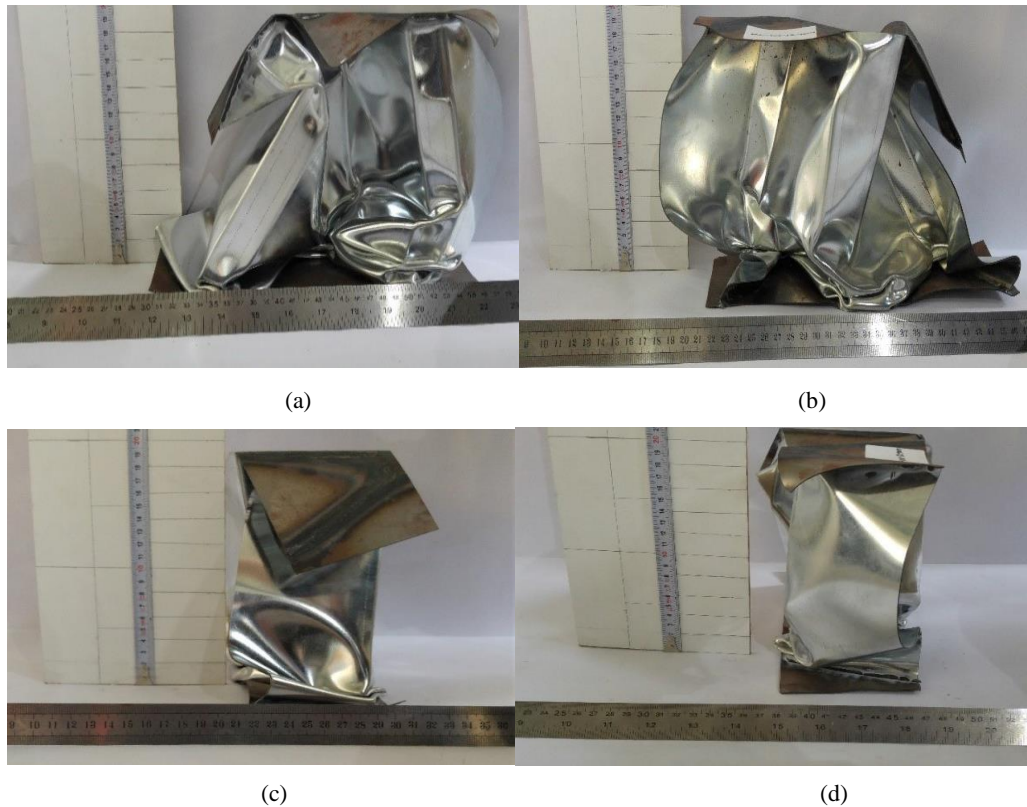
Figure 4.6. W01-I1.0-S01-T01 sample after deformation (a) Front side (b) Back side (c) Left Side (d) Right Side

As a result of the test, excessive deformation was observed in the left column of the sample.

It has been observed that the material is subjected to shear stress and the movement of the upper layer of the sample in the x-axis direction has been observed. The left column has a tendency to fold at three points. Starting from the bottom, the first folding was smooth and as seen in the foreground. The second fold is close to the base; the third fold is outwardly and 56 mm below the top of the sample. In the right column, while the folding was carried out from three points again, the first fold from the bottom to the top was smooth and the effect of the compression was observed. In the second fold,

slip, torsion and compression stresses were realized. The second fold is subjected to torsion on the Y-axis and the right side of the right column is subjected to buckling and folding on the left side of the same column with the effect of sliding and compression stresses. The third fold is on the left side of the right column. The effect of shear and torsional stresses on the middle column was clearly seen, and after the first folding, buckling was observed on the left surface of the column.

Figure 4.7. W01-I1.0-S01-T01 sample slow motion recording photographs when the drop plate hit the crash-box

-W01-I1-S02-T01- As a result of the experiments carried out with the sample with a thickness of 1mm sheet, it was thought that it would be more accurate to change the size as the desired results were approached. Therefore, the results obtained by reducing the size of the specimen from 300mm to 250mm were examined. It was seen that the sample had an ideal plastic deformation after the impact force. Post-collision photographs of the specimen in the Figure 4.8. The middle column of the sample was folded in half from 250mm to 116mm. The height of the right column decreased from 250mm to 100mm, and the height of the left column decreased to 114mm.

Figure 4.8. W01-I1.0-S02-T01 sample after deformation Front & Back side view

-W01-I1-S03-T01- As an efficient results obtained from the W01-I1-S02-T01 test, retesting the sample length to 200mm, it is important to reach the most accurate results and the new test sample was prepared and the reduction test was performed (Figure 4.9.). There are four folds in the sample, which is 66mm on average, and the extremely stable folding in the columns is proof that the impact is best absorber. However, due to excessive deformation, it is seen that it is not successful enough to absorb the impact force. For this reason, it was decided that the sample having the thickness of 1mm sheet and having 250mm length is the ideal size.

Figure 4.9. W01-I1.0-S03-T01 sample after deformation Front & Back side view

Table 4.1. Energies were calculated by W01 shaped profile samples

S.No.	Sample Code	Sample height (mm)	K.E. (KJ)	P.E. (KJ)	A.E. (KJ)
1	W02-I1.0-S01-T01	300	3.458	0.361	3.097
2	W02-I1.0-S02-T01	250	3.506	0.169	3.336
3	W02-I1.0-S03-T01	200	3.506	0.097	3.409

After the first test with 1mm thickness sample, when the image records and the deformed sample are examined, it is seen that this thickness approaches the desired damping effect. To obtain healthier results and for this thickness value. The test was repeated on samples having a thickness of 1mm to better examine the behavior of the sample.

4.1.5. 0.8mm thickness of the sample

In order to see if it will give better results after tests with sheet thickness of 1 mm, tests were carried out with plates of 0.8 mm thickness. Because the samples were subjected to very deformation in the first tests performed with the samples of 0.8 mm thickness,

the tests were not continued and the samples of 0.8mm thickness were selected from the sheet thickness selection. During the tests, no acceleration sensor was used, considering the possibility of excessive deformation of the samples having a thickness of 0.8 mm.

-W01-I08-S01-T01- 0.8mm thickness sample with steel St37 material, No torsional stress is observed in the sample after the experiment. The buckling formed on the right and left surface of the sample is different from each other and it is seen that the buckling on the left surface is more. The reason caused by the slope of the drop plate as a result of contact with the sample. After the experiment, the sample was subjected to excessive deformation due to the tensile stress of 0.8mm thickness, the sample length was reduced from 300mm to 44mm (Figure 4.10.).
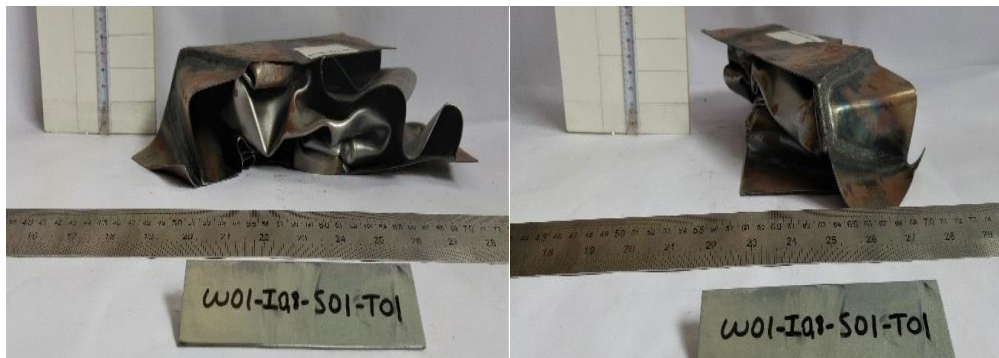
Figure 4.10. W01-I0.8-S01-T01 sample after deformation Front & Back side view

The amount of energy absorbed by the sample during the test is calculated below.

$$KE_{Impcat} = \frac{1}{2} \times 150 \times (6.741)^2 = 3.408KJ$$

$$PE_{Last} = 150 \times 9.81 \times \frac{44}{1000} = 0.065 \text{ KJ}$$

$$E_{absorb} = 3.408 - 0.065 = 3.343KJ$$

As a result of the calculation, the amount of energy absorbed by the sample was found to be 3.343 KJ. As a result of the experiments and investigations, it was decided that the W section profile having 1mm thickness is the optimum profile that we can use for our study. It was observed that the profiles with 2mm and 1.5mm thickness did not

show sufficient damping, whereas the profile with 0.8mm thickness was deformed to absorb all of the energy by excessive deformation. Material thickness and shape optimizations are considered.

-Finite Element Analysis Result- In the previous chapter (Section 3.2) everything has been explained that how to perform the finite element analysis. Here only the FEA results will be discussed, and will be compared with experimental analysis with different shapes crash-boxes under quasi-static or impact condition can collapse in one of these distinct crashing model shapes.
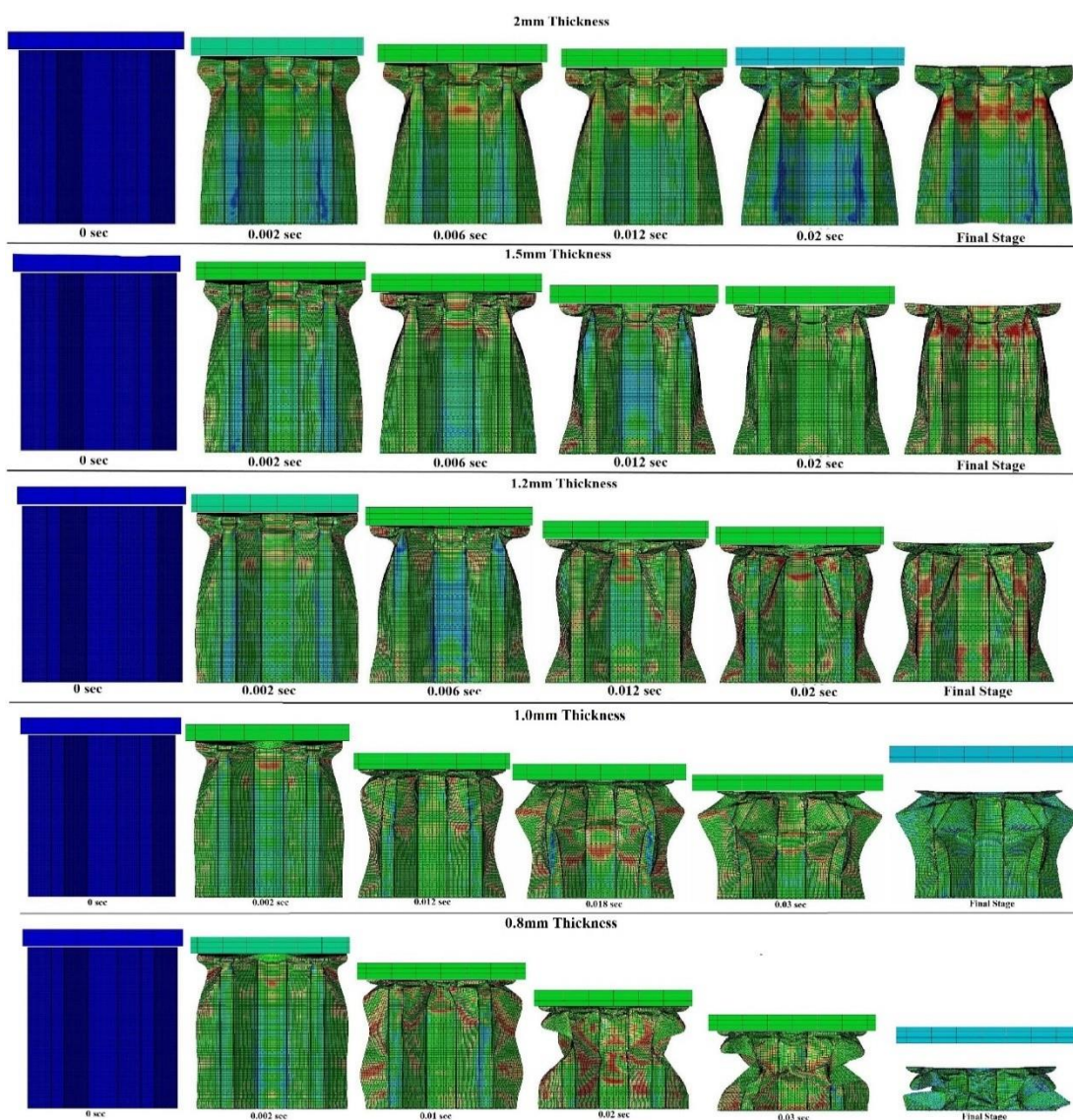
Figure 4.11. Finite Element Deformation Results of W01 Shaped Profile 300mm height of the Crash-box with all thickness

At the result of simulation with the 2mm thickness of sample and investigated, it is observed that buckling formed on both sides of the crash-box is same. This is caused by no inclination in the drop plate when hit the sample like an experimental analysis. It was determined that the length of the specimen which was 300mm decreased to (300-20.6=279.4) mm on average.

At the result of simulation 1.5mm, 1.2mm, 1.0mm, 0.8mm thickness of sample investigated (Figure 4.11.), it is found out deformation (crashing) of the crash-box in the same manner such as a corner of the W-shape profile just folding layer by layer. In 1.5mm sample deformation is just more than 2mm thickness so isn't appropriate for absorbing energy and 1mm is good enough to absorb kinetic energy arise after the frontal collision of the vehicles and will prevent the transfer to occupants. Otherwise, 0.8mm sample have absorbed more energy after crashing, crash-box crumbled layer by layer, in other word say that is just trash that's why with this thickness of crash-box, will not control shock and transfer kinetic energy to the occupants of the vehicles (Figure 4.11.). The comparison of the crash-box deformation FEA and experimental analysis results are given below in the Table 4.2 with percentage error.

Table 4.2. Experimental and FEA result of W01 Shaped profile with % error.

Height (mm)	Thickness (mm)	Mean Def. Exp.	Mean Deformation FEA	Error (%)
300	2.0	279.8	270.56	3.3
300	1.5	244.4	247.52	1.28
300	1.2	226.4	232.5	2.696
300	1.0	188.8	194	2.70
300	0.8	66.6	75.4	9.02
250	1.0	123.8	123.2	2.39
200	1.0	70.0	75.8	8.34

In the Figure 4.12. (Energy vs. Time), we see that 0.8mm thickness sheet of the crash box have long time (till 0.06 sec) of the energy absorbing process and then after graph start to move in the stabilities condition, however, the energy absorbing capacities no longer endure of the crash box condition when see the simulation result of it in this

figure but kinetic energy remain therefore this kinetic energy could be transfer to the occupant of the vehicles. Further 2.0mm, 1.5mm thickness sheet of the crash-box have an opposite properties of the energy absorbing process. So enough energy remains for transfer to occupants of vehicles. 1.2mm & 1.0mm thickness sheet of the crash boxes crash-box has moderate condition. Thus , 1.0mm is good energy absorber than 1.2mm thickness sheet of the crash -box The energy absorbing process in this crash-box starts from 0.002sec to 0.03sec then graph line starts to liner status and according to crash-box condition in this figure almost energy is absorbed by it so there is no energy remained to transfer to the occupants which means no harmful conditions would be arising for the occupant of the vehicle.

Figure 4.12. Energy graph of W01-Shaped Profile all thickness (t) with 300mm height Crash-Box

On the basis of the Figure 4.13. (Displacement vs. Time), we can find that the 1mm thickness W01 shape profile is best for deformation with the time of the frontal collision. 2.0mm & 1.5mm thickness sheets are not appropriate for the best deformation, it deformed just 22mm & 55mm respectively along 300mm length crash-box 1.2mm showed more displacement than both thickness but is not sufficient for preventing the shock and kinetic energy transfer to the occupants of the vehicles. 0.8mm thickness sheet deformed 300mm to 234mm so some of kinetic energy could be remaining to transfer to the occupant. In this figure, although simulation has been compared with experimental analysis for all thickness.

Figure 4.13. FEA & Experimental analysis results graph of W01-Shaped Profile all thickness with 300mm height
of the Crash-Box

4.2. W02 Shaped Profile Results

W02-Shape profile has six variants in thickness 1.5mm, 1.2mm, 1.0mm & 0.8mm with 300mm length of crash-box and '1mm' thickness have also 250mm and 200mm length.

4.2.1. 1.5mm thickness of the sample

There are six samples of 1.5mm thickness of W02 Shape Profile which have been experimented in the laboratory.

-W02-I1.5-S01-T01- After the collision of the drop plate and crash-box, it was observed that the sprain on the left was almost same on the right surface. Initial folding starting from the base of the crash-box. The folding was observed to be 63mm high from the base. Plastic deformation was noticed from the peak of the sample at 30mm in the right and 28mm in the left column (Figure 4.14.).

Figure 4.14. W02-I1.5-S01-T01 sample's front and back view after collision

The amount of energy absorbed by this sample during the test is calculated below.

$$\text{KE}_{\text{Impcat}} = \frac{1}{2} \times 150 \times (6.741)^2 = 3.408\text{KJ}$$

$$\text{PE}_{\text{Last}} = 150 \times 9.81 \times \frac{232}{1000} = 0.341 \text{ KJ}$$

$$\text{E}_{\text{absorb}} = 3.408 - 0.341 = 3.067 KJ$$

As a result of the calculation, the amount of energy absorbed by the sample was found to be 3.067 KJ. The details and experimental results of the rest of the samples of the W02 profile with 1.5mm thickness (see Appendix A3).

4.2.2. 1.2mm thickness of the sample

After the collision, it is seen that the folding started from the middle portion of the sample. The sign of the bucking are much more in the left portion than right portion but bottom plate turned upward direction at the right portion corner. The maximum plastic deformation was observed in the bottom portion of the sample. After calculated the deformation of the sample; 300mm length decreased to 163mm from the top.
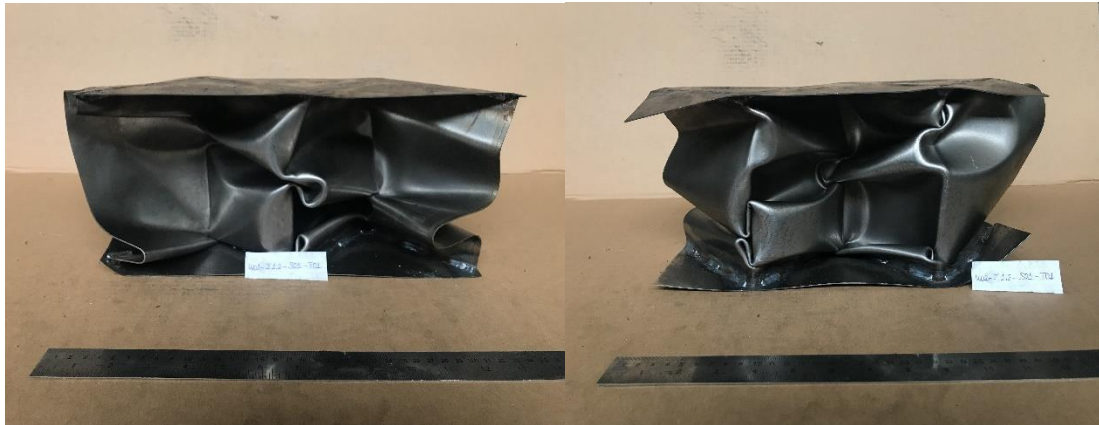
Figure 4.15. W02-I1.2-S01-T01 sample's front and back view after collision

The amount of energy absorbed by this sample during the test is calculated below.

$$KE_{Impcat} = \frac{1}{2} \times 150 \times (6.695)^2 = 3.367KJ$$

$$PE_{Last} = 150 \times 9.81 \times \frac{164.7}{1000} = 0.242 \; KJ$$

$$E_{absorb} = 3.367 - 0.242 = 3.125KJ$$

As a result of the calculation, the amount of energy absorbed by the sample was found to be 3.125 KJ.

4.2.3. 1.0mm thickness of the sample

There are 26 samples of 1.0mm thickness of W02 Shape Profile which have been experimented in the laboratory although 9 samples with 300mm height of crash-box, 8 samples with 250mm & 9 samples of 200mm height.

-W02-I1.0-S01-T01- The experiment carried out with a thickness of 1mm sheet. When specimen was examined, it was observed that there were no yielded results due to the folding and deformations on the sample surfaces and columns. The average length of the specimen was 300mm before the collision and approximately decreased to 180 mm (Figure 4.16.).

-W02-I1.0-S02-T01- After the collision test of the 1mm thick sample, it was decided to re-test the sample by decreasing length size 300mm to 250mm. As a result of the impact, in the left column there is an inward twisting, while in the right column and in the middle column there is a fold that resembles like English letter 'S'. The result of the deformation decreased to 70 mm in average (Figure 4.17.).

-W02-I1.0-S03-T01- After the completion of the test of 250mm height of the crash-box, it is reduced to length of 200mm, it is seen that it has excessive amount of energy after the impact of the drop plate. This energy could be transferred to the occupants of the vehicles (Figure 4.18.). The amount of energy absorbed by the sample is calculated below in the Table 4.3. The details and experimental results for rest of the samples see Appendix A3.

Figure 4.16. W02-I1.0-S01-T01 sample's front and back view after collision

Figure 4.17. W02-I1.0-S02-T01 sample's front and back view after collision
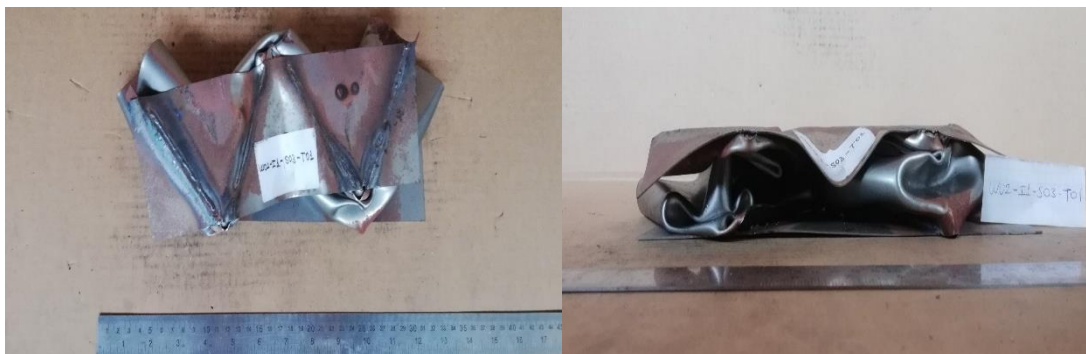
Figure 4.18. W02-I1.0-S03-T01 sample's front and back view after collision

Table 4.3. Energies were calculated by W02 shaped profile samples

S.No.	Sample Code	Sample Height (mm)	K.E. (KJ)	P.E. (KJ)	A.E. (KJ)
1	W02-I1.0-S01-T01	300	3.468	0.185	3.283
2	W02-I1.0-S02-T01	250	3.458	0.103	3.353
3	W02-I1.0-S03-T01	200	3.484	0.060	3.424

4.2.4. 0.8mm thickness of the sample

In order to see if it will give better results after tests with sheet thickness of 1 mm, tests were carried out with plates of 0.8 mm thickness. There are five samples of the 0.8mm thickness, here only details of first sample are mentioned and for rest of sample details see Appendix A3.

W02-I0.8-S01-T01-A drop test was performed with a sample of 0.8mm thickness, the sample was subjected to excessive deformation due to the tensile stress of 0.8mm. The sample length was reduced from 300mm to 68mm. The profile shape of crash-box is just look like a trash after the collision see in the Figure 4.19.

Figure 4.19. W02-I0.8-S01-T01 sample's front and back view after collision

The amount of energy absorbed by this sample during the test is calculated below.

$$KE_{Impcat} = \frac{1}{2} \times 150 \times (6.69)^2 = 3.367KJ$$

$$PE_{Last} = 150 \times 9.81 \times \frac{57}{1000} = 0.084 \ KJ$$

$$E_{absorb} = 3.367 - 0.084 = 3.283KJ$$

-Finite Element Analysis- In the finite element analysis result of W02 shape profile is almost same as W01 shape profile in the crashing manner for every thickness.
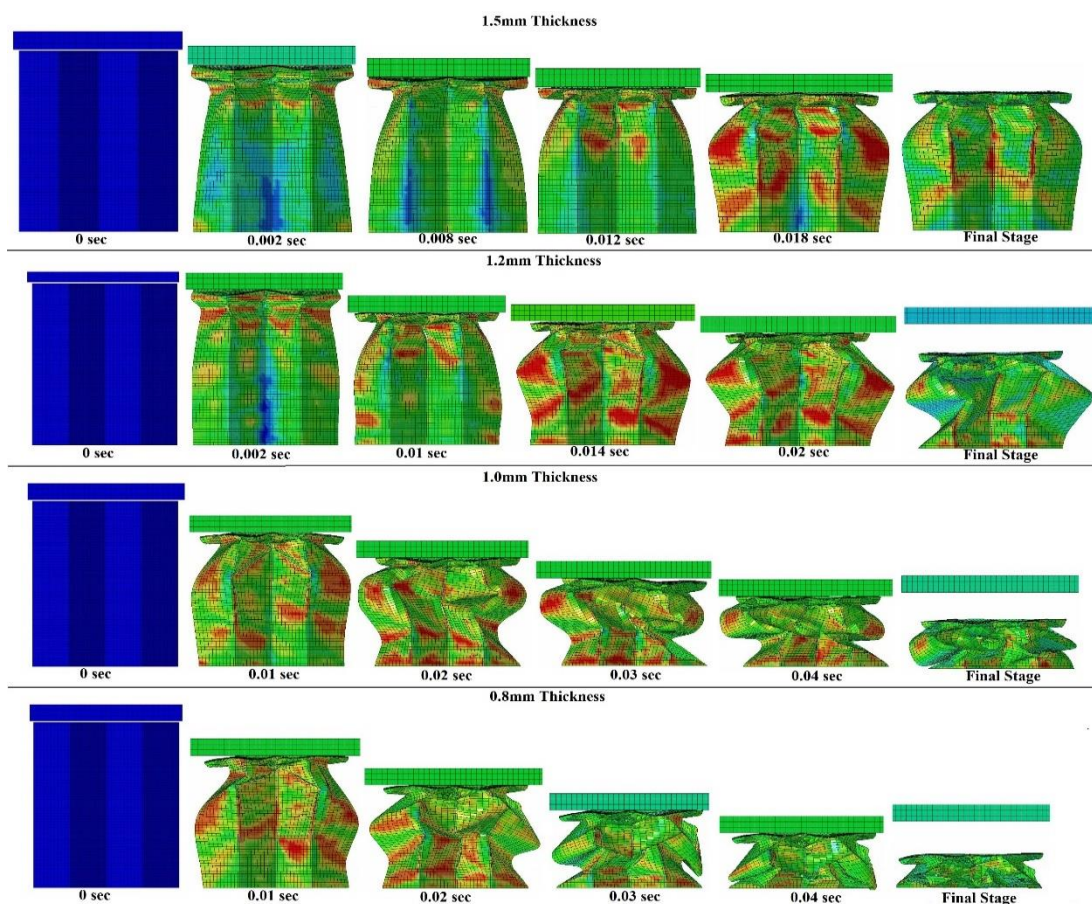
Figure 4.20. Finite Element Deformation Results of W02 Shaped Profile 300mm height of the crash-box with all thickness

Figure 4.20. shows the crash-box few time step after hit the drop plate to the crash-box in the FEA analysis. The deformation and energy absorbing properties are more than W01 shape profile. After collision of the W02 shape profile resembled like a trash.

The one corner was going ~~to~~ outside the perimeter, other side folded layer by layer in half portion of the crash-box. 1.5mm thickness sample profile deformation 300mm decreased to 242mm, 1mm thickness sample profile deformation 300mm length decreased to 120mm; it is double deformation from W01 shape profile 1mm thickness sheet, and 0.8mm thickness sheet sample does not have the capacity to absorb more energies shows properties same as previous profile of 0.8mm thickness. The experimental and FEA result comparison are provided in the Table 4.4.

Table 4.4. Experimental and FEA result of W02 Shaped profile with % error

Height (mm)	Thickness (mm)	Mean Deformation Experimental (mm)	Mean Deformation FEA (mm)	Error (%)
300	1.5	232.8	228.2	2.46
300	1.2	164.6	175.8	6.83
300	1.0	83.4	86.4	2.83
300	0.8	52.2	55	8.36

In the Figure 4.21 (Energy vs. Time), we see that 0.8mm & 1mm thickness sheet of the crash box have long time (till 0.06 sec) of the energy absorbing process and then after graph start to move in the stabilities condition, however, the energy absorbing capacities no longer endure of the crash box condition when see the simulation result of it in this figure but kinetic energy remain therefore this kinetic energy could be transfer to the occupant of the vehicles. After this 1.5mm, & 1.2mm thickness sheet of the crash-box start energy absorbing process from 0.001sec to 0.02sec then after this it move to stability condition. So enough energy remains for transfer to occupants of vehicles.
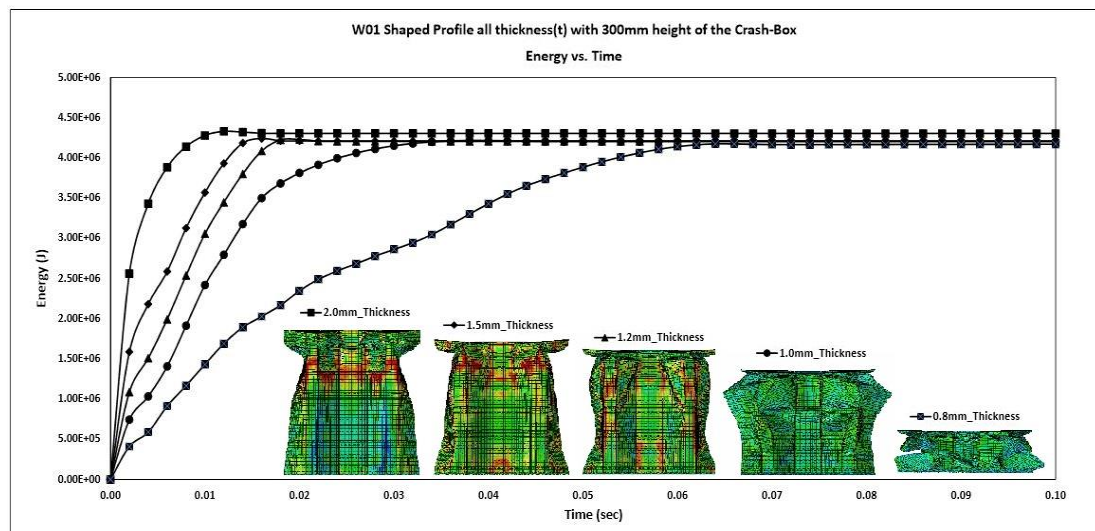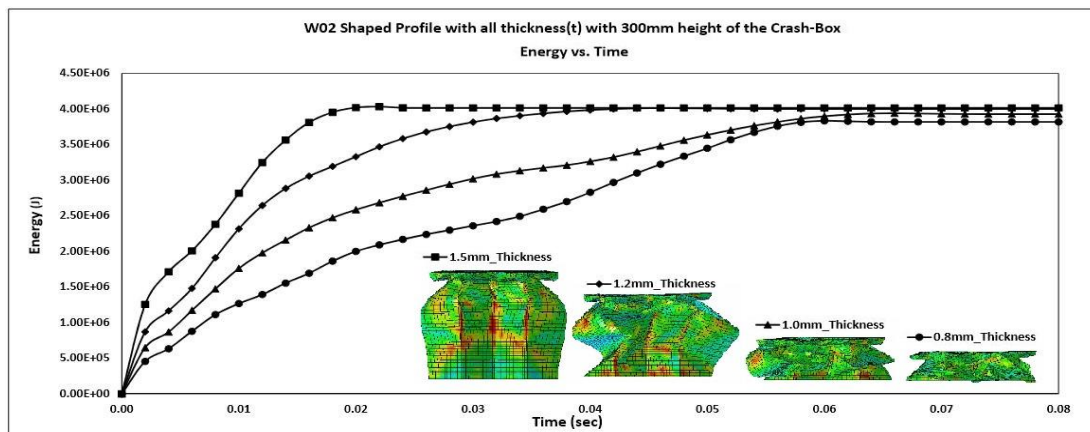

Figure 4.21. Energy graph of W02-Shaped Profile all thickness (t) with 300mm height Crash-Box

On the basis of Figure 4.22 we can say that 1mm sheet thickness crash-box has sufficient deformation after hit the drop plate. 1.5mm, 1.2mm & 0.8mm sheet thickness of the crash-box have been deformed as same as W01 shape profile and energy absorbing capacities of crash-box accordingly to sheet thickness see in the below Figure.
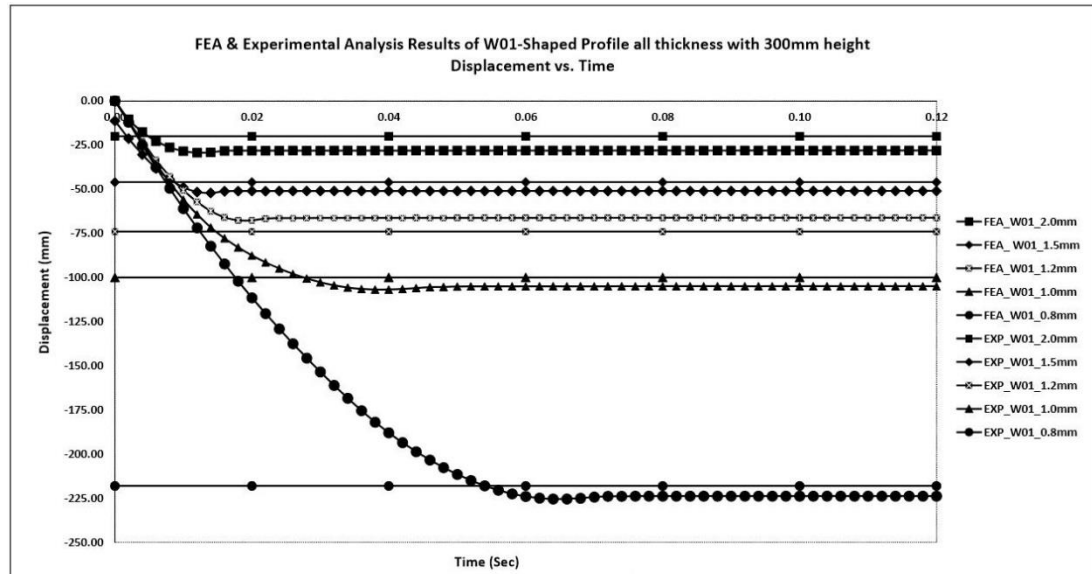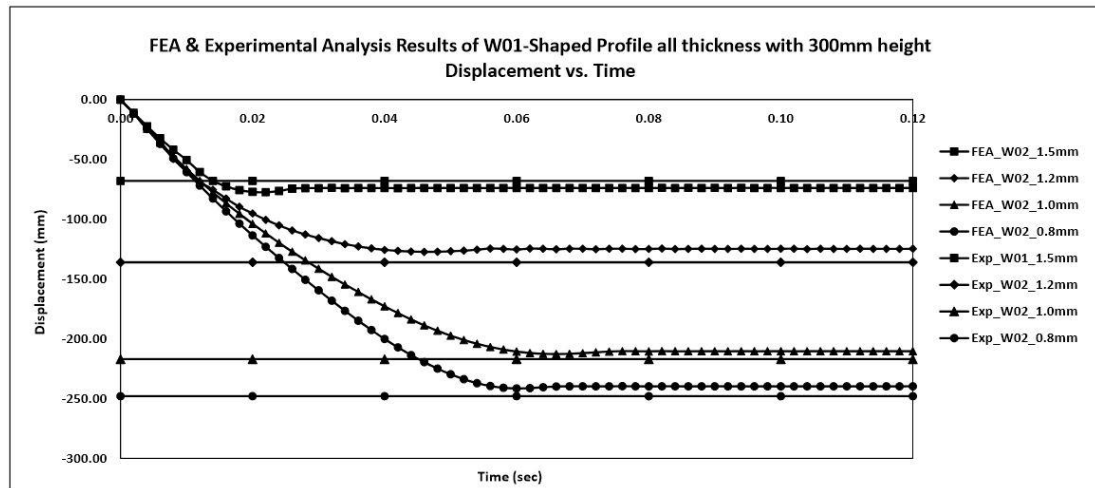

Figure 4.22. FEA & Experimental analysis results graph of W02-Shaped Profile all thickness with 300mm height Crash-Box

We have decided more length of the shaped profile of W01 & W02 will be analyzed from the length decreasing from 300mm to 250mm and further decreased to 200mm with 1mm sheet thickness profile. The experimental analysis of the 250mm & 200mm height of W01 and W02 shape profiles have been already discussed in the section (4.1.4) & (4.2.3) respectively there are finite element analysis only have been discussed.

On the basis of the Figure 4.23 it was seen that sample had ideal plastic deformation after impact collision. In the simulation, length decreased from 250mm to126mm. It has been seen good kinetic energy and shock absorbing properties than 300mm length of the crash-box and also it would not transfer much more energy to the occupant of the vehicles but 250mm length crash-box of W02 shape profile does not have good energy absorbing properties like a W01 shape profile. At the end of simulation, crash-box profile has been transformed into trash see in the Figure 4.24.
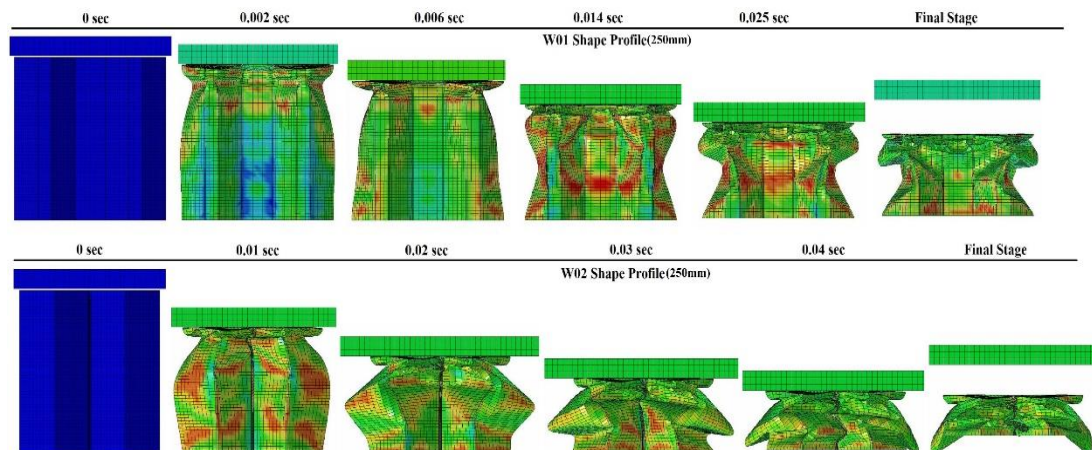
Figure 4.23. Finite Element Deformation Results for 250mm height of the crash-box of W01 & W02 Shaped Profile
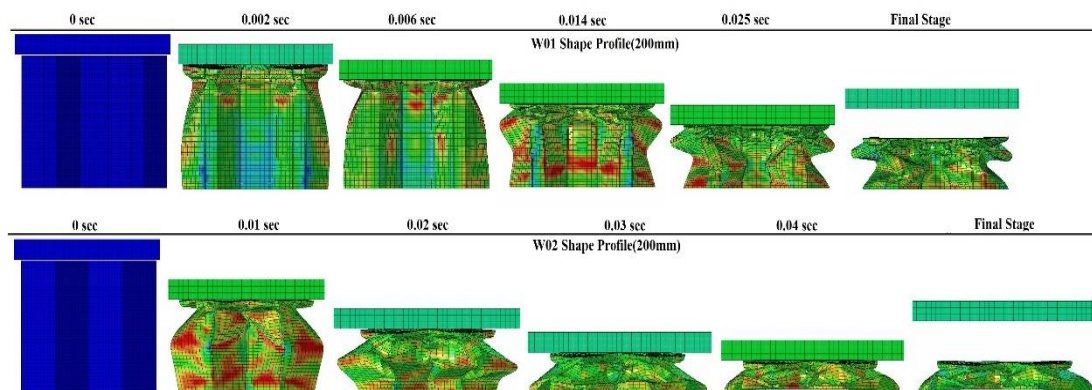
Figure 4.24. Finite Element Deformation Results for 200mm height of the crash-box of W01 & W02 Shaped Profile

Table 4.5. Experimental and FEA result of W01-250mm & W02-200mm shaped profile with % error

Height (mm)	Shaped Profile	Mean Deformation Experimental (mm)	Mean Deformation FEA (mm)	Error (%)
250	W01	123.8	123.2	2.39
250	W02	60	58.6	6.96
200	W01	70.0	75.8	8.34
200	W02	41	40.2	7.02

Accordingly to result of the experimental and simulation of all thickness of the crash-box (W01 & W02 shape profiles) along 300mm length profiles. The next step would be validation of these shaped profiles with previous studied and researched work We have decided more shape profile (Circle, Hexagonal & Square) will be analyzed from the length 300mm and also decreasing length from 300mm to 250mm and further

decreased to 200mm with 1mm sheet thickness profile. These analyzed have been discussed in the next sections.

4.3. Experimental Result of Circle, Square, Hexagonal Shaped Profile

In the following section the circle, square & hexagonal shaped profile experimental result will be discussed in detail.

4.3.1. Circle shaped profile

In the circle shaped profile crash-box; sixteen samples were analyzed in the laboratory 8 samples of 300mm length. 250mm & 200mm height crash-boxes having 4-4 samples each. Below only first sample of the each height have been discussed. For rest of the experimental result of the samples see Appendix A3.

The circle shaped profile sample code is a C01-I1-S01-T01 with height 300mm. The table hits the sample at a rate of 6.863 m/s. The contact plate of the table in the first case neck fell 300mm to 210mm was observed. At the second contact point of the table, the height remained at 214 mm (Figure 4.25). The deformations ended at a height of 180 mm from the sample base. Deformation length is around 60mm. Shapes formed in the welding section of the piece indicate that the structure dips the generated energy all over the place.

250mm height sample code is C01-I1-S02-T01 of the crash-box, crashing has been done in the same manner of the above sample. In the first contact plate of the table, the piece length decreased from 250 mm to 155mm. In the second contact, it was observed that the height decreased from 250 mm to 160 mm and there is a 30 mm deformation agglomeration area. It was observed that the resistance is higher in the weld zone (Figure 4.26).

The description of the 200mm height of the sample code C01-I1-S03-T01 is not different from above length samples but some difference is at the edge of the weld seam place. The piece length decreased from 200 mm to 110 mm. In the second

contact, it was observed that the height decreased from 200mm to 114mm. The end point of deformations at a height of 80mm is observed from the base and there is a 30mm deformation agglomeration. There was no bending fold at the edge of the weld seam (Figure 4.27).

Figure 4.25. 300mm height of the sample after deformation and weld zone of Circle Profile

Figure 4.26. 250mm height of the sample after deformation and weld zone of Circle Profile

Figure 4.27. 200mm height of the sample after deformation and weld zone of Circle Profile

4.3.2. Hexagonal shaped profile

In the Hexagonal shaped profile crash-box; 15 samples were analyzed in the laboratory 8 samples of 300mm height. 250mm height crash-boxes have 4 samples & 200mm have 3 samples. Only first sample of the each height is discussed. For rest of experimental result of the samples see Appendix A3.

Hexagonal Shaped profile sample code is a H01-I1-S01-T01 with a piece height is 300mm. The table hits the sample at a rate of 6,888 m/s. After impact of the plate on the crash-box, the crash-box length decreased from 300mm to 180mm. The deformations caused by the accumulation were mostly observed at the base of the sample. Deformations length from the bottom is 90mm. The welding seam section, there was only bending and not twisting (different from the other corner edges) (Figure 4.28).

The 250mm height sample of crash-box with code is H01-I1-S02-T01, crashing has been done in the same way of the 300mm length sample, however, the deformation area does not lie on the bottom section. The deformations at a height of 30mm from the base and continued down to 10mm from the ceiling. The folds are irregularly shaped. The welding zone is trying to oppose bending, which is also affected the general bending and folding of the piece. Other corner edges were subjected to bending, internal and external buckling is observed at the side edges (see Figure 4.29).

The same description can be given for the 200mm sample which is H01-I1-S03-T01, the part length was reduced to 100 mm. The deformation is concentrated in the upper part of the sample. The corner edge where the weld seam is bent is tilted to the other corner edges which have a fold that resists bending (see Figure 4.30).

Figure 4.28. 300mm height of sample after deformation and weld zone of Hexagonal Profile

Figure 4.29. 250mm height of sample after deformation and weld zone of Hexagonal Profile

Figure 4.30. 200mm height of sample after deformation and weld zone of Hexagonal profile

4.3.3. Square shaped profile

In the square shaped profile crash-box; sixteen samples were analyzed in the laboratory 8 samples of 300mm height. 250mm & 200mm height crash-boxes have 4-4 samples

each. Below only first sample of each height is discussed. For rest of experimental result of the samples see Appendix A3.

Square shape of sample S01-I1-S01-T01 of the crash-box height is 300 mm. The table hits the sample with the speed of 6.806 m/s. The length of the piece on the first contact edge decreased after collision from 300mm to 106-110mm range. In the second contact, it was observed that the other edge length decreased from 300mm to 110mm. The corner edge with welded seams has shown resistance against crashing other edges. Therefore, this has affected the deformation of other corner edges (Figure 4.31).

250mm height of the sample S01-I1-S02-T01 of the crash-box is similar as above with the way of crashing but the sample of length decreased from 250mm to 70mm. Deformation started after 15 mm from the bottom ceiling. When viewed from the top, the assemblage are overfilled beyond the geometry and resulted with complexions. The welding seam has shown resistance to bending and this has affected the bending of the sample (Figure 4.32).

However, the same description can be given for the 200mm height of the sample which is S01-I1-S03-T01. Here deformations have started from the base 10mm and 5mm from the ceiling of the crash-box. The weld seam has not been folded properly, it affected the overall folding. The deformation length decreased from to 200mm to 52mm (Figure 4.33).

Figure 4.31. 300mm height of the sample after deformation and weld zone of Square Profile

Figure 4.32. 250mm height of the sample after deformation and weld zone of Square Profile

Figure 4.33. 200mm height of the sample after deformation and weld zone Square Profile

4.4. FEA Result of Circle, Square, Hexagonal Shaped Profile

The effects of the impact collision on the crashing behavior of the different shape of profile crash-boxes were analyzed by extracting of the deformation behavior from the FEA model. In this section the simulation analysis of the circle, the Hexagonal and square shape profile of crash-boxes with all length has been discussed.

4.4.1. 300mm height of the crash-box

The deformation result from the FEA simulation of all models are shown in the Figure 4.34. The result of the simulation of the 300mm height of the crash-box, circle profile crushing has been started from the top portion of the crash-box when drop plate hit the sample. The amalgamation of crushing is only 40mm length from the top. Here 300mm length decresed to 91.5mm (remaining length of the crash-box after collison is 208.5mm). In the hexagoanl shape profile crash-box crashing has been started as same

as circle crash-box but energy and shock absrober properties are more than circle crash-box. Deformation has happened till 117mm length from the top. On the investigating of square shape profile, deformation has been found more than both of the profiles but crushing behavior was not in proper manner such as profile shape warped outward from square shape layer by layer. The length of the crash box was decreased from the 300mm to 182mm (remaining length of the crash-box after collison is 118mm). The comparison of the Experimental (best sample) and FEA analysis with percentage error and absorbing energy capacity of the crash box see in the Table 4.6.
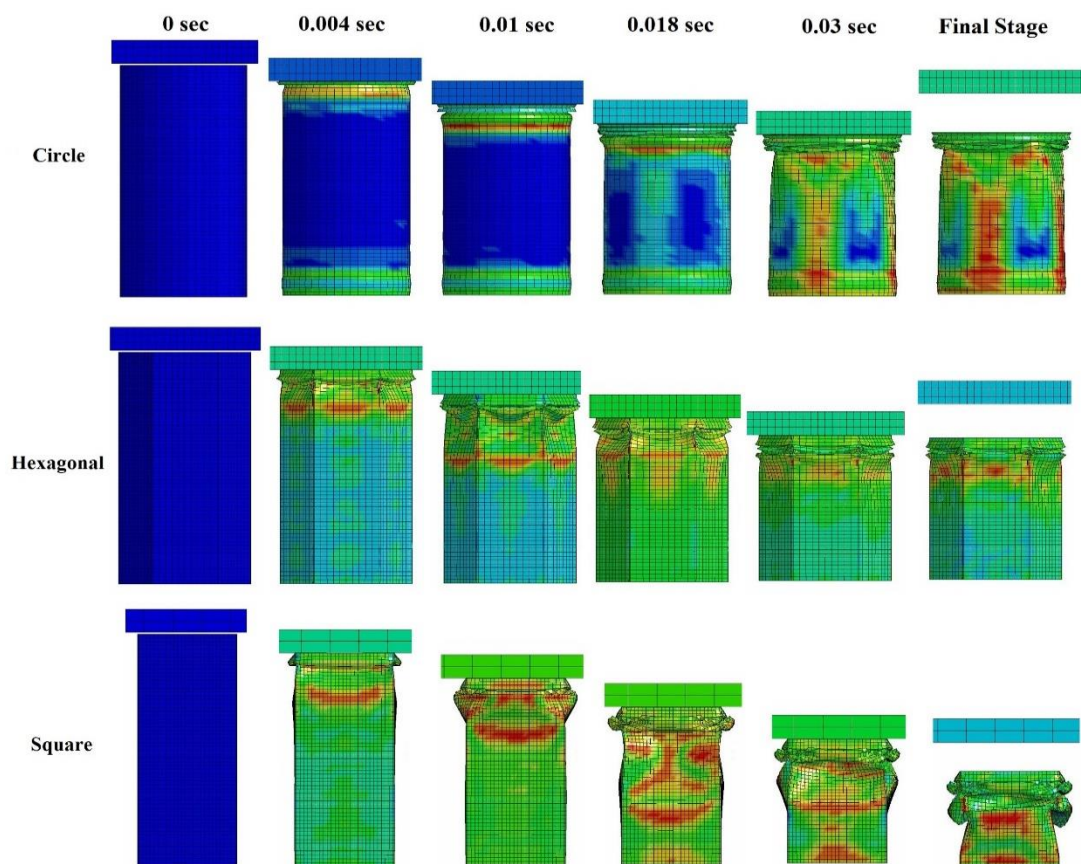
Figure 4.34. Circle, hexagonal & square shaped profiles FE model deformation results of 300mm height of the Crash-box

Table 4.6. Experimental & FEA result with percentage error and energies data of 300mm height of the crash-box

Profile Shape	Experimental mean H (mm)	FEA mean H (mm)	Error (%)	K.E. (kj)	P.E. (kj)	A.E. (kj)
Circle	215.3	208.4	3.20	3.532	0.442	3.119
Hexagonal	180	183	1.5	3.560	0.265	3.295
Square	120	122	1.64	3.474	0.159	3.315

The investigating of the Figure 4.35, in this graph, we see that W02 & S01 shape profile crash box have long time (till 0.06 sec) of the energy absorbing process and then after graph start to move in the stabilities condition, however, the energy absorbing capacities no longer endure of the crash box condition when see the simulation result of it in this figure but kinetic energy remain therefore this kinetic energy could be transfer to the occupant of the vehicles. Further W01 & C01 shape profiles crash-box have an opposite properties of the energy absorbing process. So enough energy remains for transfer to occupants of vehicles. H01 shape profile crash-box has moderate condition. The energy absorbing process in the H01 crash-box starts from 0.002sec to 0.03sec then graph line starts to liner status and according to crash-box condition in this figure almost energy is absorbed by it so there is no energy remained to transfer to the occupants which means no harmful conditions would be arising for the occupant of the vehicle. Also, the deformation result is extracted from the FEA simulation of all models of the cash-box, shown in the graph Figure 4.36.
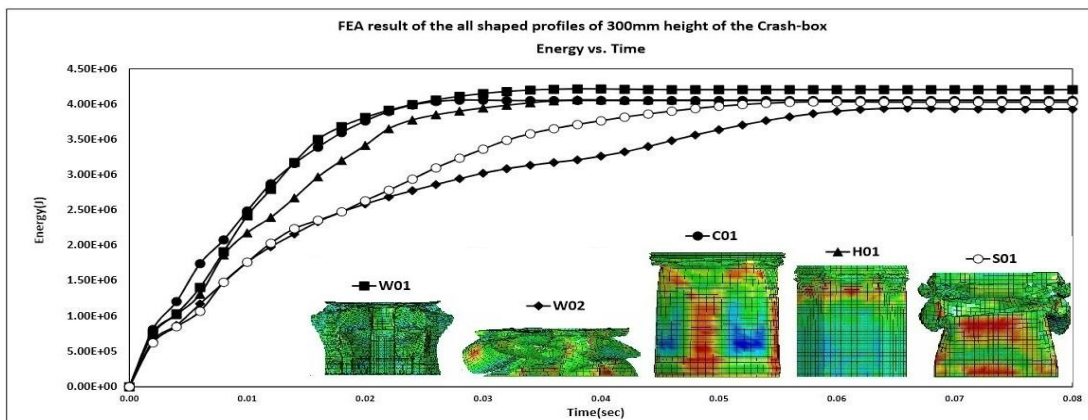
Figure 4.35. Energy vs. Time graph of all shaped profiles of 300mm height of the crash-box
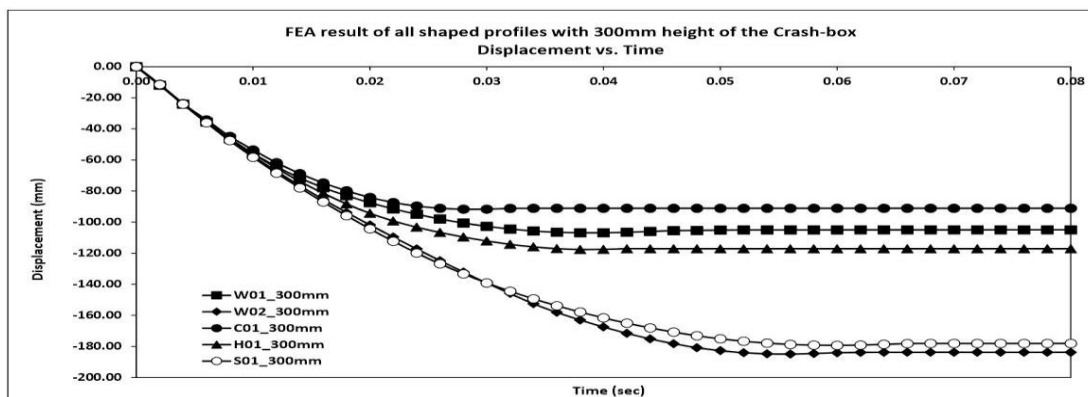
Figure 4.36.Displacement vs. Time graph of all shaped profiles of 300mm height of the crash-box

4.4.2. 250mm height of the crash-box

After getting an appropriate results from the 300mm height crash-box, 250mm length crash-box analysis was started. The deformation result from the FEA simulation of the all models are shown in the Figure 4.37. In these crash-boxes, the crashing has happened in the same as previous crash-box. The circle shaped profile deformation length decreased from 250mm to 159mm (deformation length of the crash-box after collison is 91.7mm), for the hexagonal shape profile the deformation length decreased from 250mm to 117mm (deformation length of the crash-box after collison is 83mm) and same for square shape profile deformation length decresed from 250mm to 153mm (deformation length of the crash-box after collison is 97mm).
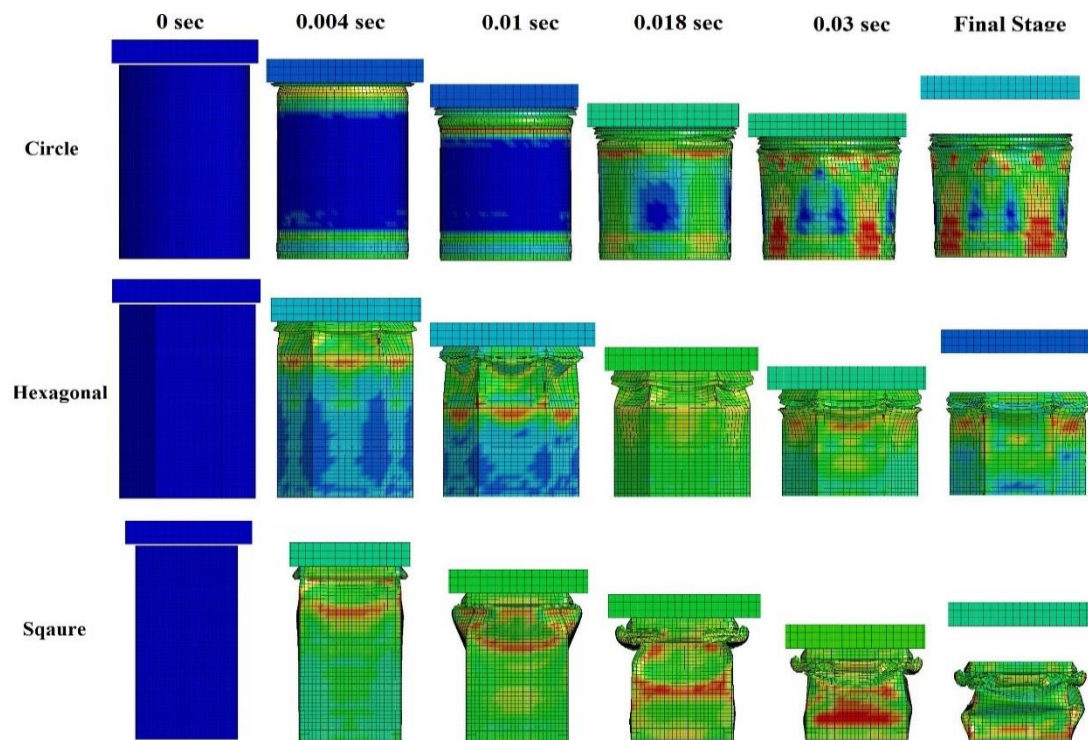
Figure 4.37. Circle, hexagonal & square shaped profiles FE model deformation results of 250mm height of the Crash-box

Table 4.7. Experimental & FEA result with percentage error and energies data of 250mm height of the Crash-box

Shape Profile	Experimental mean h (mm)	FEA mean h (mm)	Error (%)	K.E. (kj)	P.E. (kj)	A.E. (kj)
Circle	156.8	158.2	0.89	3.533	0.368	3.669
Hexagonal	129.5	132	1.54	3.606	0.191	3.458
Square	102	98.3	3.63	3.583	0.125	3.458

The investigating of the Figure 4.38. We see that W02, S01 & C01 shape profile crash-box have a same absorbing process as a 300mm length crash-box, deformation length is less than previous one. The energy absorbing process in the W01 & H01 profiles start from the 0.002sec to 0.035sec then graph line turn to stabilities condition. According to crash-box condition in this figure almost energy is absorbed by it so there is no energy remained to transfer to the occupants. However, when both the simulation and total energy results of crash-box have been analyzed. The 250mm height of it has been found that, it has more appropriate and desirable results than the others. Also, the deformation result is extracted from the FEA simulation of all models of the cash-box, is shown in the graph (Figure 4.39).
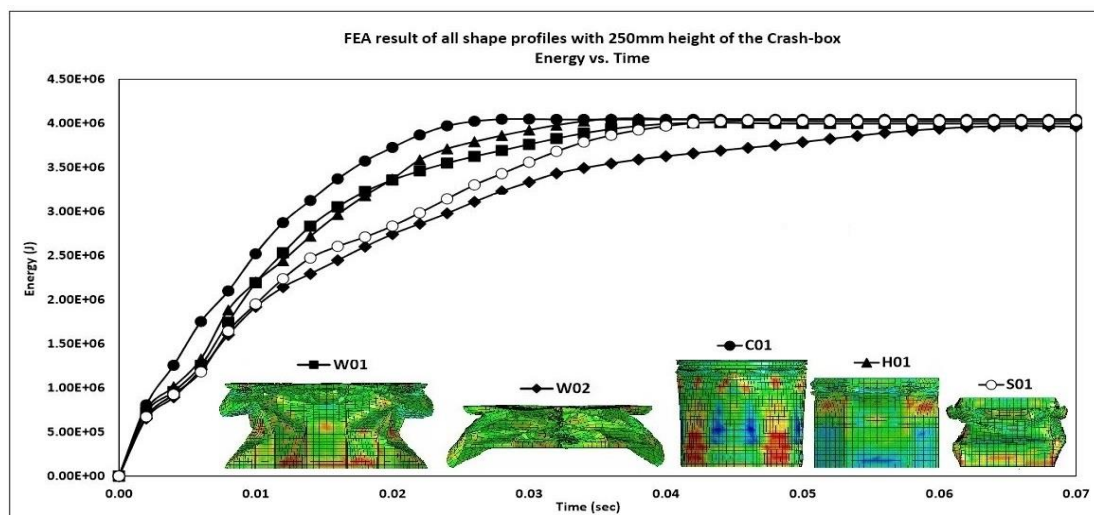
Figure 4.38. Energy vs. Time graph of all shaped profiles of 250mm height of the crash-box
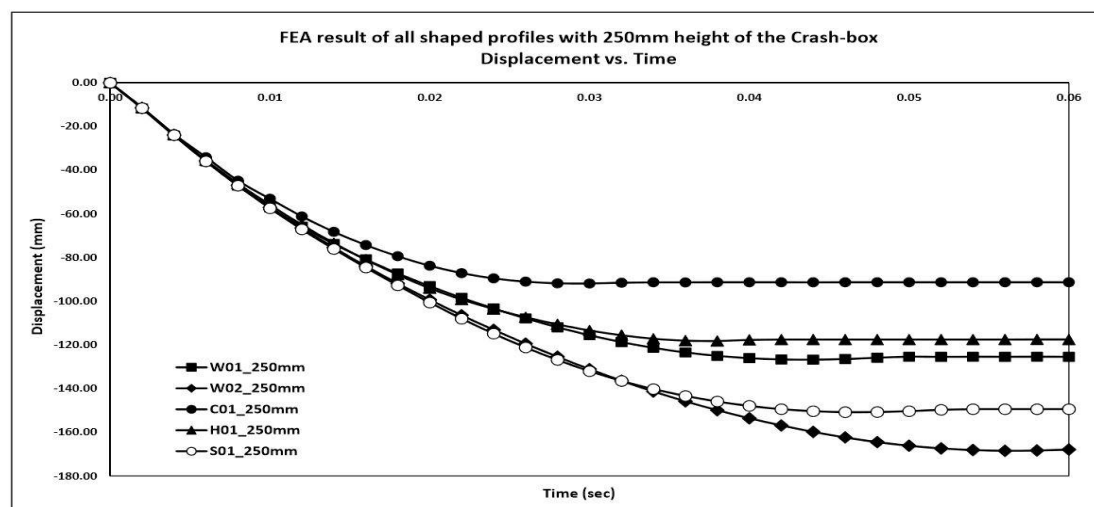
Figure 4.39. Displacement vs. Time graph of all shaped profiles of 250mm height of the crash-box

4.4.3. 200mm height of the crash-box

After getting a desirable results from the 300mm & 250mm height crash-box, 200mm length crash-box analysis was started. The deformation results from the FEA simulation of all the models are shown in the Figure 4.40 but deformation length is not sufficient for absobing the kinetic energy, when axial impact of the drop collides on the crash-box. In these crash-boxes, the crashing has happened in the same way as previous crash-box. In the circle shape profile deformation length decreased from 200mm to 111.4mm (deformation length of the crash-box after collison is 88.6mm), the hexagonal shape profile the deformation length decreased from 200 to 104mm (deformation length of the crash-box after collison is 96mm) and same square shape profile deformation length decreased from 200 to 150mm (deformation length of the crash-box after collison is 50mm).
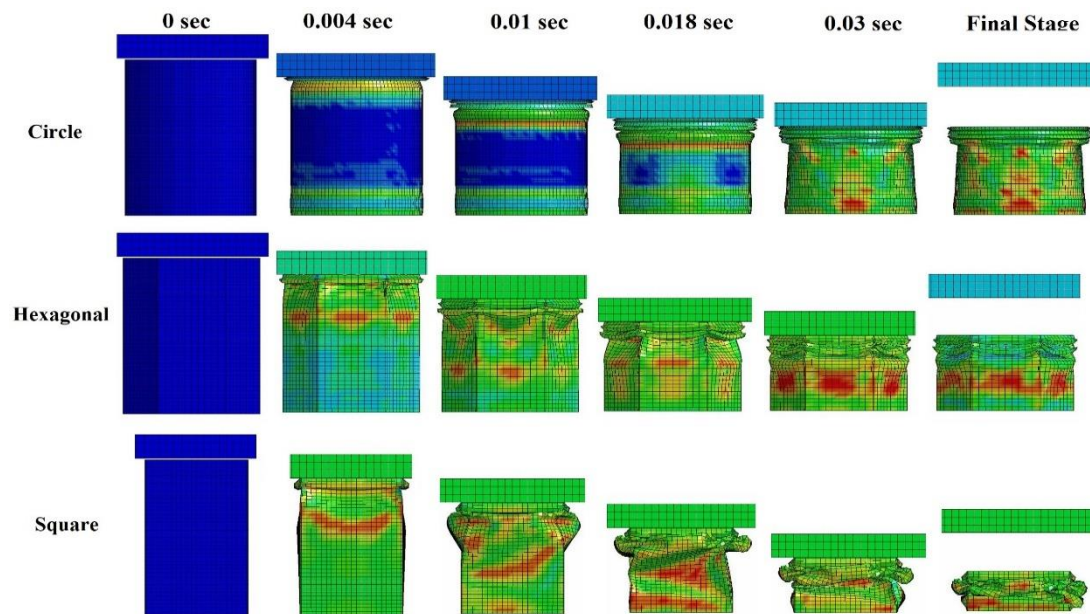
Figure 4.40. Circle, hexagonal & square shape profiles FE model deformation results of 200mm height of the
Crash-box

Table 4.8. Experimental & FEA result with percentage error and energies data of 200mm height of the Crash-box

Profile Shape	Experimental mean h (mm)	FEA mean h (mm)	Error (%)	K.E. (kj)	P.E. (kj)	A.E. (kj)
Circle	113.3	111.5	1.59	3.594	0.2944	3.740
Hexagonal	98.5	96	2.54	3.595	0.162	3.468
Square	48	50	2.56	3.642	0.074	3.468

The investigation of the Figure 4.41, all of profiles of the crash-box, the energy absorbing process start from 0.002sec to 0.04sec. After this the graph of line starts to stabilize. Although in pictures of the FEA simulation of all models, almost energy is absorbed by the crash-boxes so there is no energy remained to transfer occupants which means no harmful conditions would be arising for the occupant of the vehicle. After this, when all of the length of the crash-boxes, simulation and total energy results have been evaluated. The 250mm height of it has been found that it has more appropriate and desirable results than other. Also, the deformation result is extracted from the FEA simulation of all models of the cash-box, shown in the graph (see in the Figure 4.42).
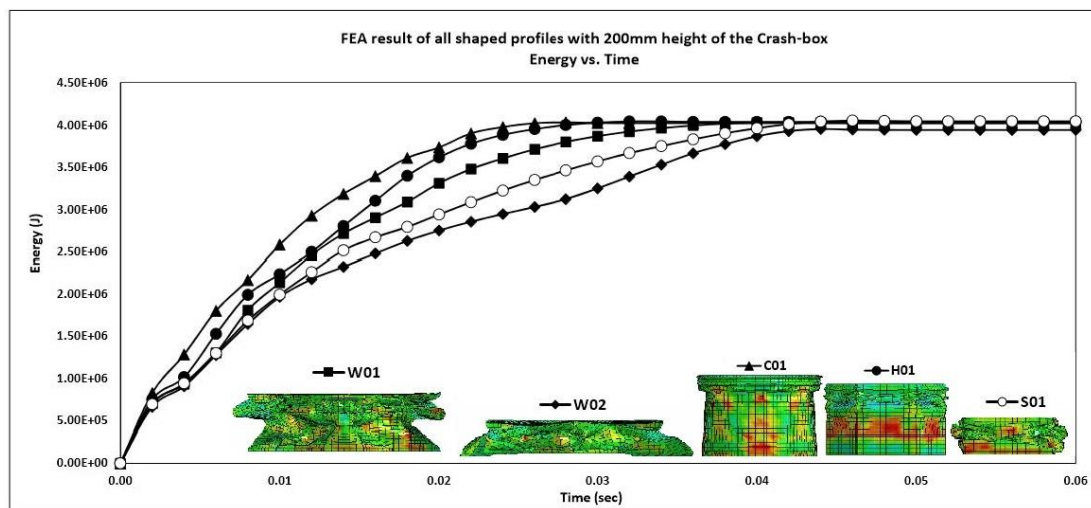
Figure 4.41. Figure 4.38. Energy vs. Time graph of all shaped profiles of 200mm height of the crash-box
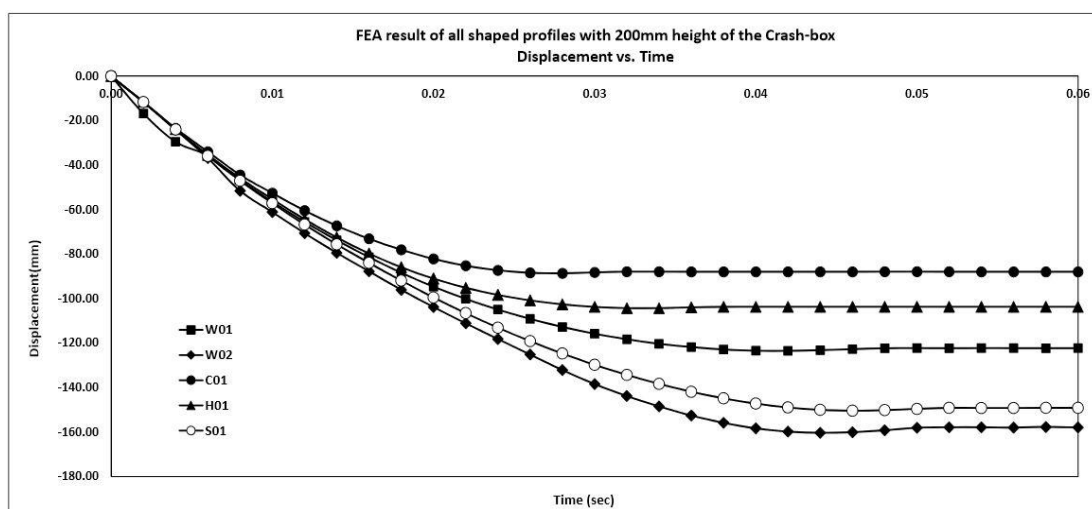
Figure 4.42.Displacement vs. Time graph of all shaped profiles of 200mm height of the crash-box

4.5. Comparison of All Experimental and FEA Analysis

All analysis photograph results of FE and experimental have been compared each other under this heading.
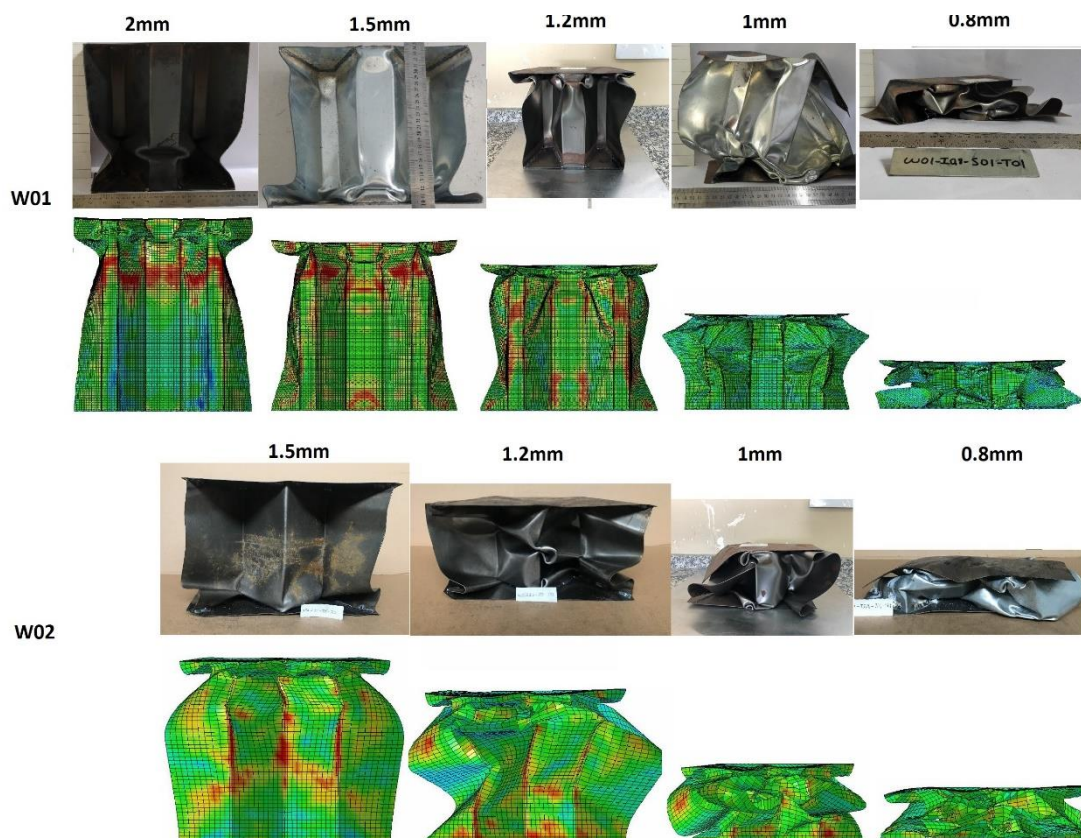
Figure 4.43. FEA & Experimental photograph results comparison of the W01 & W02 300mm profiles
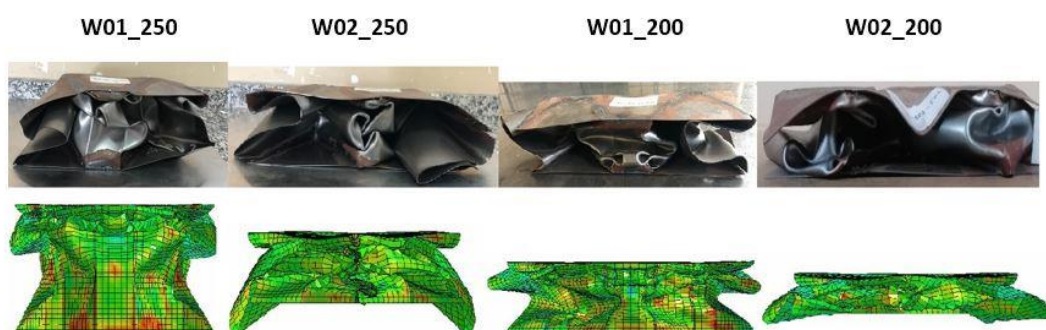
Figure 4.44. FEA & Experimental photograph results comparison of the W01 & W02 250 & 200mm profiles
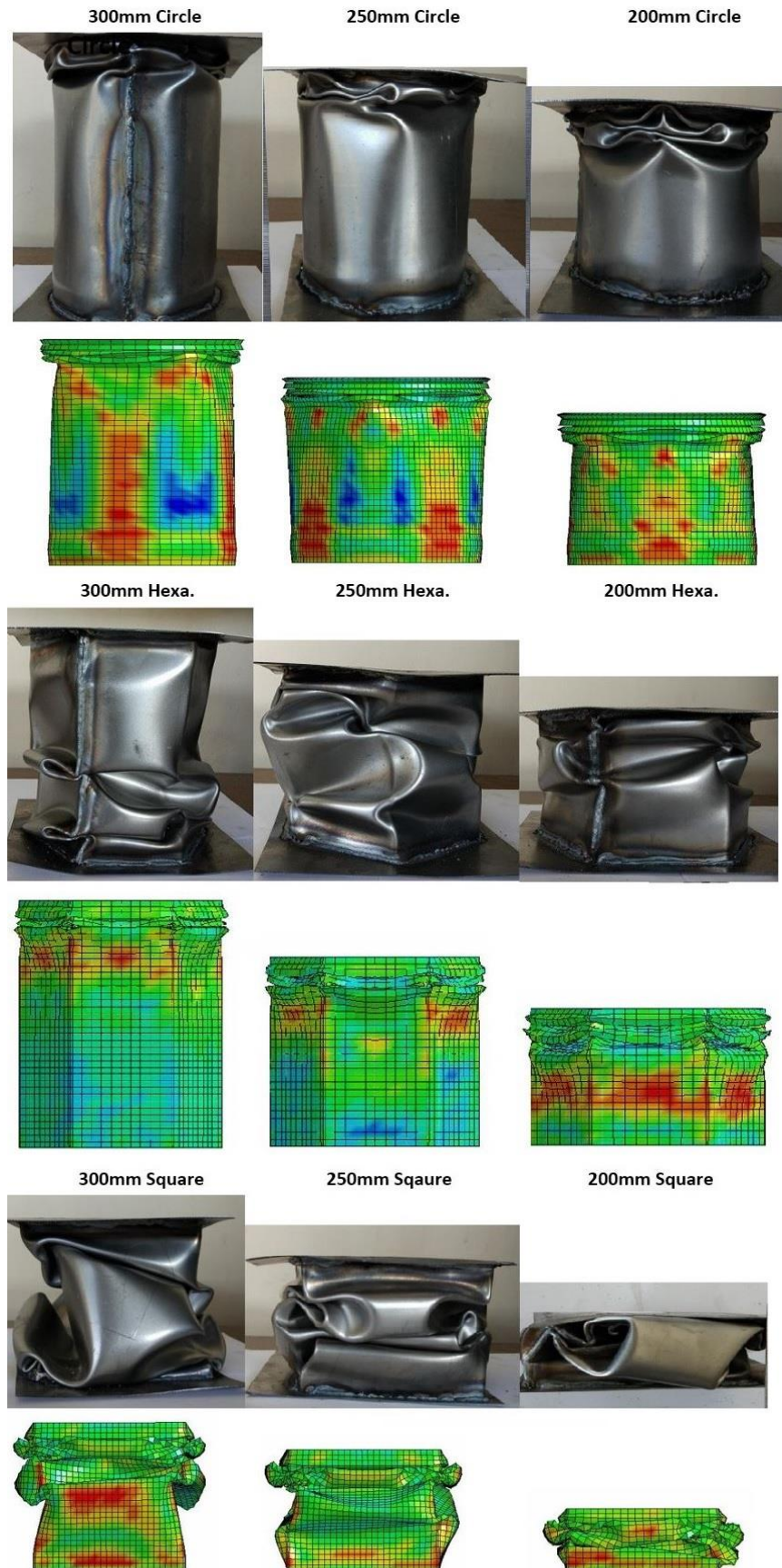
Figure 4.45. FEA & Experimental results comparison of the Circle, Hexagonal & Square profiles

CHAPTER 5. CONCLUSION

The usage of the steel material gives to create an economically and light weight crash-boxes of the vehicles. In this work number of the variables of the crash-box were investigated such as thickness, profile shape, and length. This work is based on the drop test setup (Experimental Analysis) in the laboratory as well as FEA simulation (LS-Dyna) of the crash-boxes with drop plate.

First, the number of the thickness of the crash-boxes such as W01 & W02 with 300mm length was analyzed and also compared with FE simulation. After optimization of thickness of the crash-boxes, further shaped profile and length of the crash-boxes analysis was started. Variants of the profiles are W01, W02, Circle (C01), Hexagonal (H01) & Square (S01) and 300mm, 250mm, & 200mm height of the crash-boxes with 1.0mm thickness have been evaluated. Even though finite element analysis was done by LS-Dyna software and compared each other results.

According to the experimental study of the frontal impact simulations via drop test setup is admissible to describe the direct collisions as expected. Although crash-box developments spread on spacious studies, there are still sufficient amount of undiscovered areas exist. To saturate some part of not defined areas of the impact absorbing field, this study has accomplished using not regular shapes.

Thickness optimization of the crash-box has been done by the experimentally and FEA result. The frontal imp act absorbing capacity of the 2mm, 1.5mm thickness is not appropriate because it has a rigid properties and does not have deformable behavior as per as expected requirements. When 0.8mm thickness of the crash-box was found so much deformable and does not have enough capacity to absorb impact energy of the collision.

According to the result, most appropriate thickness of the crash-box must be remained between 1.5mm to 0.8mm. Therefore, here 1.2mm and 1.0mm thick crash-box was investigated. By the both results, 1.0mm thick crash-box is capable to enough impact energy absorption by folding two times on itself while the rigid ones just fold once and the soft samples fold all the way.

After optimizing the thickness, height of the crash boxes was investigated and by the results of the experimentally and FEA, 250mm height of the crash-box was found that it has capacity to enough impact energy absorption. When shaped profiles of the crash-boxes were investigated. The hexagonal shaped profile was found that optimum features such as deformable capacity, energy absorption capacity and is capable to absorb enough impact energy than others shaped profiles of the crash-box.

Finally, repeated 1mm thick, 250mm height and hexagonal shaped profile sample of the crash-box verify by the experimentally the absorbing ability in many drop tests and though verify by finite element analysis result.

The long selection of the length of the samples used in the studies carried out to lead a clear idea about the amount of damping when working with thin materials and these samples undergoing extreme deformation. The number of samples required for a damping system to be generated using samples with a thickness of 1mm, 250mm height & hexagonal shaped profile and the value of the speed at which the impact can be completely absorbed as calculated as follows for Peugeot 301.

In this work, we suppose that the crash-box would be fixed between the bumper and chassis structure of the vehicles. In this idea, the number of crash box (according to calculation) will be fixed on the supporting sheet, which will clamp on the chassis with the help of bolt or weld joints. The exact procedure will be applied on the adjacent side. The only difference is the attachment of the crash-box with the bumper. The whole procedure is shown in the Figure (5.1). In the following, how many crash boxes will be attached to the supporting sheet has been calculated. The number of crash boxes

six would be better for the absorbing energy and coupled with the vehicle according to calculations and the dimension of the car.
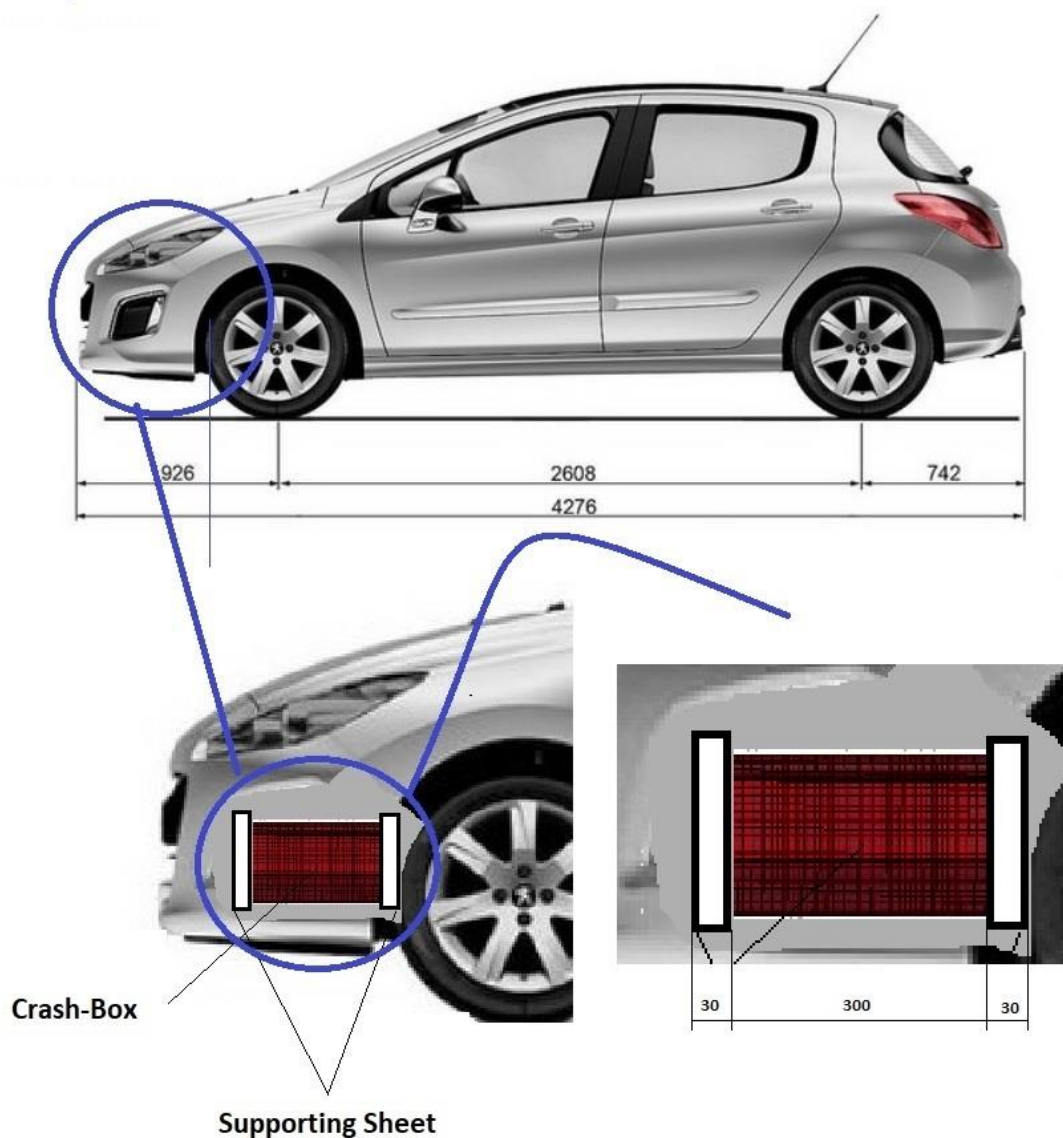
Figure 5.1. Idea of the will be attached the crash-boxes with vehicles

Features of the vehicle and weight that has been used in the calculation

(a) Selected vehicle: Peugeot 301 1.2L Pure Tech.

(b) Weight of the empty car: 980 kg.

$$m_{vehicle} = vehicle(980kg) + Driver(75kg) + N \times Profil(1.238kg)$$

N= number of the profile(Crash-box)

$$m_{drop\ plate} = 150\ kg$$

1.238 kg of the 1mm thikcness of the H01 profile with 250mm height of the crash-box

Vehicle Speed Calculation

$$\underbrace{m_{vehicle} \times V_{vehicle}}_{\text{Vehicle}} = \underbrace{N \times m_{drop\ plate} \times V_{experiment}}_{\text{Drop Plate}}$$

$$V_{vehicle} = \frac{N \times m_{drop\ plate} \times V_{experiment}}{m_{vehicle}}$$

(a) N= 6

$$m_{vehicle} = \text{vehicle}(980kg) + \text{Driver}(75kg) + N \times \text{Profil}(1.238kg)$$
$$= 980 + 75 + 6 \times 1.238$$
$$= 1062.43\ kg$$

$$V_{car} = \frac{N \times m_{drop\ plate} \times V_{experiment}}{m_{vehicle}}$$
$$= \frac{6 \times 150 \times 6.815}{1062.42}$$

$$= 5.73\ m/s\ or\ 20.75\ km/h$$

(b) N=8

$$m_{vehicle} = \text{vehicle}(980kg) + \text{Driver}(75kg) + n \times \text{Profil}(1.238kg)$$
$$= 980 + 75 + 8 \times 1.238$$
$$= 1064.99kg$$

$$V_{vehicle} = \frac{N \times m_{drop\ plate} \times V_{experiment}}{m_{vehicle}}$$
$$= \frac{8 \times 150 \times 6.815}{1064.99}$$

$$= 7.67\ m/s\ or\ 27.58\ km/h$$

(c) N=10

$$m_{vehicle} = \text{vehicle(980kg)} + \text{Driver(75kg)} + \text{n x Profil(1.528kg)}$$

$$= 980 + 75 + 10 \times 1.238$$

$$= 1067.38 \text{ kg}$$

$$V_{vehicle} = \frac{N \times m_{drop\ plate} \times V_{experiment}}{m_{vehicle}}$$

$$= \frac{10 \times 150 \times 6.815}{1067.38}$$

$$= 9.57 \text{ m/s or } 34.38 \text{km/h}$$

According to the above calculation of N=6 (Crash-boxes) and resulting velocity indicates that absorbing energy capacity of the vehicle is adequate to prevent the transfer kinetic energy to the occupant. The experimental speeds used in the calculations are those which can be extracted by the capacity of the experimental setup. The presence of non-deformable regions in the samples indicates that the samples still have the ability to absorb energy. With tests that can reach higher speeds in test installations, or with more severe drop plates, the maximum energy damping capacity of the current design can be measured. If the speed values obtained in these tests are used, it can be calculated how much the maximum impact speed can be absorbed by the selected vehicle. Measures and weight values in the tool used in the selection of the vehicle is one of the light vehicles in the segment and a sufficiently larger number of samples in the buffer zone.

REFERENCES

[1]   Alghamdi, A., Collapsible impact energy absorbers: An overview. Thin-Walled Structures, 39: 189-213, 2001.

[2]   Ghadianlou, A., Abdullah, S., Crashworthiness design of vehicle side door beams under low-speed pole side impacts. Thin-Walled Structures 67: 25-33, 2013.

[3]   Ambrósio, J., Contact and impact models for vehicle crashworthiness simulation. International Journal of Crashworthiness, 73-86, 2003.

[4]   http://www.oica.net, International Organization of Motor Vehicle Manufacturers (OICA), Access Date: 25.01.2018.

[5]   Blaszkiewicz, M. Urbanek, M., FEM Based Improvement of CAD for Non-Conventional Railway Track. Acta Phys. Polonica A 128: B241-242, 2015

[6]   Jingwen, H., Flannagan, C., Bao, S., Integration of Active and Passive Safety Technologies - A Method to Study and estimate field capability. Stapp Car Crash Journal, 59: 15S-37, 2015.

[7]   Zhou, C., Zhou, Y., Wang, B., Crashworthiness design for trapezoid origami crash boxes. Thin-Walled Structures, 257-267, 2017.

[8]   G. Belingardi, A. B. E. K. a. B. M., 2014. Alternative lightweight materials and component manufacturing technologies for vehicle frontal bumper beam. Composite Structures, 120: 483-495, 2014.

[9]   Belingardi, G., Beyene, A., Koricho, E., Martorana, B., Crashworthiness of integrated crash-box and bumper beam made by die- forming composite, 16th European Conf. on Composite Material, Seville-Spain, 22-26, June 2014.

[10]   Chul, H., Shin, K, Lee, J., Kwon, J., Crashworthiness of aluminum/CFRP square hollow section beam under axial impact loading for crash box application, Composite Structures, 112: 1-10, 2014.

[11]   Ozer, H., Can, Y., Yazici, M., Investigation of the Crash Boxes Light Weighting with Syntactic Foams by the Finite Element Analysis. Acta Phys. Pol. A 132: 734-737, 2017.

[12] Tarlochan, F., Samer, F., Hamouda, A., Singh, R., Design of thin wall structures for energy absorption applications: Enhancement of crashworthiness due to axial and oblique impact forces. Thin-Walled Structures 71: 7-17, 2013.

[13] Sun, G., Pang, T., Xu, C., Zheng, G., Song, J., Energy absorption mechanics for variable thickness thin-walled structures. Thin-Walled Structures 118: 214-228, 2017.

[14] Wierzbicki, T., Abramowicz, W., A., On the Crushing Mechanics of Thin-Walled Structures. Appl. Mech 50(4a): 727-734, 1983.

[15] Meguid, S., Yang, F., Hou, P., Crush behaviour of foam-filled thin-walled conical frusta: analytical, numerical and experimental studies. Acta Mechanica 227(12): 3391–3406, 2016.

[16] Zhou, F., Lan, F., Chen, J., Crashworthiness research on S-shaped front rails made of steel–aluminum hybrid materials. Thin-Walled Structures 49 (2): 291-297, 2011.

[17] Tanlak, N., Sonmez, F., Senaltun, M., Shape optimization of bumper beams under highvelocity impact loads. Engineering Structures 95: 49-60, 2015.

[18] http://www.oica.net/category/production-statistics/2017-statistics/, International Organization of Motor Vehicle Manufacturers (OICA), Access Date: 27.01.2018.

[19] Qui, N., Gao, Y., Fang, J., Feng, Z., Crashworthiness analysis and design of multi-cell hexagonal columns under multiple loading cases, Finite Elements in Analysis and Design, 104: 89–101, 2015.

[20] Peroni, L., Avalle, M., Belingardi, G., Experimental investigation of the energy absorption capability of bonded crash boxes, Politecnico di Torino, Italy, 07-35, 2006.

[21] Husain, N., Regalla, S., Rao, Y., Low velocity Impact Characterization of Glass Fiber Reinforced Plastics for Application of Crash Box, Materials Today, 4: 3252–3262, 2016.

[22] https://data.oecd.org/transport/road-accidents.html, The Organization for Economic Cooperation and Development, Access Date: 05.02.2018.

[23] Boria, S., Crashworthiness Optimization of an Automotive Front Bumper in Composite Material, International Journal of Mechanical and Mechatronics Engineering, 11: No-11, 2017.

[24] Ozturk, I., Kaya, N., Crash Analysis of Vehicle Front Bumper and Its Optimization, Uludağ Üniversitesi Mühendislik-Mimarlık Fakültesi Dergisi, Vol: 13, Issue: 1, 2008.

[25] Costas, M., Diaz, J., Romera, L., Hernandez, S., Static and dynamic axial crushing analysis of car frontal impact hybrid absorbers, International Journal of Impact Engineering 62: 166-181, 2013.

[26] Paz, J., Diaz, J., Romera, J., Costas, M., Crushing analysis and multi-objective crashworthiness optimization of GFRP honeycomb-filled energy absorption devices, Finite Elements in Analysis and Design, 91: 30–39, 2014.

[27] Abbasi, M., Reddy, S., Nazari, A., Farz, M., Multiobjective crashworthiness optimization of multi-cornered thin-walled sheet metal members, Thin-Walled Structures, 89: 31–41, 2015.

[28] https://www.hagerty.com/articles-videos/articles/2013/04/09/antilock-brakes, Access Date: 10.02.2108.

[29] http://www.safetyresearch.net/blog/articles/brief-history-electronic-stability-controls-and-their-applications, Access Date: 10.02.2018.

[30] https://babyseat.fundacionmapfre.org/children/images/child-safetycars_tcm726 93770.pdf, Access Date: 10.02.2018.

[31] Lee, D., Kim, S., Kim, C., Huh, K., Development of an autonomous braking system using the predicted stopping distance, International Journal of Automotive Technology, 341−346, 2014.

[32] https://www.crashtest.org/history-car-safety/, Access Date: 12.02.2018.

[33] https://triblive.com/business/headlines/3917853-74/safety-car-cars, Access Date: 15.02.2018.

[34] https://en.wikipedia.org/wiki/Seat_belt, Access Date: 15.02.2018.

[35] https://en.wikipedia.org/wiki/Center_console_(automobile), Access Date: 21.02.2018.

[36] https://didyouknowcars.com/history-of-airbags/, Access Date: 21.02.2018.

[37] https://en.wikipedia.org/wiki/Side_Impact_Protection_System#cite_note-1, Access Date: 21.02.2018.

[38] https://www.firehouse.com/rescue/article/10519423/knee-airbag supplemental-restraint systems, Access Date: 21.02.2018.

[39] Shone, R., Dynamic Study and Analysis of Active Head Restraint Systems, ME490 RISE, University of Michigan.

[40] Lim, K., Ang, L., Seng, K., Chin, S., Lane-Vehicle Detection and Tracking, Proceedings of the International Multi Conference of Engineers and Computer Scientists Vol II IMECS, 18 - 20, Hong Kong, 2009.

[41] www.rospa.com/rospaweb/docs/advice-services/road.../vehicles/pop-up-bonnets.pdf, Access Date: 25.02.2018.

[42] https://www.iihs.org/iihs/ratings, Access Date 02.03.2018.

[43] https://www.nhtsa.gov/vehicle/1966, Access Date: 02.03.2018.

[44] https://www.euroncap.com/en, Access Date: 02.03.2018.

[45] Khalil, T., Vehicles crashworthiness and occupants protection. Chapter: Introduction, First Edition, American Iron and steel institute, 1-10, 2004.

[46] https://www.nhtsa.gov/, Access Data: 05.03.2018.

[47] https://en.wikipedia.org/wiki/Federal_Motor_Vehicle_Safety_Standards, Access Date: 05.03.2018.

[48] https://www.lifewire.com/car-safety-features-534860, Access Date: 05.03.2018.

[49] Lefer, B., Rebolloso, I., Car-to-Truck Frontal Crash Compatibility-Quantification of the possible crash severity reduction from an additional truck frontal structure. Chalmers University of Technology, Department of Applied Mechanics-Division of Vehicle Safety, Master's Thesis in Automotive Engineering, 2012.

[50] Khattab, A., Investigation of an adaptable crash energy management system to enhance vehicle crashworthiness. Concordia University, The department of Mechanical and Industrial Engineering, PhD's Thesis in Mechanical and Industrial Engineering 2010.

[51] Liu, Y., Ding, L., A Study of using Different Crash Box Types in Automobile Frontal Collision, International Journal of Simulation - Systems, Science & Technology 17(38), 21.1-21.5, 2016.

[52] Zhou, Y., Lan, F., Chen, J., Crashworthiness research on S-shaped front rails made of steel–aluminum hybrid materials, Thin-Walled Structures, 49: 291–297 2011.

[53] Li, P., Petrinic, N., Quantification of impact energy dissipation capacity in metallic thin-walled hollow sphere foams using high speed photography, Journal of Applied Physics, 8: 110, 2011.

[54] https://compass.astm.org/EDIT/html_annot.cgi?A370+18, Access Date: 05.03.2018.

[55] Garud, O., Pawar, K., Analysis and Experimentation of Crash Box, International Journal for Research in Applied Science & Engineering Technology (IJRASET), 6: 2347-2358, 2018.

[56] Reddy, J., An Introduction to the Finite Element Method. Chapter: Introduction, Third Edition, Department of the mechanical engineering Texas A&M University, 1-26, 2006.

[57] Liu, G., Quek, S., The Finite Element Method. Chapter: Introduction, Second Edition, Elsevier, 2014.

[58] Logan, D., First course in the Finite Element Method. Chapter: Introduction to matrix notation, Fifth Edition, University of Wisconsin–Platteville, 1-29, 2012.

[59] Reddy, J., An Introduction to Nonlinear Finite Element Analysis. Chapter: Introduction and The Finite Element Method: A review, First Edition, Department of the mechanical engineering Texas A&M University, 1-59, 2004.

[60] LS-DYNA, Theory Manual. Livermore Software Technology Corp., Copyright © 2008 Livermore Software Technology Corp.

[61] Engineering Research Nordic AB — DYNA more Types". November 8, 2011.

APPENDIX

A1: Mesh Information

The meshing of the crash-box structure was prepared in the ANSYS Mechanical APDL 17.2.
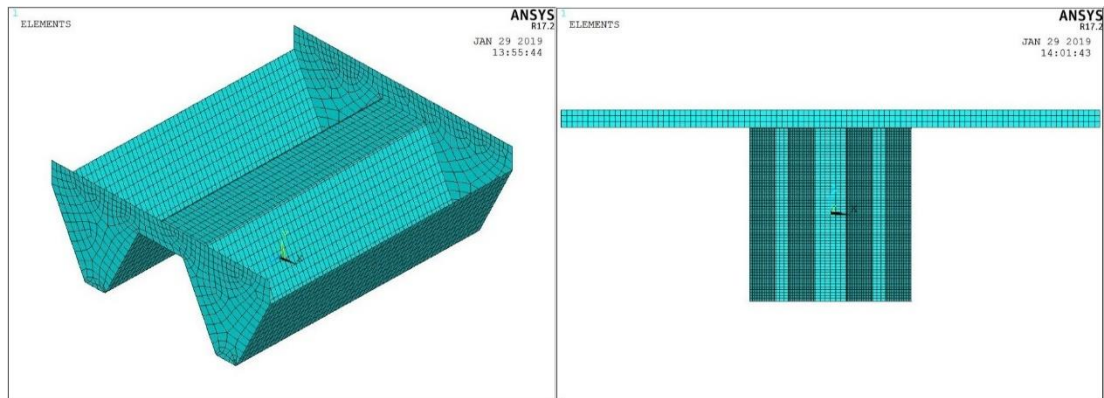
Figure A.1. W01 shaped profile with meshing elements
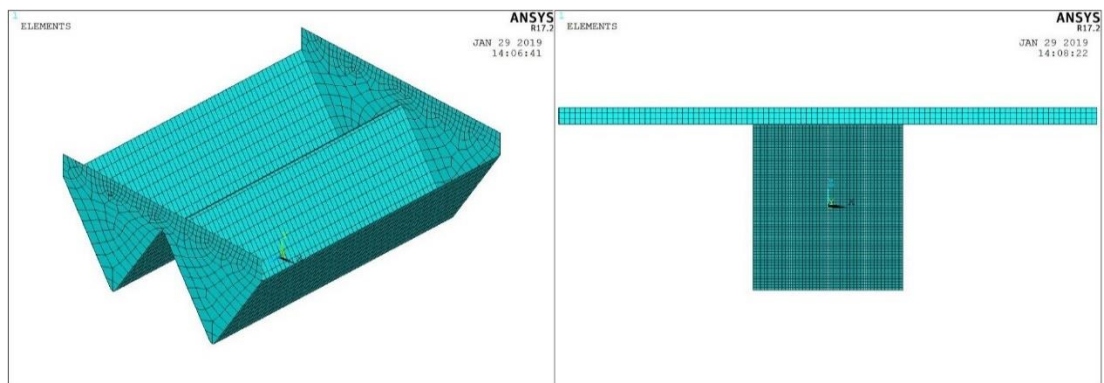
Figure A.2. W02 shaped profile with meshing elements
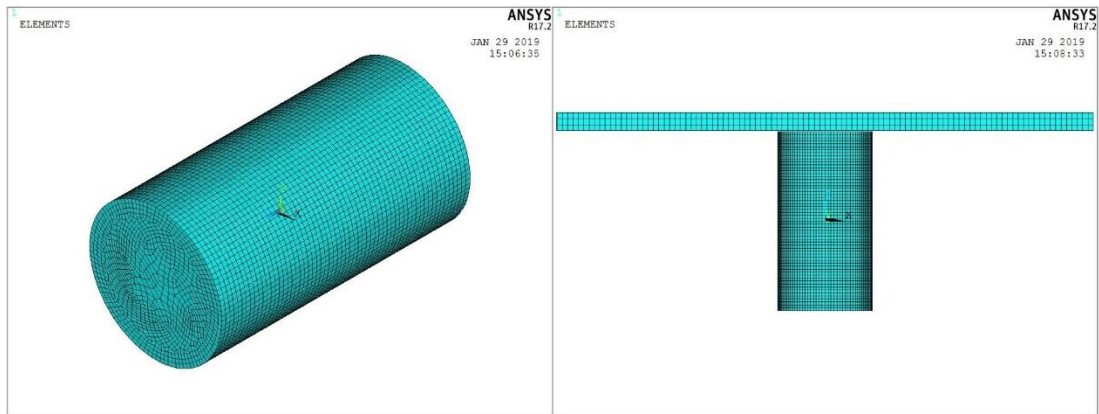
Figure A.3. C01 shaped profile with meshing elements
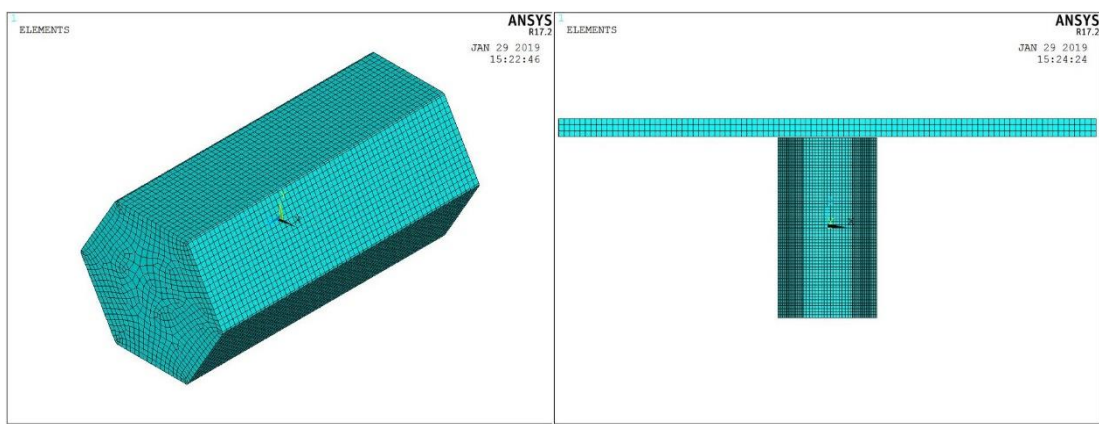
Figure A.4. Hexagonal shaped profile with meshing elements
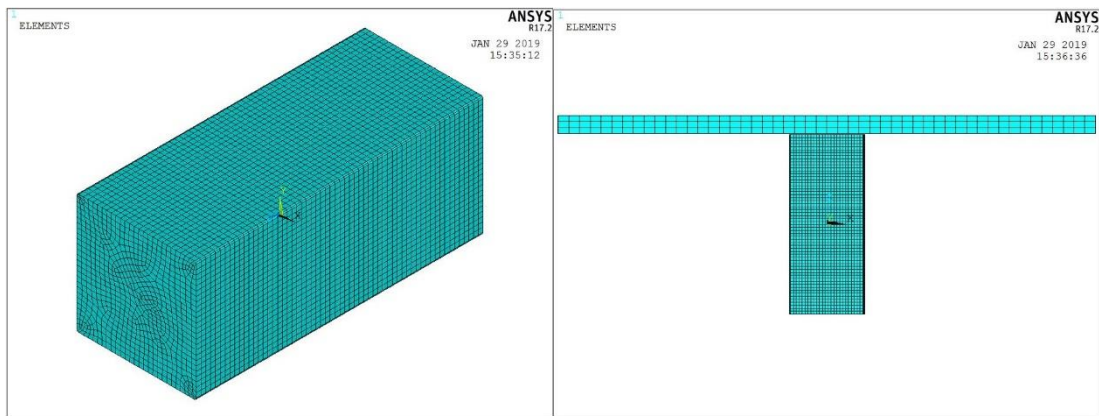
Figure A.5. Square shaped profile with meshing elements

A2:   Technical Drawing with 3-D Geometries of the all Crash-box

Circle (C01), Hexagonal (H01) & Square (S01)

Circle (C01) Shape Profile

Hexagonal (H01) Shape Profile

Square (S01) Shape Profile
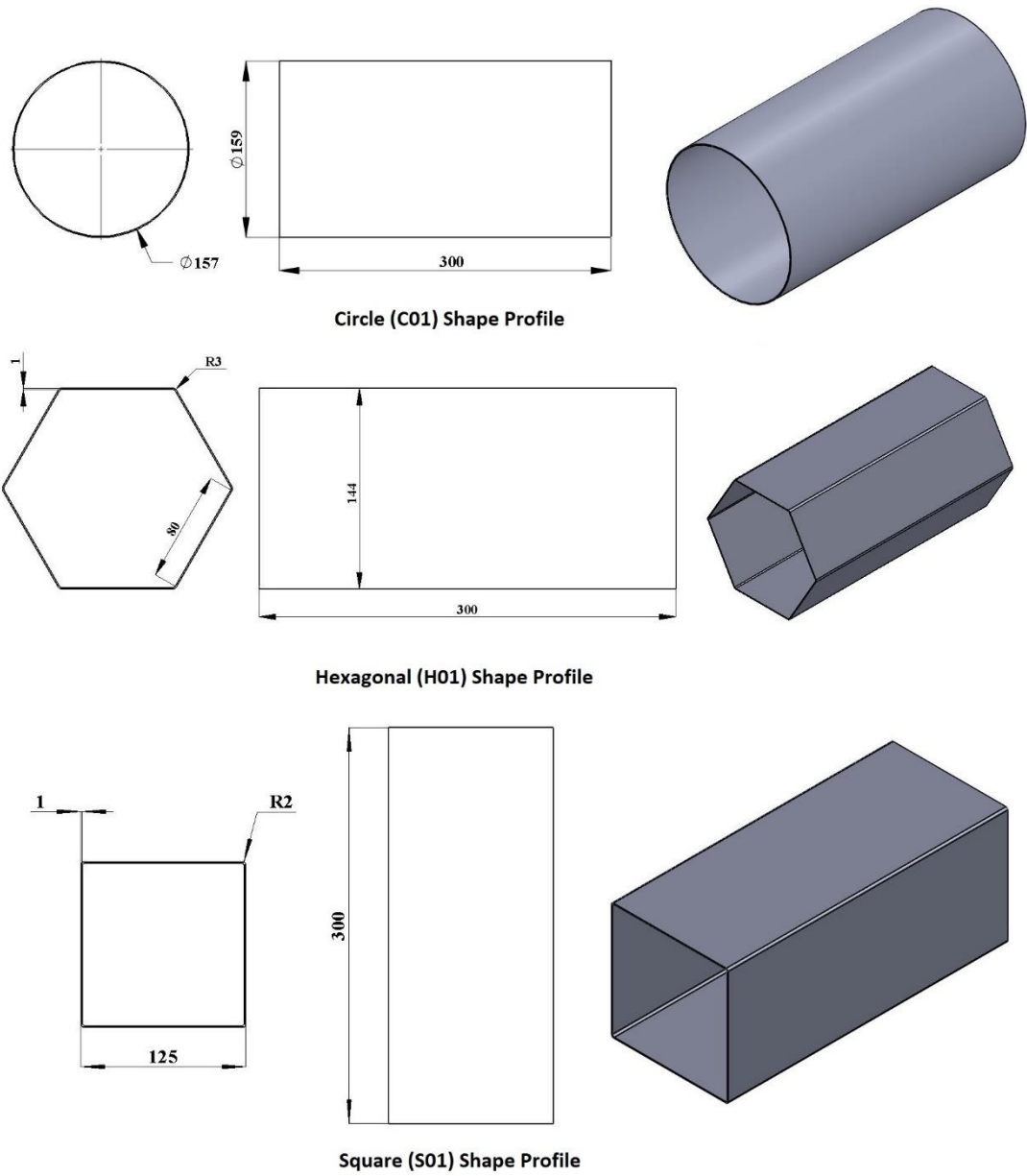
Figure A.6. Technical drawings of Circle (C01), Hexagonal (H01) & Square (S01) with 3-D geometries
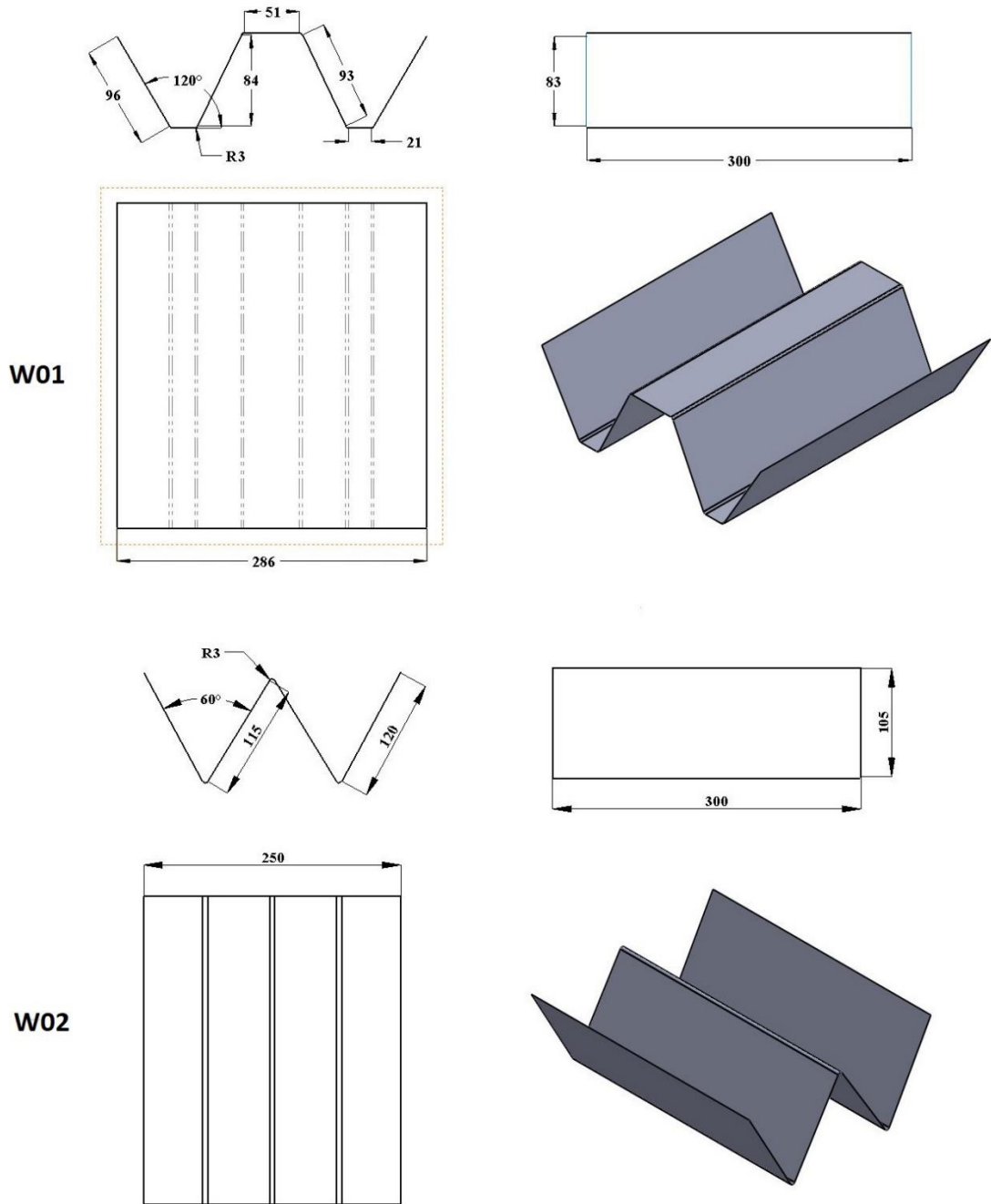
Figure A.7. Technical drawings of W01& W02 shaped profile with 3-D geometries

A3: Experimental & FE Analysis Results

W01-Shaped Profile
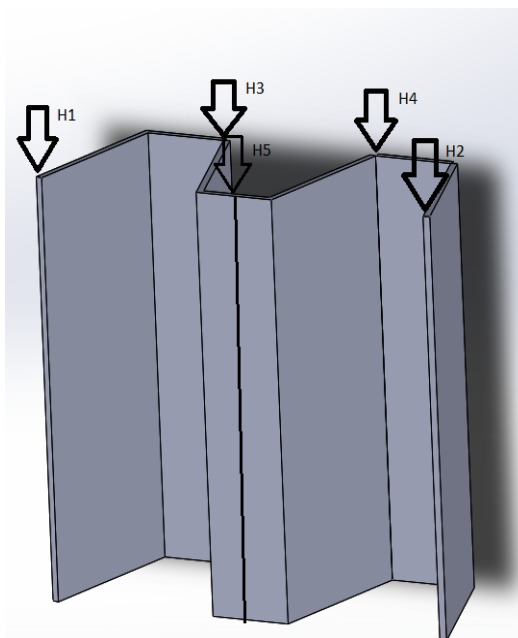
In this figure meaning of these notations (H1, H2, H3, H4 & H5) are representing the height (mm) which measures from the bottom of the crash-box after collision. In the simple word; remaining height of the crash-box after deformation. Mean deformation height is the summation of the all of height which mention in the notations.

Table B.1. Experimental & FEA result of all samples of W01 shaped profile

Specimen No	H (mm)	H1 (mm)	H2 (mm)	H3 (mm)	H4 (mm)	H5 (mm)	Mean (H)
Experimental Analysis Result							
W01-I2-S01-T01	*300*	280	281	278	279	281	*279.8*
W01-I2-S01-T02	*300*	276	276	274	276	276	*275.6*
W01-I1.5-S01-T01	*300*	243	245	245	245	244	*244.4*
W01-I1.5-S01-T02	*300*	247	246	246	246	246	*246.2*
W01-l1,2-S01-T01	*300*	220	220	224	223	222	*221.8*
W01-l1.2-S01-T02	*300*	220	221	225	222	219	*221.4*
W01-l1.2-S01-T03	*300*	222	222	222	223	222	*222.2*

Table B.1. Experimental & FEA result of all samples of W01 shaped profile(Continued.)

W01-l1.2-S01-T04	*300*	223	211	223	224	222	*220.6*
W01-l1.2-S01-T05	*300*	206	207	214	208	204	*207.8*
W01-l1.2-S01-T06	*300*	205	205	204	204	206	*204.8*
W01-l1.2-S01-T07	*300*	220	219	225	223	222	*221.8*
W01-I1.2-S01-T08	*300*	229	225	225	226	227	*226.4*
W01-I1.2-S01-T09	*300*	221	220	222	222	222	*221.4*
W01-I1.0-S01-T01	*300*	192	190	191	190	181	*188.8*
W01-l1.0-S01-T02	*300*	200	195	197	190	196	*195.6*
W01-l1.0-S01-T03	*300*	150	160	150	150	165	*155.0*
W01-l1.0-S01-T04	*300*	175	186	185	190	187	*184.6*
W01-l1.0-S01-T05	*300*	210	210	203	206	210	*207.8*
W01-l1.0-S01-T06	*300*	180	185	182	183	186	*183.2*
W01-l1-S01-T07	*300*	182	180	175	180	180	*179.4*
W01-l1.0-S01-T08	*300*	160	165	170	175	180	*170.0*
W01-l1.0-S01-T09	*300*						
W01-l1.0-S01-T10	*300*	175	172	180	178	177	*176.4*
W01-I1.0-S01-T11	*300*	199	168	203	202	199	*194.2*
W01-I1.0-S01-T12	*300*	188	116	195	200	190	*177.8*
W01-I1.0-S01-T13	*300*	172	172	171	172	173	*172*
W01-I1.0-S01-T14	*300*	174	169	172	177	173	*173*
W01-I1.0-S01-T15	*300*	175	159	175	174	177	*172*
W01-I1.0-S01-T16	*300*	186	170	178	181	185	*180*
W01-I1.0-S01-T17	*300*	121	155	170	161	159	*153.2*
W01-I1.0-S01-T18	*300*	164	150	164	162	165	*161*
W01-l1.0-S02-T01	*250*	114	116	95	100	116	*108.2*
W01-I1.0-S02-T02	*250*	122	120	122	120	120	*120.8*
W01-I1.0-S02-T03	*250*	100	115	110	114	115	*110.8*
W01-I1.0-S02-T04	*250*	122	129	121	122	125	*123.8*
W01-I1.0-S02-T05	*250*	111	88	109	105	110	*104.6*
W01-I1.0-S02-T06	*250*	125	92	126	127	123	*118.6*
W01-I1.0-S02-T07	*250*	83	90	90	90	91	*88.8*
W01-I1.0-S02-T08	*250*	95	107	112	112	113	*107.8*
W01-I1.0-S02-T09	*250*	124	119	121	122	120	*121.2*
W01-I1.0-S02-T10	*250*	110	91	115	110	110	*107.2*
W01-l1.0-S03-T01	*200*	68	67	65	60	68	*65.6*
W01-I1.0-S03-T02	*200*	58	45	65	58	61	*57.4*
W01-I1.0-S03-T03	*200*	68	26	65	58	68	*57*
W01-I1.0-S03-T04	*200*	63	48	65	65	67	*61.6*
W01-I1.0-S03-T05	*200*	66	63	65	62	65	*64.2*
W01-I1.0-S03-T06	*200*	48	45	53	55	57	*51.6*
W01-I1.0-S03-T07	*200*	69	66	69	69	68	*68.2*

Table B.1. Experimental & FEA result of all samples of W01 shaped profile(Conti.)

W01-I1.0-S03-T08	*200*	57	58	66	67	66	*62.8*
W01-I1.0-S03-T09	*200*	58	60	61	60	59	*59.6*
W01-I1.0-S03-T10	*200*	71	72	69	67	71	*70.0*
W01-l0.8-S01-T01	*300*	52	52	47	57	55	*52.6*
W01-l0.8-S01-T02	*300*	42	45	45	44	43	*43.8*
W01-l0.8-S01-T03	*300*	67	68	65	66	67	*66.6*
W01-l0.8-S01-T04	*300*	57	32	73	71	71	*60.8*
W01-l0.8-S01-T05	*300*	90	100	100	100	100	*98.0*
W01-I0.8-S01-T06	*300*	58	57	70	68	69	*57.0*
W01-I0.8-S01-T07	*300*	82	63	80	85	75	*77.0*
FEA Result							
W01-I2.0-S01-T01	*300*	270.5	270.6	270.5	270.5	270.7	*270.6*
W01-I1.5-S01T01	*300*	247.3	247.4	247.4	248.1	247.4	*247.5*
W01-I1.2-S01T01	*300*	232.3	232.4	232.3	232.5	233	*232.5*
W01-I1.0-S01T01	*300*	193	193	194	195	194	*194*
W01-l1.0-S02-T01	*250*	125	121	123	123	124	*123.2*
W01-l1.0-S03-T01	*200*	75	76	76	75	77	*75.8*
W01-I0.8-S01T01	*300*	75	76	75	76	75	*75.4*

W02-Shaped Profile
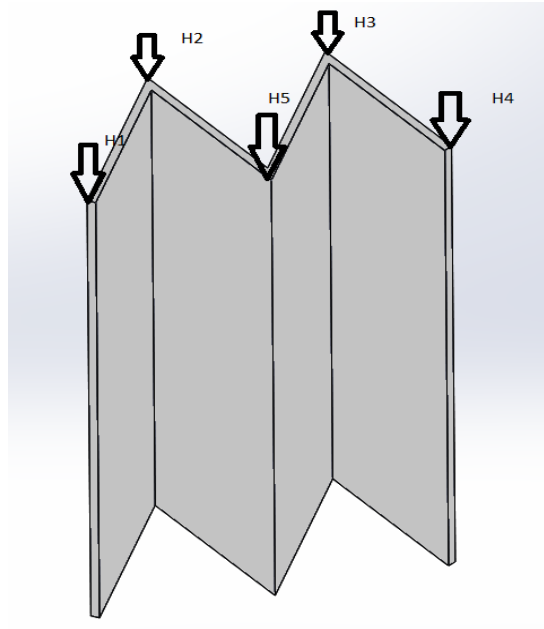
In this figure meaning of these notations (H1, H2, H3, H4 & H5) are representing the height (mm) which measures from the bottom of the crash-box after collision. In the simple word; remaining height of the crash-box after deformation. . Mean deformation height is the summation of the all of height which mention in the notations

Table B.2. Experimental & FEA result of all samples of W02 shaped profile

Specimen No	H (mm)	H1 (mm)	H2 (mm)	H3 (mm)	H4 (mm)	H5 (mm)	Mean(H) (mm)
Experimental Analysis Results							
W02-I1.5-S01-T01	300	237	233	230	230	234	232.8
W02-I1.5-S01-T02	300	186	194	215	212	211	203.6
W02-I1.5-S01-T03	300	208	177	206	205	202	205.3
W02-I1.5-S01-T04	300	215	177	221	218	210	216.0
W02-I1.5-S01-T05	300	205	188	209	207	204	202.6
W02-I1.5-S01-T06	300	127	183	212	213	210	189.0
W02-I1.2-S01-T01	300	167	165	163	161	167	164.6
W02-I1.2-S01-T02	300	106	71	121	113	121	106.4
W02-I1.2-S01-T03	300	81	146	183	184	182	155.2
W02-I1.2-S01-T04	300	111	130	159	156	159	143.0
W02-I1.2-S01-T05	300	116	151	151	151	150	143.8
W02-I1-S01-T01	300	120	122	130	122	120	122.8
W02-I1-S01-T02	300	65	106	104	103	106	96.8
W02-I1-S01-T03	300	74	84	88	86	85	83.4
W02-I1-S01-T04	300	102	103	102	104	103	102.8
W02-I1-S01-T05	300	71	123	123	124	127	113.6
W02-I1-S01-T06	300	97	56	94	91	92	86
W02-I1-S01-T07	300	44	78	80	79	78	71.8
W02-I1-S01-T08	300	34	90	95	96	94	81.8
W02-I1-S01-T09	300	92	57	90	87	86	82.4
W02-I1-S02-T01	250	71	68	73	72	68	70.4
W02-I1-S02-T02	250	69	32	75	67	70	59.5
W02-I1-S02-T03	250	22	49	70	69	69	55.8
W02-I1-S02-T04	250	63	56	57	63	61	60
W02-I1-S02-T05	250	21	25	49	46	45	37.2
W02-I1-S02-T06	250	31	56	61	56	60	52.8
W02-I1-S02-T07	250	57	46	70	68	70	66.3
W02-I1-S02-T08	250	51	59	60	58	60	59.3

Table B.2. Experimental & FEA result of all samples of W02 shaped profile (Continued)

W02-I1-S03-T01	*200*	43	36	42	41	43	*41.0*
W02-I1-S03-T02	*200*	30	32	30	30	30	*30.4*
W02-I1-S03-T03	*200*	24	2	27	27	25	*21.0*
W02-I1-S03-T04	*200*	35	32	38	38	38	*36.2*
W02-I1-S03-T05	*200*	24	34	37	37	36	*33.6*
W02-I1-S03-T06	*200*	30	29	39	37	40	*35.0*
W02-I1-S03-T07	*200*	33	30	41	43	42	*37.8*
W02-I1-S03-T08	*200*	34	28	37	34	36	*33.8*
W02-I1-S03-T09	*200*	32	28	39	35	34	*33.6*
W02-I0.8-S01-T01	*300*	68	22	69	64	62	*57.0*
W02-I0.8-S01-T02	*300*	62	60	58	63	63	*61.2*
W02-I0.8-S01-T03	*300*	62	53	64	59	62	*60.0*
W02-I0.8-S01-T04	*300*	43	53	52	61	52	*52.2*
W02-I0.8-S01-T05	*300*	48	34	43	43	44	*42.4*
FEA Results							
W02-I1.5-S01-T01	*300*	222.6	229.6	229.6	223.3	230.1	228.2
W02-I1.2-S01-T01	*300*	176	175	176	176	176	*175.8*
W02-I1.0-S01-T01	*300*	81	87	87	87	85	*86.5*
W02-I1.0-S02-T01	*250*	45	58	58	57	57	*55*
W02-I1.0-S03-T01	*200*	58	60	60	57	58	*58.6*
W02-I0.8-S01-T01	*300*	39	41	41	39	41	*40.2*

Circle shaped profile
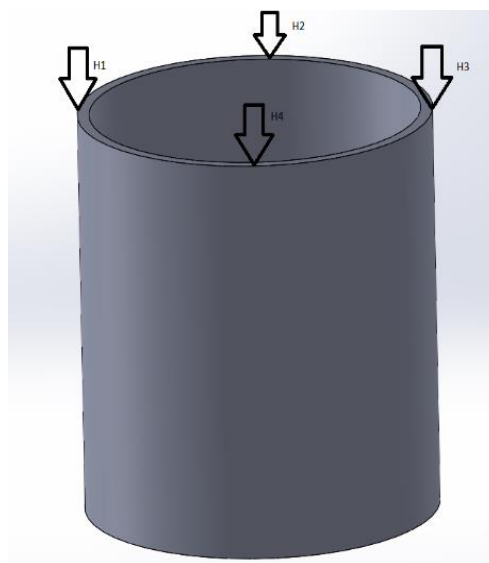
In this figure meaning of these notations (H1, H2, H3, & H4) are representing the height (mm) which measures from the bottom of the crash-box after collision. In the simple word; remaining height of the crash-box after deformation. . Mean deformation height is the summation of the all of height which mention in the notations

Table B.3. Experimental & FEA result of all samples of C01 shaped profile

Specimen No	H (mm)	H1 (mm)	H2 (mm)	H3 (mm)	H4 (mm)	Mean (mm)
Experimental Analysis Results						
C01-l1-S01-T01	*300*	222	212	214	213	*215.3*
C01-l1-S01-T02	*300*	223	224	224	225	*224*
C01-l1-S01-T03	*300*	225	224	224	221	*223.5*
C01-l1-S01-T04	*300*	222	222	218	215	*219.3*
C01-l1-S01-T05	*300*	216	219	220	221	*219*
C01-l1-S01-T06	*300*	220	216	223	213	*218*
C01-l1-S01-T07	*300*	224	219	220	221	*221*
C01-l1-S01-T08	*300*	227	224	227	224	*225.5*
C01-l1-S02-T01	*250*	159	157	155	156	*156.8*
C01-l1-S02-T02	*250*	162	162	164	164	*163*
C01-l1-S02-T03	*250*	160	165	165	162	*163*
C01-l1-S02-T04	*250*	**Experimental Error**				
C01-l1-S03-T01	*200*	114	111	114	114	*113.3*
C01-l1-S03-T02	*200*	125	122	124	125	*124*
C01-l1-S03-T03	*200*	119	121	115	120	*118.8*
C01-l1-S03-T04	*200*	115	110	100	110	*108.8*
FEA Result						
C01-l1-S01-T01	*300*	208.3	208.3	208.4	208.4	*208.4*
C01-l1-S02-T01	*250*	158.1	158.2	158.1	158.2	*158.2*
C01-l1-S03-T01	*200*	111.4	111.4	111.5	111.6	*111.5*

Hexagonal Shaped Profile
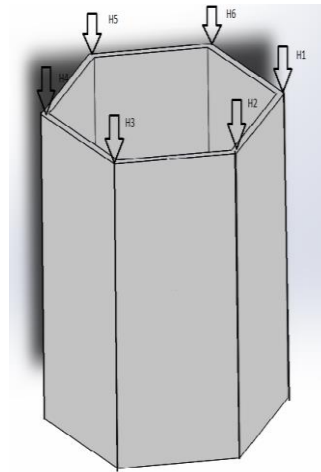
In this figure meaning of these notations (H1, H2, H3, H4, H5 & H6) are represent the height (mm) which measure from the bottom of the crash-box after collision. In the simple word; remaining height of the crash-box after deformation. . Mean deformation height is the summation of the all of height which mention in the notations

Table B.4. Experimental & FEA result of all samples of H01 shaped profile

Specimen No	H (mm)	H1 (mm)	H2 (mm)	H3 (mm)	H4 (mm)	H5 (mm)	H6 (mm)	Mean (mm)
Experimental Analysis Results								
H01-l1-S01-T01	*300*	180	180	180	180	180	180	*180*
H01-l1-S01-T02	*300*	200	200	200	203	190	200	*198.3*
H01-l1-S01-T03	*300*	204	202	204	202	204	204	*203.3*
H01-l1-S01-T04	*300*	195	195	195	193	194	195	*194.5*
H01-l1-S01-T05	*300*	204	209	203	201	197	201	*202.5*
H01-l1-S01-T06	*300*	202	198	202	199	203	198	*200.3*
H01-l1-S01-T07	*300*	191	195	193	190	185	193	*191.2*
H01-l1-S01-T08	*300*	200	202	203	203	203	201	*202*
H01-l1-S02-T01	*250*	130	130	131	125	130	131	*129.5*
H01-l1-S02-T02	*250*	128	132	134	128	133	128	*130.5*
H01-l1-S02-T03	*250*	145	150	155	146	145	150	*148.5*
H01-l1-S02-T04	*250*	135	154	150	148	148	150	*147.5*
H01-l1-S03-T01	*200*	100	98	97	100	101	95	*98.5*
H01-l1-S03-T02	*200*	89	86	86	87	85	85	*86.3*

Table B.4. Experimental & FEA result of all samples of H01 shaped profile (Countined)

H01-l1-S03-T03	*200*	93	97	95	95	96	97	*95.5*
FEA Result								
H01-l1-S01-T01	*300*	183	183	183	182	183	182	*182.7*
H01-l1-S02-T01	*250*	132	132	132	132	132	132	*132*
H01-l1-S03-T01	*200*	96	96	96	96	96	96	*96*

Square Shaped Profile
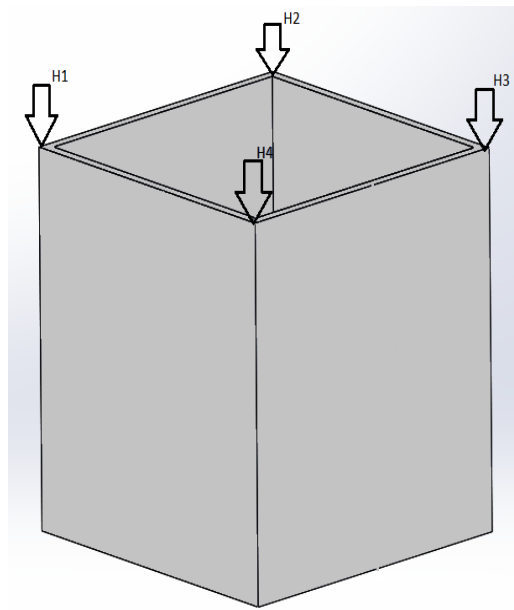
In this figure meaning of these notations (H1, H2, H3, & H4) represents the height (mm) which measures from the bottom of the crash-box after collision. In the simple word; remaining height of the crash-box after deformation. . Mean deformation height is the summation of the all of height which mention in the notations.

Table B.5. Experimental & FEA result of all samples of S01 shaped profile

Specimen No	H (mm)	H1 (mm)	H2 (mm)	H3 (mm)	H4 (mm)	H Mean (mm)
Experimental Analysis Results						
S01-l1-S01-T01	300	112	110	105	104	*107.8*
S01-l1-S01-T02	300	120	123	123	122	*122*
S01-l1-S01-T03	300	158	158	160	159	*158.8*

Table B.5. Experimental & FEA result of all samples of S01 shaped profile (Continued)

S01-l1-S01-T04	300	161	163	163	161	*162*
S01-l1-S01-T05	300	162	164	165	163	*163.5*
S01-l1-S01-T06	300	166	145	142	145	*149.5*
S01-l1-S01-T07	300	134	130	133	131	*132*
S01-l1-S02-T01	250	70	85	88	85	*82*
S01-l1-S02-T02	250	110	107	109	110	*109*
S01-l1-S02-T03	250	109	104	95	100	*102*
S01-l1-S02-T04	250	103	104	99	100	*101.5*
S01-l1-S03-T01	200	52	46	50	47	*48.8*
S01-l1-S03-T02	200	57	61	61	64	*60.8*
S01-l1-S03-T03	200	37	58	53	54	*50.5*
S01-l1-S03-T04	200	78	79	75	76	*77*
FEA Result						
S01-l1-S01-T01	300	118	120	121	121	*120*
S01-l1-S02-T01	250	97	99	99	98	*98.3*
S01-l1-S03-T01	200	50	50	50	50	*50*

Details all files of Crash-boxes FEA model which run in the LS-Dyna software-

Abbreviation

SOL= Drop plate- Solid, Crash-Box_Solid
SUR= Drop plate- Solid, Crash-Box_Shell
ASSC= Automatic Single Surface Contacts
ANSC= Atuomatic Node to Surface Contacts
F.S.= Failure Strain
SUR_   MAT_003_Linear plasticity kinematics
SUR_Piec_   MAT_024_Piecewise kinematics
[highlighted] Selected files which are used in the thesis

Contcat Type= ASSC, ANSC
Velocity= -6944 m/s
Mesh Type= Quadrilateral

Crash-Box Test Analysis Result

Note SUR_026= Crashing has been happened in a proper manner, no material destroyed/disappered and displacement is approximately same with experimental anlysis that's why it has been selected for further anlysis with same parameter such as mesh element size, contact, others.

S.No.	File No.	Profile type	F.S.	Result	Remark
1	SOL_01	W01-I02-S01-T01	0.2	k file did not start in LS dyna manager	Analysis run didn't start that's why don't have analysis picture
2	SOL_02	W01-I02-S01-T02	0.2	k file did not start in LS dyna manager	Analysis run didn't start that's why don't have analysis picture
3	SOL_03	W01-I02-S01-T03	0.2	k file did not start in LS dyna manager	Analysis run didn't start that's why don't have analysis picture
4	SOL_04	W01-I02-S01-T04	0.2	k file did not start in LS dyna manager	Analysis run didn't start that's why don't have analysis picture
5	SOL_05	W01-I02-S01-T05	0.2	k file did not start in LS dyna manager	Analysis run didn't start that's why don't have analysis picture
6	SUR_001	W01-I02-S01-T06	0.2	k file ran in the LS dyna manager	Crashing did not happen in a proper manner
7	SUR_002	W01-I02-S01-T07	0.2	k file ran in the LS dyna manager	Crashing did not happen in a proper manner
8	SUR_003	W01-I02-S01-T08	0	Error termination	Analysis dose not processe and drop plate didn't move down
9	SUR_004	W01-I02-S01-T09	0.2	k file ran in the LS dyna manager	Crashing did not happen in a proper manner
10	SUR_005	W01-I02-S01-T10	0.2	k file ran in the LS dyna manager	Crashing did not happen in a proper manner
11	SUR_006	W01-I02-S01-T11	0.2	k file ran in the LS dyna manager	Crashing did not happen in a proper manner
12	SUR_007	W01-I02-S01-T12	0.2	k file ran in the LS dyna manager	Crashing did not happen in a proper manner
13	SUR_008	W01-I02-S01-T13	0	Error termination	Analysis has not proceed and drop plate didn't move down
14	SUR_009	W01-I02-S01-T14	0.1	k file ran in the LS dyna manager	Deformation of crash-box did not happen like a crashing manner, apart of this, the parts of the material are being disappeared from the crash box profile
15	SUR_010	W01-I02-S01-T15	0.01	k file ran in the LS dyna manager	Deformation of crash-box did not happen like a crashing manner, apart this material are disappeared from the crash box profile
16	SUR_011	W01-I02-S01-T16	0.05	k file ran in the LS dyna manager	Deformation of crash-box did not happen like a crashing manner, apart this material are disappeared from the crash box profile
17	SUR_012	W01-I02-S01-T17	0.2	Error termination	Analysis dose not processe and drop plate didn't move down
18	SUR_013	W01-I02-S01-T18	0	k file ran in the LS dyna manager	Crashing did not happen in a proper manner, some material is destroyed where drop plate hit the crash-box
19	SUR_014	W01-I02-S01-T19	0.2	k file ran in the LS dyna manager	Crashing did not happen in a proper manner, some material is destroyed where drop plate hit the crash-box
20	SUR_015	W01-I02-S01-T20	0.2	k file ran in the LS dyna manager	Crashing did not happen in a proper manner, some material is destroyed where drop plate hit the crash-box
21	SUR_016	W01-I02-S01-T21	0	Error termination	Analysis dose not processe and drop plate didn't move down
22	SUR_017	W01-I02-S01-T22	0.001	k file ran in the LS dyna manager	Crashing did not happen in a proper manner, some material is destroyed where drop plate hit the crash-box
23	SUR_018	W01-I02-S01-T23	0.2	k file ran in the LS dyna manager	Analysis dose not processe and drop plate didn't move down
24	SUR_019	W01-I02-S01-T24	0	Error termination	Crashing did not happen in a proper manner, some material is destroyed where drop plate hit the crash-box.
25	SUR_020	W01-I02-S01-T25	0.2	k file ran in the LS dyna manager	Crashing did not happen in a proper manner, some material has been destroyed where drop plate has hit the crash-box
26	SUR_021	W01-I02-S01-T26	0.2	k file ran in the LS dyna manager	Crashing has been happened in a proper manner, some material with some error, some material is destroyed where drop plate hit the crash-box
27	SUR_022	W01-I02-S01-T27	0.2	Normal termination	May be meshing problem
28	SUR_023	W01-I02-S01-T28	0	Error termination	May be meshing problem
29	SUR_024	W01-I02-S01-T29	0	Error termination	Crashing has been happened in a proper manner, some material may be destroyed due to failure strain after collision of drop plate with crash-box
30	SUR_025	W01-I02-S01-T30	0.2	Normal termination	Crashing has been happened in a proper manner, no material destroyed/disappered and displacement is approximately same with experimental analysis
31	SUR_026	W01-I02-S01-T31	0	Normal termination	Crashing has been happened in a proper manner, but piecewise material has a more accurate result than linear plastics material when compared result with exp. analysis
32	SUR_026_Piec	W01-I02-S01-T32	0	Normal termination	Crashing has been happened in a proper manner, no material destroyed/disappered but displacement is not greater than 60 elements mesh structure
33	SUR_027	W01-I02-S01-T33	0	k file did not start in LS dyna manager	Crashing did not happen because 250 meshing elements have much more nodes. To run these nodes' analysis, our system's memory is unsufficent
34	SUR_028	W01-I02-S01-T34	0	Normal termination	Crashing has been happened in a proper manner, no material destroyed/disappered but displacement is not greater than quadrilateral mesh structure
35	SUR_029	W01-I02-S01-T35	0	Normal termination	Crashing has been happened in a proper manner, no material destroyed/disappered but displacement is not greater than quadrilateral mesh structure
36	SUR_030	W01-I02-S01-T36	0	Normal termination	Crashing has been happened in a proper manner, no material destroyed/disappered but displacement is not greater than 60 elements mesh structure
37	SUR_031	W01-I02-S01-T37	0	Normal termination	Crashing has been happened in a proper manner, no material destroyed/disappered but displacement is not greater than 60 elements mesh structure
38	SUR_032	W01-I02-S01-T38	0	Normal termination	Crashing has been happened in a proper manner, no material destroyed/disappered but displacement is not greater than 60 elements mesh structure
39	SUR_033	W01-I02-S01-T39	0	Normal termination	Crashing has been happened in a proper manner, no material destroyed/disappered but displacement is not greater than 60 elements mesh structure

#	ID	Code		Status	Description
40	SUR_034	W01-I02-S01-T40	0	Normal termination	Crashing has been happened in a proper manner , no material destroyed/disappered but displacement is not greater than 60 elements mesh structure
41	SUR_035	W01-I1.5-S01-T1	0	Normal termination	Crashing has been happened in a proper manner , no material destroyed/disappered and displacement is not near to experimental anlysis and more than 15 % error
42	SUR_035_Piec	W01-I1.5-S01-T2	0	Normal termination	Crashing has been happened in a proper manner , no material destroyed/disappered and displacement is approximately same with experimental anlysis
43	SUR_036	W01-I1.2-S01-T01	0	Normal termination	Crashing has been happened in a proper manner , no material destroyed/disappered and displacement is not near to experimental anlysis and more than 30 % error
44	SUR_036_Piec	W01-I1.2-S01-T02	0	Normal termination	Crashing has been happened in a proper manner , no material destroyed/disappered and displacement is approximately same with experimental anlysis
45	SUR_037	W01-I1.0-S01-T01	0	Normal termination	Crashing has been happened in a proper manner , no material destroyed/disappered and displacement is not near to experimental anlysis and more than 44 % error
46	SUR_037_Piec	W01-I1.0-S01-T02	0	Normal termination	Crashing has been happened in a proper manner , no material destroyed/disappered and displacement is approximately same with experimental anlysis
47	SUR_038	W01-I0.8-S01-T01	0	Normal termination	Crashing has been happened in a proper manner , no material destroyed/disappered and displacement is not near to experimental anlysis and more than 60 % error
48	SUR_038_Piec	W01-I0.8-S01-T02	0	Normal termination	Crashing has been happened in a proper manner , no material destroyed/disappered and displacement is approximately same with experimental anlysis
49	SUR_039	W01-I1.5-S01-T03	0	Normal termination	Crashing has been happened in a proper manner , no material destroyed/disappered and displacement is not near to experimental anlysis and more than 20 % error
50	SUR_040	W01-I1.2-S01-T03	0	Normal termination	Crashing has been happened in a proper manner , no material destroyed/disappered and displacement is not near to experimental anlysis and more than 40 % error
51	SUR_041	W01-I1.0-S01-T03	0	Normal termination	Crashing has been happened in a proper manner , no material destroyed/disappered and displacement is not near to experimental anlysis and more than 60 % error
52	SUR_042	W01-I0.8-S01-T03	0	Normal termination	Crashing has been happened in a proper manner , no material destroyed/disappered and displacement is not near to experimental anlysis and more than 67 % error
53	SUR_043_Piec	W02-I1.0-S01-T01	0	Normal termination	Crashing has been happened in a proper manner , no material destroyed/disappered and displacement is approximately same with experimental anlysis
54	SUR_044_Piec	S01-I1.0-S01-T01	0	Normal termination	Crashing has been happened in a proper manner , no material destroyed/disappered and displacement is approximately same with experimental anlysis
55	SUR_045_Piec	C01-I1.0-S01-T01	0	Normal termination	Crashing has been happened in a proper manner , no material destroyed/disappered and displacement is approximately same with experimental anlysis
56	SUR_046_Piec	H01-I1.0-S01-T01	0	Normal termination	Crashing has been happened in a proper manner , no material destroyed/disappered and displacement is approximately same with experimental anlysis
57	SUR_047_Piec	W01-I1.0-S02-T01	0	Normal termination	Crashing has been happened in a proper manner , no material destroyed/disappered and displacement is approximately same with experimental anlysis
58	SUR_048_Piec	W01-I1.0-S03-T01	0	Normal termination	Crashing has been happened in a proper manner , no material destroyed/disappered and displacement is approximately same with experimental anlysis
59	SUR_049_Piec	W02-I1.0-S02-T01	0	Normal termination	Crashing has been happened in a proper manner , no material destroyed/disappered and displacement is approximately same with experimental anlysis
60	SUR_050_Piec	W01-I1.0-S03-T01	0	Normal termination	Crashing has been happened in a proper manner , no material destroyed/disappered and displacement is approximately same with experimental anlysis
61	SUR_051_Piec	S01-I1.0-S02-T01	0	Normal termination	Crashing has been happened in a proper manner , no material destroyed/disappered and displacement is approximately same with experimental anlysis
62	SUR_052_Piec	S01-I1.0-S03-T01	0	Normal termination	Crashing has been happened in a proper manner , no material destroyed/disappered and displacement is approximately same with experimental anlysis
63	SUR_053_Piec	C01-I1.0-S02-T01	0	Normal termination	Crashing has been happened in a proper manner , no material destroyed/disappered and displacement is approximately same with experimental anlysis
64	SUR_054_Piec	C01-I1.0-S03-T01	0	Normal termination	Crashing has been happened in a proper manner , no material destroyed/disappered and displacement is approximately same with experimental anlysis
65	SUR_055_Piec	H01-I1.0-S02-T01	0	Normal termination	Crashing has been happened in a proper manner , no material destroyed/disappered and displacement is approximately same with experimental anlysis,
66	SUR_056_Piec	H01-I1.0-S03-T01	0	Normal termination	Crashing has been happened in a proper manner , no material destroyed/disappered and displacement is approximately same with experimental anlysis
67	SUR_057_Piec	W02-I1.5-S01-T01	0	Normal termination	Crashing has been happened in a proper manner , no material destroyed/disappered and displacement is approximately same with experimental anlysis
68	SUR_058_Piec	W02-I1.2-S01-T01	0	Normal termination	Crashing has been happened in a proper manner , no material destroyed/disappered and displacement is approximately same with experimental anlysis
69	SUR_059_Piec	W02-I0.8-S01-T01	0	Normal termination	Crashing has been happened in a proper manner , no material destroyed/disappered and displacement is approximately same with experimental anlysis

RESUME

Ahmad Bakhtiyar is an Indian citizen born in January 1992, in Uttar Pradesh, India. High School Graduated from the Adarsh Janta Inter college Tanda Ambedkar Nagar, UP, India, finished his Bachelor of Mechanical Engineering at the Aligarh Muslim University, Aligarh in 2015. Mr. Ahmad Bakhtiyar started his master studies in Sakarya University in the field of Machine Design & Production in 2016 after completing one year of Turkish preparatory class. It is worth to be mentioned that he has worked in Federal Electrics Sakarya, Turkey. He is a Masters student in Department of Mechanical Engineering.